CONTENTS

# Biomedical Research

Volume 14 Number 2 October 2003



Edited, printed and published by M.A. Qayyum
For Scientific Publishers of India, 87 Greater Azad Enclave, Aligarh 202 002, India

# Biomedical Research

*An international Journal*

**Chief Editor:** M.A. Qayyum: 6-B Manzar, Sir Syed Nagar, Aligarh 202 002, India

Phone: 0091 571-2703043 e-mail: biomedical@sancharnet.in biomedical44@hotmail.com



**Scientific Publishers of India, 87-Greater Azad Enclave, Aligarh 202 002, India**

*Biomedical Research 2003; 14 (2): 117-120*

# Effects of alendronate on the expression of osteoclasts in the transplanted bone

**Toshitsugu Kawata, Kaoru Tenjo, Chiyoko Tokimasa, Tadashi Fujita, Masato Kaku, Akira Matsuki, Shinya Kohno, Keisuke Tsutsui, Junji Ohtani, Masahide Motokawa, Mao Shigekawa, Yuiko Tohma and Kazuo Tanne**

Department of Ortodontics and Craniofacial Developmental Biology, Graduate School of Biomedical Sciences, Hiroshima University, 1-2-3 Kasumi, Minami-ku, Hiroshima 734-8553, Japan

**Key words:** Alendrnate, bone resorption, bone transplantation

*Accepted June 21, 2003*

## Abstract

**Alendronate, a bisphosphonates was examined for inhibitory effect on bone resoption. The mice were divided into two groups: $10^{-7}$ M alendronate immersed group and saline group. The tarsal bone to transplanted after immersing in $10^{-7}$ M alendronate for 15 minutes at 37°C. While the grafted bone disappeared within one month in the control group, 80% of the alendronate-tested bone tissue remained over 14 days postoperation, decreasing slightly thereafter. The osteoclasts were significantly less in number in the alendronate. These results indicated that the alendronate inhibits resorption of ectopic bone graft at a concentration of $10^{-7}$ M.**

## Introduction

In osseous defects resulting from maxillary alveolar clefts as well as in craniofacial bone clefts and in craniofacial bone clefts of the palate, regeneraton of bone is of importance in the morphological and functional restoration. The most reliable regenerative bone materials for maxillary alveolar clefts and cleft palate are fresh autografts, while it may cause ill effects at the donor site such as excessive blooding pneumothorax, wound infection, and chronic pain [1]. On the other hand, the resorption of the grafted tissue is a problem. Alenronate, a biophosphonates, is known to have an inhibitory effect on bone resorption, suppressing osteoclastic resorption and are used to treat bone disorders including metastatic bone disease and osteoporosis [2]. The antiresorptive action is supposed to the suppression of differentiation of osteoclasts from hemapoietic precursors originated in the bone marrow [3]. The relative contribution of these mechanisms to the action of biophosphonates in vivo is not known and may not be the same for every individual compound. In the previous studies, the influence of immersing transplanted bone in biophosphonates was not considered. This study investigated the effects of alendronate on ectopic bone graft resorption.

## Materials and Methods

This study is to investigate the effects of alendronate on the resorption of the ectopic bone onto graft. C57BL/6J mice (Jackson Laboratory, Bar Harbor, ME, USA) were used as experimental animals. They were kept in cages under alternating 12 h light and dark cycle, and fed either a solid or granulated diet (CE2; Clea Japan, Tokyo, Japan) and water ad libitum. Mice were divided into two groups of 50 each (Table1), 20-day old mice of 30g were used. In the control group, segments of chopped tarsal bone immersed in saline solution were grafted. From 20-day old mice tarsal bone weighing 1 mg was removed from each mouse and chopped and the samples were immersed in $10^{-7}$ M alendronate solution according to the method designed by Tenjou et al [4] and Kawata et al [5] while those from the remaining 100 mice were immersed in saline solution. Each bone material was autografted into the subcutis of the body side. All the operations were made under general anesthesia (Fig. 1). At 7, 14, 21, 28, 35, 42, 49, 56, 63-day-old postgrafting, 5 mice of each group were examined for dorsoventral and lateral x-ray examination using an apparatus (Asahi Roentogen Ind. Co., Kyoto, Japan) and Kodak Dental Ultra-speed film® (Eastman Kodak Co., Rochester, USA) at 20-25kV and 6mA with an exposure time of 3.0 s. The radiographs of transplanted bone volumes were analyzed by an image-analyser programme (NIH) 1.59; National Institutes of Health, Bethesda, MD, USA). And then, one mouse from each group was sacrificed under general anesthesia by intraperitoneal injection of sodium pentobarbital and the bone graft was removed and fixed in 4% paraformaldehyde. The specimens were decalcified in 14% EDTA (pH 7.4) for 14 days at 4°C, embedded in paraffin, 7 μm longitudinal sections were made.

μm longitudinal sections were made. The sections were stained with tartarate-resistant acid phosphatase (TRAP) and counterstained with hematoxylin for counting the number of osteoclasts.

## Results and Discussion

With the body weight, diameter of transplanted bone and number of osteoclasts, analysis of variance (ANOVA) and Fisher's test were performed using Stat View® (Abacus Concepts). There were no significant differences in body weights among the two groups throughout the whole experimental period (Fig. 2), revealing no surgical invasions and growth retardation.

In the control group the grafted bone remarkably decreased in area and volume at 14-days postgrafting and disappeared at about 35 days postgrafting (Fig. 3), significantly less in all. The alendronate immersed graft, however, showed less significant decrease in area and volume. These was noted 20% decrease in bone volumes at 14-day postoperation (Fig. 3).

The number of osteoclasts was significantly less in the alendronate treated graft than in controls at 21-days postgrafting (Fig. 4). Whereas numerous osteoclasts appeared along the surface of the non-treated grafts at 14 days postgrafting, decreasing suddenly upto 35 days postoperation (Figs. 4,5,6). The earlier studies demonstrated the induction of apoptosis in osteoclasts after treatment with biophosphonates [6,7,8,9,10]. The apoptotic osteoclasts might show less active bone resorption. Biophosphonates are known to have no direct effect on the intestinal calcium transport [11] or renal calcicium resorption in laboratory animals [12], Morever, no effects have been demonstrated on hypercalcemia due to malignancy in patients [13].

Thus, alendronate may prevent differentiation of osteoclasts and/ or induce apoptosis of osteoclasts. The present study suggests that the bone resorption in early stages of transplantation is controlled by a local action of alendronate.

*Table 1: Summary of experimental animals*

| Group | 0-day Postoperation | 7-day postoperation | 14-day postoperation | 28-day postoperation | 35-day postoperation | 42-day postoperation | 49-day postoperation | 56-day postoperation | 63-day postoperation |
|---|---|---|---|---|---|---|---|---|---|
| Saline | 5 | 5 | 5 | 5 | 5 | 5 | 5 | 5 | 5 |
| 10-7M Alendronate | 5 | 5 | 5 | 5 | 5 | 5 | 5 | 5 | 5 |

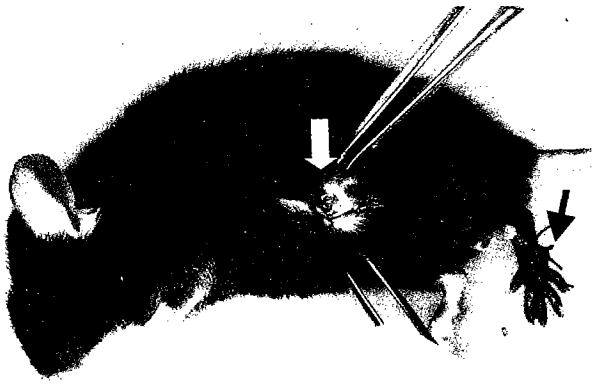

*Fig. 1: Bone material was autografted into the subcutaneous layer under general anesthesia. A solid arrow indicates tarsal bone fragment. An open arrow indicates the subcutaneous layer where the bone fragment should be transplanted.*

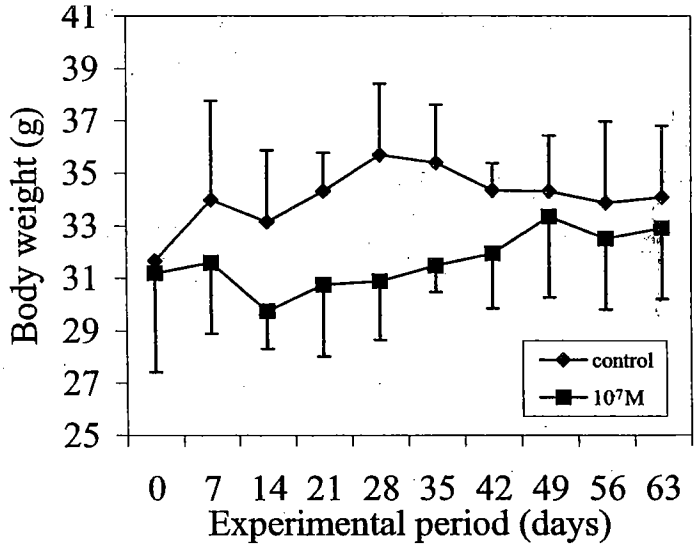


*Fig. 2: Changes in body weight. The receiving bones were immersed in 10-7 M alendronate (n= 3) or saline (n= 3)*

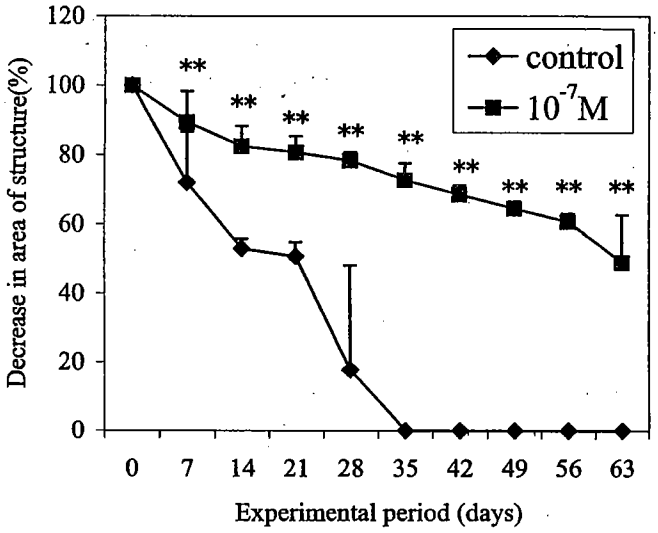


*Fig. 3: Changes in the bone volume of transplanted bone, as analysed by dorsoventral and lateral x-rays of each mouse. Significantly different ($p<0.01$) vs control*

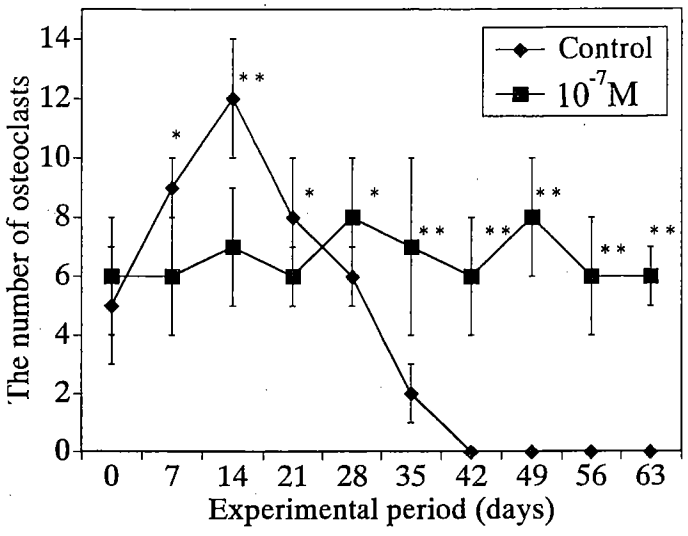


*Fig. 4: Changes in the number of osteoclasts detected by TRAP histochemically different **($p<0.01$) and *($p<0.05$) vs control*

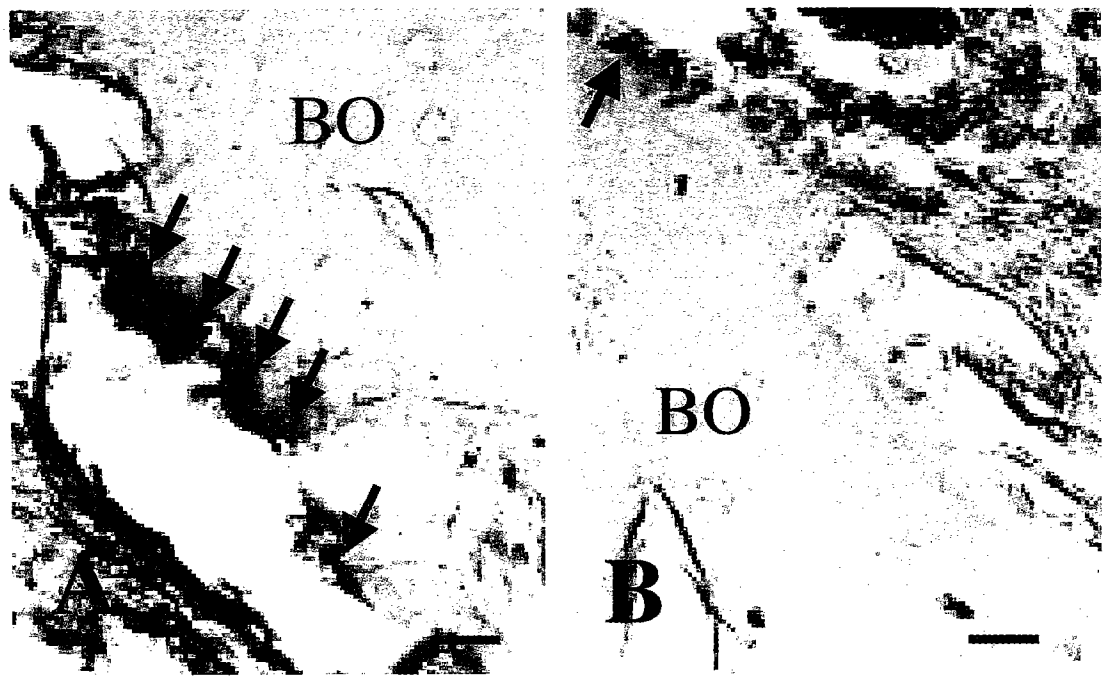


*Fig. 5: TRAP-positive cells appeared around the grafted bone (Bo) by TRAP 14 days after bone grafting. Control (A) and10-7 M alendronate-treated mouse (B). Arrows indicate TRAP=positive cells. (TRAP activity counterstained with hematoxylin, horizontal bar= 50 μm)*

Thus it is concluded that the transplanted bone volume in alendronate-treated mice was substantially higher than that of non-treated ones. These results suggest that alendronate inhibits resorption of ectopic bone graft at a concentration of $10^{-7}$ M.

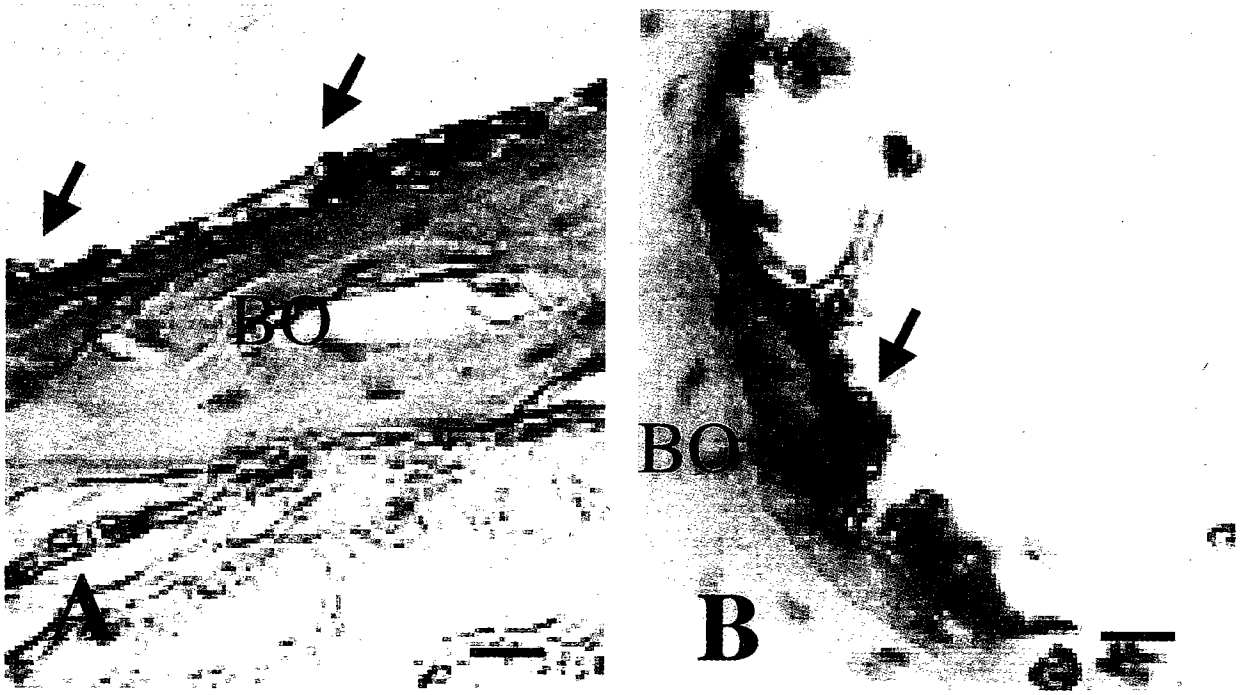


*Fig. 6: Photomicrograph of transplanted bones (Bo) 28 days after bone transplantation. Contol (A) and 10-7 M alendronate-treated mouse (B). Arrow heads indicate osteoclasts (TRAP activity counterstained with hematoxylin, horizontal bar= 50 μm)*

**Acknowledgements**

The authors are grateful to the staff of the Laboratory Animal Science, Hiroshima University School of Medicine for their assistance.

**References**

1. Glowacki J, Kaban LB, Murray JE, Folkman J, Mulliken JB. Lancet 1981; 1: 959-962.
2. Fleisch H. Drugs 1991; 42: 919-944.
3. Rodan GA, Fleisch HA. J Clin Invest 1996; 97: 2692-2696.
4. Tenjo K, Kawata T, Tokimasa C, Kohno S, Kaku M, Fujita T, Tsutsui K, et al Jap Dent Res 2002; 50: 92 (Abstract).
5. Kawata T, Tenjo K, Tokimasa C, Fujita T, Kaku M, Matsuki A, Kohno S, et al. Effect of alendronate on resorption of transplanted bone in mice. Biomed Res (Tokyo) 27 (in press).
6. Benford HL, Frith JC, Auriola S, Monkkonen J, Rogers MJ. Mol Pharmacol 1999; 56: 131-141.
7. Coxon FP, Helfrich MH, Van't Hof R, Ralston SH, Hamilton A, Rogers MJ. Bone Miner Res 2000; 15: 1467-1476.
8. Hughes DE, Wright KR, Uy HL, Sasaki A, Yoneda T, Roodman GD, Mundy GR, Boyce BF. J Bone Miner Res 1995; 10: 1478-1487.
9. Luckman SP, Hughes DE, Coxon FP, Graham R, Russell G, Rogers MJ. J Bone Miner Res 1998; 13: 581-589.
10. Rizzoli R, Caverzasio J, Chapuy MC, Martin TJ, Bonjor JP. J Bone Miner Rtes 1989; 4: 759-765.
11. Bonjour JP, Pussel RGG, Morgan DB, Fleisch H. Am J Physiol 1973; 224: 1011-1017.
12. Reszka AA, Halasy-Nagy JM, Masarachia PJ, Rodan GA. J Biol Chem 1999; 274: 34967-34973.
13. Bickerstaff DR, O'Doherty DP, McCloskey EV, Hamdy NA, Mian M, Kanis JA. Bone 1991; 12: 17-20.

**Correspondence:**

Dr. Toshitsugu Kawata
Department of Ortodontics
Graduate School of Biomedical Sciences
Hiroshima University, 1-2-3 Kasumi, Minami-ku
Hiroshima 734-8553
Japan Fax: +81-82-257-5687
e-mail: tenzan@hiroshima-u.ac.jp

*Biomedical Research 2003; 14 (2): 121-125*

# Attraction of phagocyte to dying cells in the uterine epithelium of mouse during postpartum involution: A ultrastructural study

**Kiyoshi Shimizu and Jinzo Yamada**

Department of Anatomy, Tokyo Medical University, 6-1-1 Shinjuku, Shinjuku-ku, Tokyo 160-8402, Japan

**Key words:** Dying cell, phagocyte, luminal epithelium, uterus, postpartum involution, mice

*Accepted April 17, 2003*

## Abstract

**Some luminal epithelial cells are eliminated by cell death such as apoptosis in an involuting organ. We observed when phagocytes engulfing dying cell appeared in the luminal epithelium as the postpartum uterus involuted. The luminal epithelial cells did not begin to undergo cell death until postpartum day 1. Phagocytes engulfing dying cell in the epithelium were observed only on postpartum day 2. These observations indicated that dying cells in the epithelium attracted phagocytes through the basement membrane and then were swiftly and entirely engulfed by phagocytes for preventing inflammation and autoimmunity.**

## Introduction

Following parturition, the weight of uterus shows a rapid decrease, known as postpartum involution [1]. The postpartum uterus eliminates rapidly excessive tissues to prepare the next pregnancy. In the mouse, most of the postpartum involution has finished until postpartum day 3 [2]. In an involuting organ, some cells diminish own cell volume by autophagy and other cells are eliminated by cell death such as apoptosis [3]. For preventing the release of potentially pro-inflammatory and pro-immunogenic intracellular contents, the dying cells must be swiftly and entirely engulfed by phagocytes [4]. For engulfment, phagocyte must touch the dying cell by means of receptors which recognize eat-me signals elicited by dining cells [for reviews see, 5,6,7]. Since the basement membrane obstructs this contact, dying cell must attract phagocytes into the epithelium.

By observing an appearance of phagocytes engulfing dying cell in the luminal epithelium of the postpartum involuting uterus by an electron microscope, we considered whether or not dying cell attracts phagocyte. To eliminate forcible deletion of the luminal epithelial cells by placental detachment and different involuting amounts of with or without fetus, we used the non-pregnant horn of unilaterally pregnant mice during the first three postpartum days.

## Materials and Methods

The animals used were female mice of the IVCS strain. They were reared 12 hours under light and 12 hours dark regime and given food and water ad libitum.

At 7 weeks of age, mice were anesthetized with ether, the right oviduct was ligated with silk thread. After one week, they were mated. Animals were killed on the day of parturition, two or three days postpartum. Three animals were killed in the morning of each day. All pups were removed on the day of parturition.

After perfusion with fixative (Karnovsky solution), the uterine horn was dissected and cut into small pieces. These pieces were postfixed in 2% osmic tetroxode in 0.1% cacodylate buffer (pH 7.5) for 2 h at room temperature. Tissue pieces were routinely dehydrated through graded ethyl alcohol and embedded in Epon. Ultrathin sections were stained with uranyl acetate and lead citrate, and observed with an electron microscope (Hitachi 7000).

## Observations

On the day of parturition (Fig. 1), the luminal epithelial cells were resting on the basement membrane. The nucleus

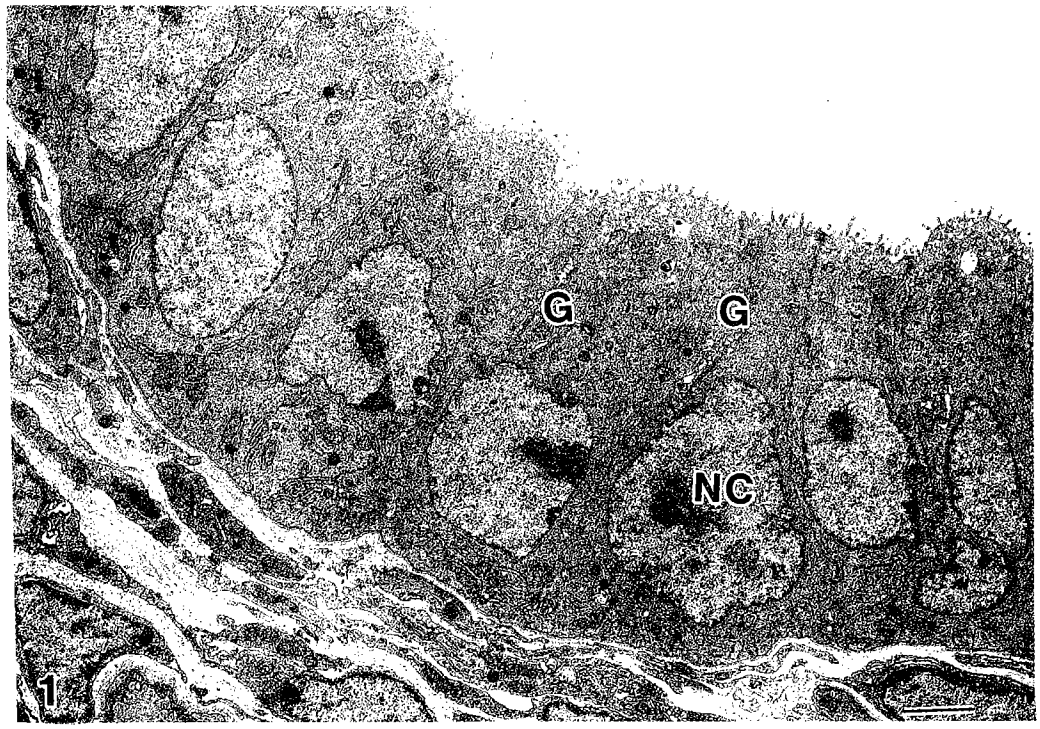


*Fig. 1: On the day of parturition. The luminal epithelial cells were resting on the basement membrane. G, Golgi apparatus; NC, Nucleolus. Bar= 2μm*

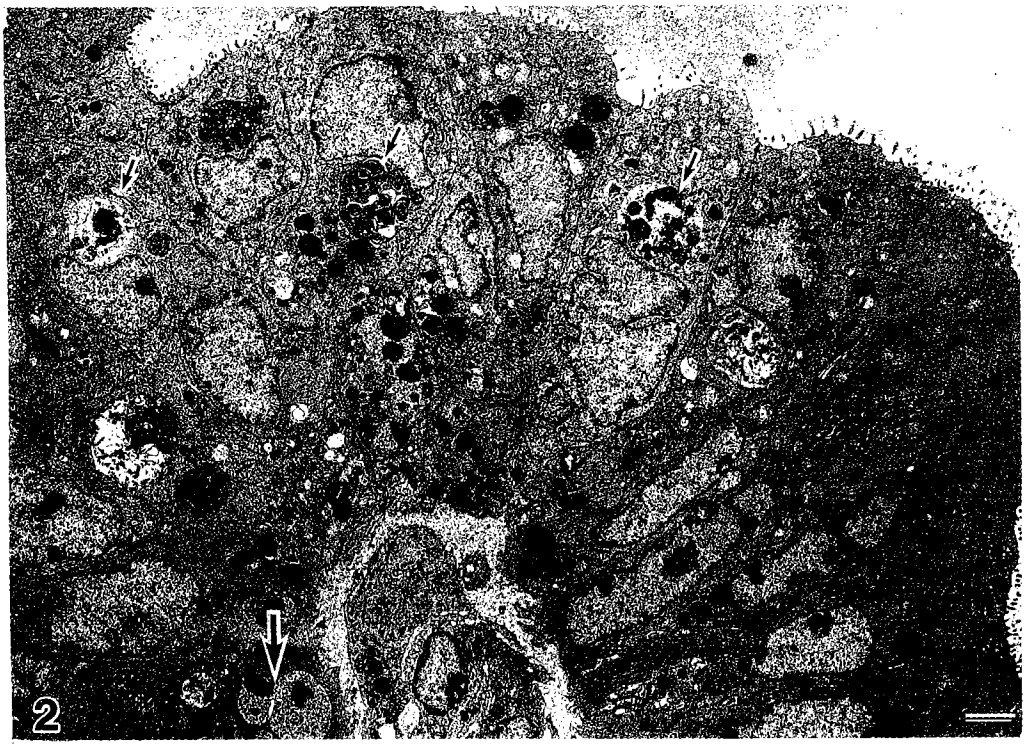


***Fig. 2**: On postpartum day 1. A lot of large vacuole (small arrow) appeared in the luminal epithelium. Cell undergoing apoptosis (large arrow) was a few in number. Bar= 2 μm*

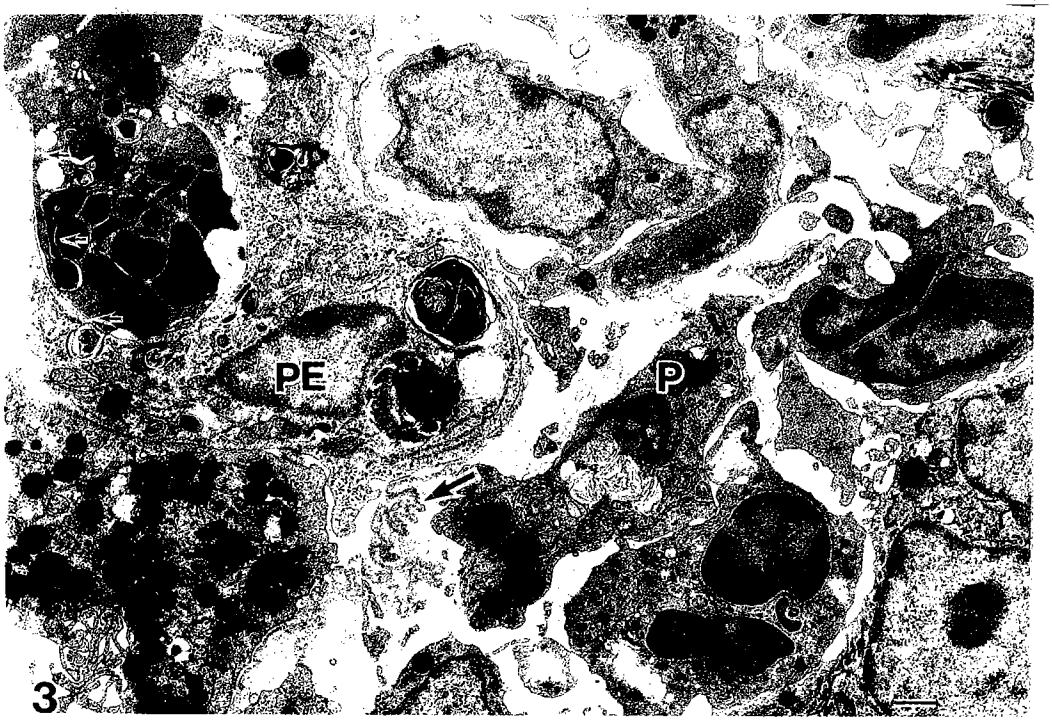


*Fig. 3: On postpartum day 2: A cell undergoing apoptosis was surrounded by a long cytoplasmic process (small arrow) of the phagocyte (PE) in the epithelium. A part of the basement membrane near this cell (large arrow) corrugated. The phagocyte (P) in the subepithelial stroma had several phagosomes.* Bar= 2 *μm*

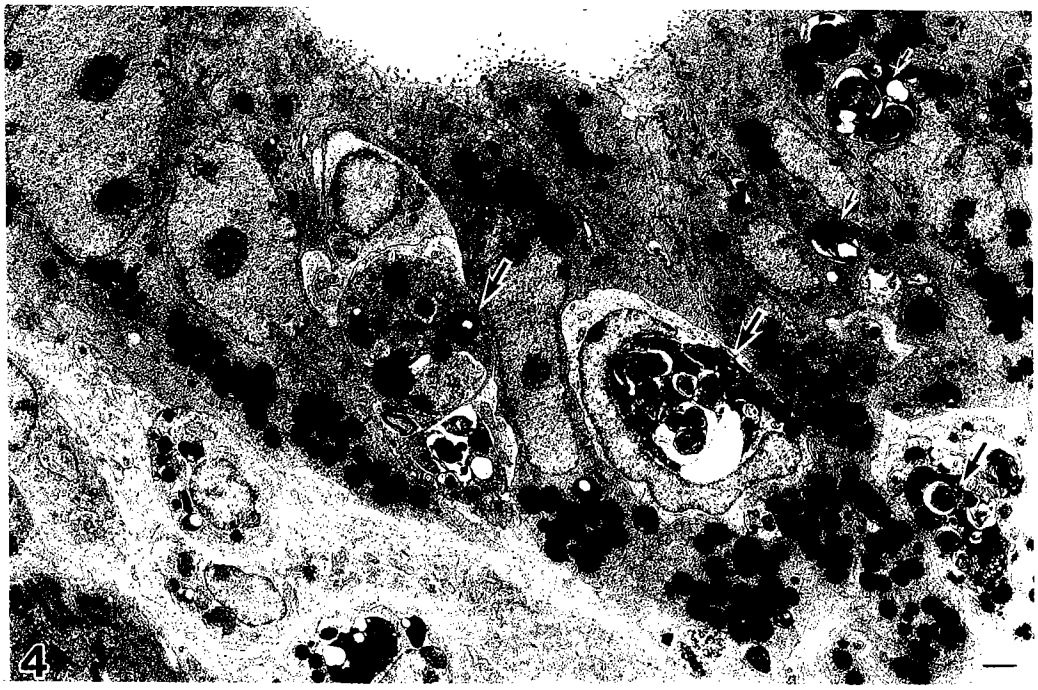


*Fig. 4: On postpartum day 4: Many phagocytes (large arrow) which had a phagosome containing a cell undergoing apoptosis or apoptotic bodies located in the basal region of the luminal epithelium. The epithelial cell (small arrow) containing a large vacuole decreased in number. Bar= 2 μm*

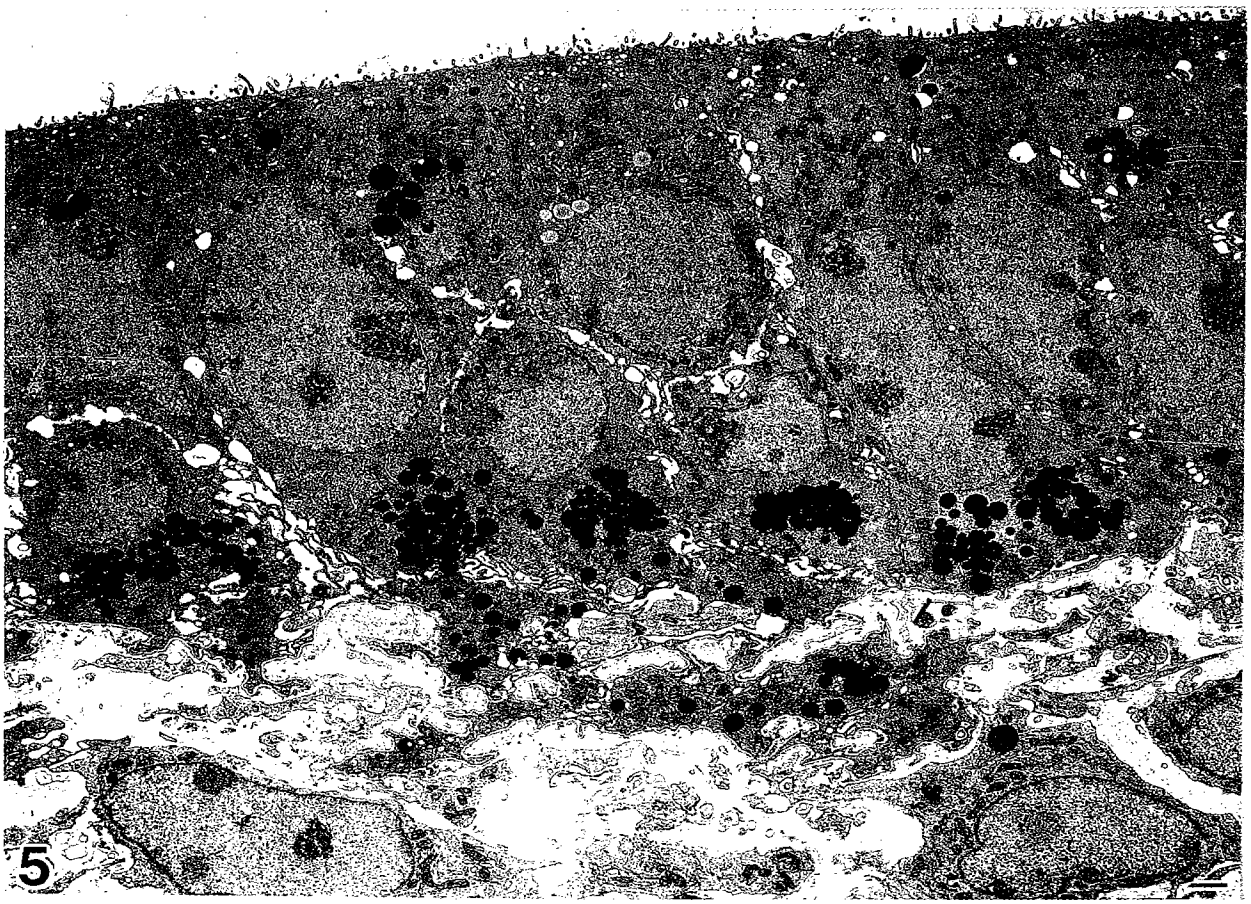


*Fig. 5: On postpartum day 3: Both phagosome and large vacuole never observed in the epithelium. Phagocyte containing a phagosome was not observed in the subepithelial stroma. Bar= 2 μm*

showed relatively oval contour with evenly dispersed chromatin throughout the nucleus. A well developed Golgi apparatus was noted in the supranuclear region.

Many epithelial cells contained a large vacuole near the nucleus on postpartum day 1 (Fig. 2). The vacuole was usually located in the central portion. This vacuole contained myelin figures and electron dense granular material. A few lipid droplets appeared in the basal region of some epithelial cells. A few cells underwent apoptosis (Fig. 2). Their nucleus was fragmented.

On postpartum day 2 (Fig. 3), many electron dense granules derived from nuclear fragments of the luminal epithelial cell were surrounded by a long cytoplasmic process of phagocyte in the epithelium. In the subepithelial stroma, the phagocyte which had several phagosomes containing filamentous material was observed.

Many phagocytes in the epithelium had a phagosome which contained a cell undergoing apoptosis or apoptotic bodies derived from the epithelial cell (Fig. 4). They are located in the basal region of the epithelium. In this study, all materials which might have originated from apoptotic cells was localized within the phagosome of the phagocyte. The epithelial cell containing large vacuole decreased in number (Fig. 4). Many spherical lipid droplets appeared in the basal region of the epithelium.

On postpartum day 3 (Fig. 5), no cell containing a phagosome or large vacuole in the epithelium was observed. Phagocyte having phagosome could not be observed in the subepithelial stroma. A wide intercellular space appeared in the basal part of the epithelium. Thick and long cytoplasmic processes projecting from the basal side of the epithelium were noticed. These processes contained lipid droplets which were similar in appearance to those in the cell body and were surrounded by the basement membrane.

## Discussion

In unilaterally pregnant rodents, the non-pregnant uterine horn showed postpartum involution that is slower to that of the pregnant uterine horn [8,9]. The large vacuole of uterine epithelial cells, which might have originated due to autophagy [10], reaches the peak of the observable frequency on postpartum day 1. The phagocytes which have en-

gulfed the dying cell I and which n the epithelium contained a phagosome in the subepithelial stroma, respectively appeared only postpartum day 2.

Plassma estradiol levels increase suddenly around parturition to induce postpartum ovulation, decrease rapidly on postpartum day 1 and then this low level continues until at least postpartum day 3 [11]. Reduction of plasma estradiol from the day of parturition to postpartum day 1 is similar to that from prooestrus to oestrus.

Withdrawl of estrogen and progesterone induces apoptosis in endometrial cell by activation in the and Fas ligand system [12]. Reduction of plasma estradiol at oestrus makes a epithelial cell to undergo apoptosis [13,14]. Therefore, some epithelial cells in the postpartum endometrium might undergo apoptosis.

Estrogen enhances uterine epithelial cell production of colony-stimulating factor-1 which is a chemoattractant for macrophage [15]. Macrophage accumulates in the subepithelial stroma at oestrus [16] and goes through the basement membrane of the epithelium on postpartum day 2 [17]. Therefore, phagocytes in the postpartum endometrium might migrate along with colony-stimulating factor-1 gradient.

Reduction of plasma estradiol levels on postpartum day 1 might induce some epithelial cells to undergo cell death and, simultaneously, to secrete a phagocyte chemoattractant which is synthesized within the epithelial cell by high estradiol levels around parturition. Phagocytes which migrate into the epithelium on postpartum day 2 recognize the eat-me signals elicited by dying cell, touch and engulf them swiftly and entirely. Ours observations suggest that dying cells might secrete a phagocyte attractant, as yet unknown, for preventing inflammation and autoimmunity.

## Acknowledgement

We would like to thank T. Sato for processing the electron micrographs used in the present study.

## References

1 Harkness RD. The physiology of the connective tissue of the reproductive tract. Int Connect Tiss Res 1964; 2: 155-211.

2 Shimizu K, Hokano M. Removal of collagen bundles in murine uterus during postpartum involution. Anat Rec 1988; 220: 138-142.

3 Zakari Z, Bursh W, Tenniswood M, Lockskin RA. Cell death: Programmed, apoptosis, necrosis, or other ? Cell Death Diff 1995; 2: 87-96.

4 Kerr JF, Wyllie AH, Currie AR. Apoptosis: A base biological phenomenon with wide-ranging implications in tissue kinetics. Br J Cancer 1972; 26: 239-257.

5 Savill J, Fadok V. Corpse clearance defines the meaning of cell death. Nature 2000; 407: 784-788.

6 Geske FJ, Monks J, Lehman L, Fadok VA. The role of the macrophage in apoptosis: Hunter, gather and regulator. Int J Hematol 2002; 76: 16-26.

7 Manfredi AA, Iannacone H, D'Auria F, Rovere-Queirni P. The disposal of dying cells in living tissues. Apoptosis 2002; 7: 153-161.

8 Adams WC, Frieden EM. Inhibition of postpartum involution in the rat by relaxin. Biol Reprod 1985; 33: 1168-1175.

9 Shimizu K, Takahashi T, Hokano M. Loss of collagen from unilaterally non-pregnant uterine horn of mice. Biomed Res (India) 1991; 2: 198-206.

10 Dunn CA. Autophagy .and related mechanisms of lysosome-mediated protein degradation. Trends Cell Biol 1994; 4: 139-143.

11 Grota LJ, Eik-Nes KB. Plasma progesterone concentration during pregnancy and lactation in the rat. J Reprod Fert 1974; 13: 83-91.

12 Song J, Rutherford T, Naftolin F, Brown S, Mor G. Hormonal regulation of apoptosis and the Fas and Fas ligand in human endometrial cells. Mol Human Reprod 2002; 8: 447-455.

13 Sandow BA, West NB, Norman RL, Brenner RM. Hormonal control of apoptosis in hamster uterine luminal epithelium. Am J Anat 1979: 150: 15-36.

14 Spornitz UM, Rinderknect BP, Elderman A, Scheidegger B, Carloi F. Ultrastructure as base for dating of rat endometrium. Anat Rec 1994; 238: 163-176.

15 Bartocci A, Pollard JW, Stanley ER. Regulation of colony-stimulating factor 1 during pregnancy. J Exp Med 1986; 164: 956-961.

16 De M, Wood GW. Influence of estrogen and progesterone on macrophage distribution in the mouse uterus. J Endocrinol 1990; 126: 417-424.

17 Padykula HA, Campbell AG. Cellular mechanisms involved in cyclic stromal renewal of the uterus. II The albino rat. Anat Rec 1976; 184: 27-48.

**Correspondence to:**

Dr. Kiyoshi Shimizu
Department of Anatomy
Tokyo Medical University
6-1-1 Shinjuku, Shinjuku-ku
Tokyo 160-8402
Japan e-mail: kshimizu@tokyo-med.ac.jp

*Biomedical Research 2003; 14 (2): 126-132*

# Okadaic acid stimulates the expression of receptor activator of nuclear factor-kappa B ligand (RANKL) in mouse osteoblastic cells

**Kaya Yoshida [a], Hirohiko Okamura [a], Hiroyuki Morimoto [b], Toshihiko Nagata [c], and Tatsuji Haneji [a]**

[a]Department of Histology and Oral Histology, [b]Department of Anatomy, and [c]Department of Periodontology and Endodontics, School of Dentistry, The University of Tokushima, Kuramoto-cho, Tokushima 770-8504, Japan

**Key words:** Cbfa1, Osteoblast, Okadaic acid, Protein phosphatase, RANKL

*Accepted July 27 2003*

## Abstract

**Receptor activator of nuclear factor-κB ligand (RANKL) is a membrane-bound signal transducer responsible for differentiation and maintenance of osteoclasts. To investigate a possible relationship between the status of protein phosphorylation and the regulation of RANKL in osteoblasts, we examined the effects of okadaic acid, a potent inhibitor of protein phosphatases, on cultured mouse osteoblastic MC3T3-E1 cells. Okadaic acid increased the amounts of RANKL protein in a dose-dependent fashion, with the maximum effective concentration being 100 nM. Okadaic acid at 100 nM stimulated the expression of RANKL mRNA and protein in MC3T3-E1 cells in a time-dependent manner up to 3 h. Okadaic acid also stimulated the expression of the Cbfa1 protein, a transcription factor required for osteoblast differentiation, in a dose-dependent manner. Binding of nuclear proteins prepared from MC3T3-E1 cells to Cbfa1 consensus sequence increased in a time-dependent manner when the cells had been treated with 100 nM okadaic acid. A 200-fold excess of unlabelled Cbfa1 oligonucleotide completely inhibited the DNA-protein complex formation. Our study demonstrate that okadaic acid stimulate RANKL production in MC3T3-E1 cells, indicating that the serine/threonine protein phosphatases play an important role in the regulation of bone metabolism.**

## Introduction

Okadaic acid is a toxic polyether fatty acid produced by several dinoflagellates and is isolated from marine sponges that feed on them [1, 2]. Okadaic acid is a potent inhibitor of protein phosphatases type1 (PP-1) and type 2A (PP-2A) that dephosphorylate serine and threonine residues of proteins in the cytosol of eukaryotic cells and increase the phosphorylation of cellular proteins [3]. The use of this agent has led to the understanding that the phosphorylation/dephosphorylation status is related to cell proliferation and differentiation in mammalian cells [4]. Protein phosphorylation and dephosphorylation are key mechanisms in the regulation of cellular metabolism and functions in various tissues [5, 6]. The level of protein phosphorylation is controlled by the activity of not only protein kinases but also protein phosphatases.

The two major processes of bone remodelling, bone formation and resorption, are regulated by osteoblasts and osteoclasts, respectively [7]. Osteoblasts responsible for bone formation are derived from multipotential stromal cells in the bone marrow through a process of proliferation and differentiation [8]. Osteoclasts are bone-resorbing multinuclear cells that originated from hematopoietic cells [9]. In response to a bone-resorbing stimulant, receptor activator of nuclear factor-κB ligand (RANKL) is expressed on the surface of osteoblasts, which binds to RANK, a receptor of RANKL, and regulate osteoclasts differentiation [10]. RANK is expressed in osteoclast precursors and mediates osteoclast formation through cell-to-cell interaction [7]. Core-binding factor alpha 1 (Cbfa1), which is required for osteoblast differentiation, is one of the important transcription factors located in the promoter region of the RANKL gene [11]. Several signals regulating the expression of RANKL have been reported.

1α, 25-dihydroxyvitamin $D_3$ [1α, 25-$(OH)_2D_3$] stimulates the production of RANKL mRNA through vitamin D receptor [12], whereas parathyroid hormone (PTH) and prostaglandin $E_2$ ($PGE_2$) increase RANKL mRNA by stimulating cAMP production in osteoblast/stromal cells [13]. Intracellular calcium and serine/threonine protein kinases such as protein kinase C also mediate the expression of RANKL in osteoblast [14], indicating that various serine/threonine protein kinases are involved in the signalling pathways for RANKL production. These findings suggest that RANKL plays important roles in bone formation and resorption. However, as the regulation of RANKL and Cbfa1 in phosphorylation status in osteoblasts is poorly understood.

## Materials and Methods

### *Materials*

Alpha Modified Eagle's Minimum Essential Medium (α-MEM) was purchased from GIBCO BRL (Grand Island, NY, USA). Fetal bovine serum (FBS) was obtained from JRH Biosciences (Lenexa, KS, USA). Okadaic acid was purchased from Wako Chemical (Osaka, Japan). Stock solutions (100 μM), prepared in dimethyl sulfoxide (DMSO) and protected from the light, were diluted to the appropriate concentrations with medium. Anti-RANKL and anti-Cbfa1antibodies were purchased from Santa Cruz Biotechnology (Santa Cruz, CA, USA). Anti-Cbfa1 antibody was also supplied by Dr. K. Yamashita (Tokushima University, Japan). Tissue culture plastic dishes were from Falcon Plastics (Los Angeles, CA, USA).

### *Cells and culture condition*

MC3T3-E1 cells were cultured in plastic dishes containing α-MEM supplemented with 10% FBS, ascorbic acid (50 μg/ml), and β-glycerophosphate (2 mM) at 37 °C in a humidified atmosphere of 5% $CO_2$ and 95% air. The cells were subcultured every 3 days by treatment of the cells with 0.25% trypsin together with 1 mM EDTA in $Ca^{2+}$-$Mg^{2+}$-free phosphate buffered-saline (PBS). For experiments, $2\times10^5$ cells in 10 ml of medium were plated in 90-mm plastic dishes and incubated for 3 days, at which time the cells were still subconfluent (~80% of confluence).

### *RNA preparation and reverse transcriptase-polymerase chain reaction (RT-PCR)*

Total RNA was isolated from okadaic acid-treated MC3T3-E1 cells by use of ISOGEN (Nippon Gene, Tokyo, Japan), followed by phenol extraction and ethanol precipitation. The purified RNA was further incubated with DNase I (Sigma) to digest the contaminating DNA. cDNA was synthesized by using Ready-To-Go RT-PCR Beads (Amersham Pharmacia Biotech, Piscataway, NJ, USA). RT-PCR was performed on the cDNA with the following sense and antisense primers:

RANKL, 5′, 5′-GACATGTGCCACTGAGAACC-3′
RANKL, 3′, 5′-CACCTGGTGACCAACATCCT-3′
β-actin, 5′, 5′-GTGGGCCGCTCTAGGCACCAA-3′
β-actin, 3′, 5′-CTCTTTGATGTCACGCACGATTTC-3′

Each RT-PCR experiment was carried out by using cDNA generated from 1 μg of total RNA. After denaturation at 95 °C for 10 min, PCR amplification was performed under the following conditions: 94 °C for 50 sec, 60 °C for 50 sec, and 72 °C for 50 sec, for total of 33 to 35 cycles. The reaction was terminated after a 5-min elongation step at 72 °C. Amplification products were analyzed on 2.0% agarose gels and visualized with an UV transilluminator following ethidium bromide staining. Photographs were taken with a Polaroid DS-300 camera. PCR products were subcloned and sequenced to confirm sequence identities.

### *SDS-PAGE and immunoblotting*

After appropriate periods of cultivation, cells were washed twice with PBS and scraped into lysis buffer containing 1 mM dithiothreitol (DTT), 1 mM phenylmethylsulfonyl fluoride (PMSF), 1 μg/ml leupeptin, 2 μg/ml aprotinin, and 5 mM EGTA in PBS. The cells were sonicated for 10 sec with a sonifier cell disrupter, and the sonicates were then centrifuged for 10 min at 10,000 g. The supernatants were denatured in sample buffer and heated in boiling water for 5 min. Equal amounts of protein estimated with a protein assay kit (Bio-Rad, Richmond, CA, USA) and prestained molecular weight markers (GIBCO BRL) were separated by 12.5% SDS-PAGE and transferred electrophoretically from the gels to polyvinylidene difluoride (PVDF) transfer membranes (Immobilon, Millipore, Bedford, MA, USA). Next, the membranes were incubated in a blocking solution containing 5% skim milk and 0.05% Tween-20 in PBS (PBS-Tween) for 2 h at ambient temperature, washed briefly in PBS-Tween, and incubated overnight at 4 °C with polyclonal anti-RANKL or anti-Cbfa1 antibodies diluted 1:100 or 1:500, respectively. After they had been washed 4 times within 30 min in PBS-Tween by using a rotary shaker at ambient temperature, the washed membranes were incubated with horseradish peroxidase (HRP)-conjugated anti goat IgG (diluted 1:10,000) in PBS-Tween for 1 h at ambient temperature. The membranes were washed as described above, and the proteins recognized by the antibody were visualized with an ECL detection kit (Pharmacia Biotech, Uppsala, Sweden) used according to the manufacturer's directions.

### *Electrophoretic mobility gel shift assay*

Nuclear extracts prepared from MC3T3-E1 cells treated with or without okadaic acid were analyzed by use of an electrophoretic mobility gel shift assay (EMSA) conducted according to the method of Schreiber et al. [15]. Nuclear extraction was performed by using a CelLytic NuClear

Extraction Kit (Sigma) as described in the instruction manual. The concentrations of nuclear proteins were determined with a protein assay kit (Bio-Rad). Double-stranded oligonucleotide probe for Cbfa1 was 3′ end-labeled with digoxigenin by using a DIG Gel Shift Kit (Roche Diagnostics, Mannheim, Germany). The binding reaction was performed as described in the instruction manual; samples (4 μg of protein in each lane) were loaded directly onto nondenaturing 4% polyacrylamide/ bisacrylamide gels prepared in 0.5×TBE (45 mM Tris, 45 mM boric acid, 1 mM EDTA). The gels were pre-run for 60 min before the samples were loaded, and electrophoresis was performed in an ice-cold water bath for 1.5-2 h at 80 V. The following 22-bp double-stranded oligonucleotides, corresponding to 2145-2167 region of the RANKL promoter, were used in this study (only the top strands are shown): 5'-GATCCAACCCACAGCCTCCACC-3'. For competition study, a 200-fold molar excess of unlabeled Cbfa1 probe was added to the mixtures.

## Results

### *Stimulation of RANKL protein expression in MC3T3-E1 cells by okadaic acid*

To determine whether MC3T3-E1 cells express RANKL protein in response to okadaic acid, we prepared cell extracts from MC3T3-E1 cells treated for 3 h with various concentrations of okadaic acid. Figure 1A shows the reaction between the antibody and the proteins extracted from the okadaic acid-treated MC3T3-E1 cells. The anti-RANKL polyclonal antibody interacted with a band having an estimated molecular weight of 40 kDa and the band intensity increased in a dose-dependent manner with the maximum effective concentration being 100 nM. In the extracts prepared from the cells without okadaic acid-treatment the intensity of this band was low. The corresponding band was not detected when the Immobilon membrane was incubated with normal rabbit serum (data not shown). Okadaic acid at 100 nM also stimulated the expression of RANKL protein in MC3T3-E1 cells in a time-dependent manner up to 3 h (Fig. 1B).

### *Expression of RANKL mRNA in MC3T3-E1 cells treated with okadaic acid*

A band of approximately 500-bp corresponding to RANKL cDNA was present in the unstimulated MC3T3-E1 cells after amplification of cDNA for 35 cycles. The RANKL mRNA was not detected in the cells when the amplification cycles were reduced to 33. The RT-PCR exponential phase was determined to be from 30 to 34 cycles and so 33 cycles was used to allow semiquantitative comparisons among cDNAs developed from identical reactions. Figure 2 shows that the expression of RANKL mRNA in MC3T3-E1 cells increased in a time-dependent manner up to 3 h with okadaic acid-treatment. The mRNA sequence was identical to those of the mouse RANKL cDNA. The RT-PCR product of β-actin prepared from the same cells and amplified for the same number of cycles is also shown in Figure 2. There were no quantitative differences in the PCR product of β-actin between the cells treated with okadaic acid for various times.

### *Okadaic acid increased Cbfa1 protein expression in MC3T3-E1 cells*

Figure 3 shows the reaction between the anti-Cbfa1 antibody and the proteins extracted from the MC3T3-E1 cells treated for 3 h with various concentrations of okadaic acid. Staining intensity was weak in the cell extracts prepared from the cells without okadaic acid-treatment. The anti-Cbfa1 antibody interacted with a band having an estimated molecular weight of 37 kDa, and the level of the staining intensity increased in a dose-dependent manner with the maximum effective concentration being 100 nM. The corresponding band was not detected when the Immobilon membrane was incubated with normal rabbit serum (data not shown).

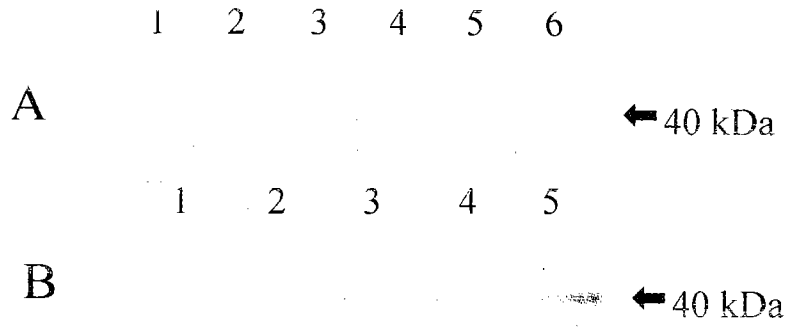


*Fig. 1: Identification of RANKL protein in MC3T3-E1 cells treated with okadaic acid. (A), Cell extracts prepared from MC3T3-E1 cells treated with various concentrations of okadaic acid for 3 h were analyzed by Western blotting. Lane 1,0 nM okadaic acid; lane 2, 1 nM; lane 3, 5 nM; lane 4, 10 nM; lane 5, 50 nM; and lane 6, 100 nM. (B), Cell extracts prepared from MC3T3-E1 cells treated for various periods of time with 100 nM okadaic acid were analyzed by Western blotting. Lane 1, 0 h; lane 2, 0.5 h; lane 3, 1 h; lane 4, 2 h; and lane 5, 3 h. The molecular weight of the protein detected by Western analysis is indicated as kDa.*

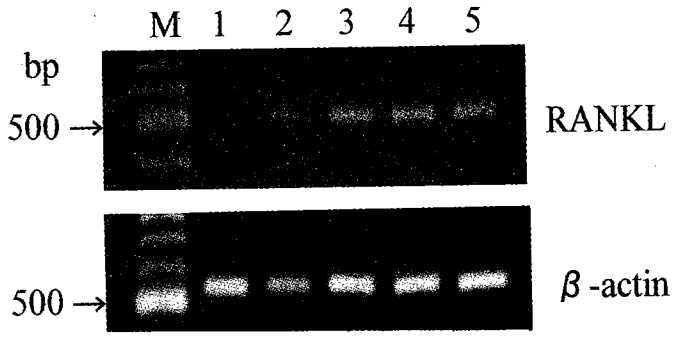


*Fig. 2: Expression of RANKL and β-actin mRNA in MC3T3-E1 cells. Total RNA was prepared from MC3T3-E1 cells treated with 100 nM okadaic acid for various periods of time and the cDNA from the mRNA was amplified for 33 cycles. The resulting products of semiquantitative RT-PCR were electrophoresed in 2% agarose gels and stained with ethidium bromide. Lane M, standard DNA marker (bp); lane 1, treatment for 0 h; lane 2, 0.5 h; lane 3, 1 h; lane 4, 2 h; lane 5, 3 h. Arrow indicates 500 bp. Upper panel, RANKL; bottom panel, β-actin.*

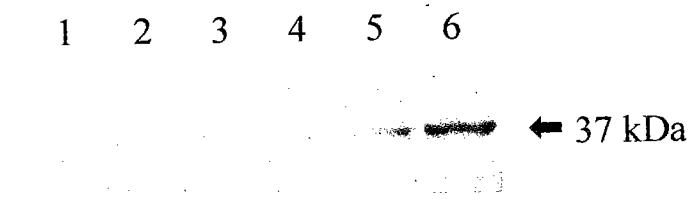


*Fig. 3: Identification of Cbfa1 protein in MC3T3-E1 cells treated with okadaic acid. Cell extracts prepared from MC3T3-E1 cells treated with various concentrations of okadaic acid for 3 h were analyzed by Western blotting. Lane 1, 0 nM okadaic acid; lane 2, 1 nM; lane 3, 5 nM; lane 4, 10 nM; lane 5, 50 nM; and lane 6, 100 nM. The molecular weight of the protein detected by Western analysis is indicated as kDa.*

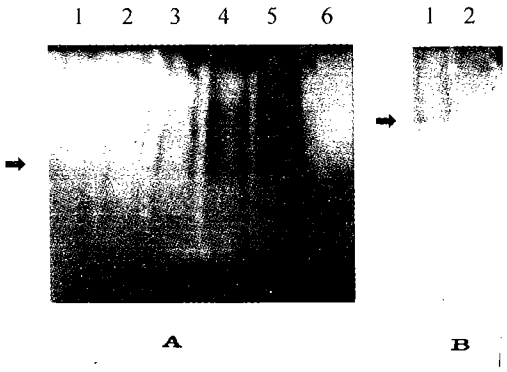


*Fig. 4: Okadaic acid stimulates nucleoprotein complex formed with consensus Cbfa1 site. (A), The Cbfa1 consensus nucleotide was incubated with nuclear extract prepared from untreated MC3T3-E1 cells (lane 1) or from those treated with 100 nM okadaic acid for 10 min (lane 2), 30 min (lane 3), 1 h (lane 4), and 3 h (lane 5). The Cbfa1 probe was also incubated without any extract (lane 6). Arrow indicates DNA-protein complex. (B), The Cbfa1 probe was incubated with the nuclear extract of MC3T3-E1 cells treated for 1 h with 100 nM okadaic acid (lane 1). For demonstrating the specificity of protein binding, a 200-fold molar excess of unlabelled Cbfa1 consensus oligonucleotide (lane 2) was added to the nuclear extract of okadaic acid-treated MC3T3-E1 cells. Arrow indicates DNA-protein complex.*

*Binding of Cbfa1 oligonucleotide to the nuclear proteins from MC3T3-E1 cells treated with okadaic acid*

Cbfa1 is one of the important transcription factors and binds to the sequence located in the promoter region of the RANKL gene. In an attempt to detect DNA-binding proteins interacting with the RANKL promoter, we performed an EMSA using a 3'end-labelled 22-bp DNA probe for Cbfa1 and the nuclear extracts from MC3T3-E1 cells. Figure 4A shows the binding activity of the nuclear proteins of MC3T3-E1 cells toward the Cbfa1 consensus sequence. Nuclear proteins prepared from the cells without

okadaic acid-treatment did not form a DNA-protein complex when incubated with the labeled Cbfa1 consensus oligonucleotide (lane 1). Binding of Cbfa1 to the consensus oligonucleotide sequence increased in time-dependent manner when the cells had been treated with 100 nM okadaic acid for 10 min (lane 2), 30 min (lane 3), 1 h (lane 4), and 3 h (lane 5). The nucleotide did not form DNA-protein complex if nuclear proteins were not added to the reaction mixture (lane 6). Figure 4B shows that the complex was specific for the Cbfa1 probe. A 200-fold excess of unlabelled Cbfa1 oligonucleotide inhibited the binding of this probe to the nuclear extracts from MC3T3-E1 cells treated with okadaic acid (Fig. 4B, lane 2).

As was a case described in Figure 4A, nuclear proteins prepared from cells treated for 1 h with 100 nM okadaic acid bound to Cbfa1 oligonucleotide (Fig. 4B, lane 1).

## Discussion

The level of RANKL mRNA and RANKL protein was low in the unstimulated MC3T3-E1 cells under the conditions used in the present study, which is accord with the previous reports [16]. In the present study, we examined the expression of the mRNA and proteins of RANKL in MC3T3-E1 cells treated with okadaic acid. Okadaic acid stimulated the expression of the mRNA and protein of RANKL in MC3T3-E1 cells in dose- and time-dependent manners. It was reported that osteoblastic cell lines and cells isolated from calvaria expressed higher levels of RANKL protein after treatment with cytokines or hormones including 1α, 25-$(OH)_2$ $D_3$, PTH, or interleukin (IL)-6-type cytokines [16]. However, it has been reported that RANKL mRNA and protein were expressed at higher levels in immature osteoblasts at the confluent stage and decreased as the cultures progressed to the mineralization stage [17]. A recent study indicated that intracellular calcium and serine/threonine protein kinases such as PKA and PKC regulated the expression of RANKL protein in osteoblasts [14]. The activity of PP-1 and PP-2A in mammalian cells has been shown to change in response to various extracellular signals [18]. Such changes in MC3T3-E1 cells might modulate RANKL production. One or more of these factors may involve in the pathway for RANKL production in MC3T3-E1 cells. It might be possible that okadaic acid increased the production of RANKL by inhibiting PP-1 or PP-2A. However, the detailed mechanisms of okadaic acid-regulation of RANKL gene expression in MC3T3-E1 cells are still obscure.

Cbfa1 is a transcription factor required for osteoblast differentiation [19]. In mice lacking Cbfa1 gene, osteoblasts are absent; and the number of osteoclasts is severely reduced [19]. The RANKL promoter contains two potential Cbfa1 binding sites, known as osteoblast-specific element 2 (OSE2) [20]. Based on these studies, we hypothesized that Cbfa1 is involved in the stimulation of RANKL production by okadaic acid. We found that okadaic acid stimulated the expression of Cbfa1 protein. Moreover, by using the EMSA we demonstrated that Cbfa1 consensus sequence was able to bind to the OSE2-like site in RANKL promoter region. These results suggest that the production of RANKL by okadaic acid resulted from the binding of Cbfa1 to the promoter region of RANKL gene. However, whether Cbfa1 regulates the production of RANKL directly or indirectly remains unknown.

There are conflicting reports about the effect of okadaic acid on bone metabolism. For example, okadaic acid inhibited calcium release from neonatal mouse calvaria stimulated by PTH, 1α, 25-$(OH)_2$ $D_3$, $PGE_2$, or 12-O-tetradecanoylphorbol-13-acetate [21, 22]. These reports indicated that okadaic acid inhibited bone resorption and suggested that protein phosphatases may play a role in bone resorption processes. Okadaic acid also inhibited alkaline phosphatase activity and collagen production in mouse and human osteoblastic cells, 2 phenotypic markers directly linked to osteoblastic differentiation and bone formation [23]. However, in a previous study, we demonstrated that okadaic acid at 5 nM increased alkaline phosphatase activity in MC3T3-E1 cells [24], indicating that lower concentration of okadaic acid stimulates bone formation. It was reported that okadaic acid at 60 nM stimulated osteopontin expression through *de novo* induction of AP-1 transcriptional factor in osteoblastic cells including MC3T3-E1 [25]. Lower concentration of okadaic acid enhanced cartilage formation in mesenchymal cell cultures and elevated the activity of cAMP-dependent protein kinase [26]. Okadaic acid also acts as a regulator of alkaline phosphatase activity at a point downstream from protein kinase C in MC3T3-E1 cells [27].

In previous reports we demonstrated that long-term treatment (48-72 h) of 10 nM okadaic acid caused apoptotic cell death in osteoblastic cells including MC3T3-E1 [28-30]. Okadaic acid at 100 nM inhibited protein synthesis and induced phosphorylation of PKR and eIF-2 proteins within 3 h in osteoblastic MG63 cells whereas at a lower concentration (20 nM), okadaic acid did not affect the level of the phosphorylated PKR (Morimoto et al, submitted). These findings suggest that okadaic acid at higher concentration may inhibit dephosphorylation of specific proteins including PKR and eIF-2 and induce RANKL or Cbfa1 proteins. Since okadaic acid inhibits PP-1 and PP-2A at different concentration [6], the opposite effects of okadaic acid on apoptosis and bone metabolism may be derived from the concentrations of okadaic acid used and okadaic acid-treated time or the combination of the inhibited enzymes. Further studies are necessary to elucidate these points. In conclusion, our study demonstrated that okadaic acid stimulated RANKL production in MC3T3-E1 cells, indicating that the serine/threonine protein phosphatases plays a positive role in bone formation by regulating RANKL production.

## Acknowledgments

We thank Mrs. Eiko Sasaki for her skillful technical assistance. This study was supported in part by a grant from the Grant-in-Aid for Scientific Research from the Ministry of Education, Science, Sports, and Culture of Japan.

## References

1. Bialojan C, Takai A. Inhibitory effect of a marine-sponge toxin, okadaic acid, on protein phosphatases. Biochem J 1988; 256: 283-290.

2. Suganuma M, Fujiki H, Suguri H, Yoshizawa S, Hirota M, Nakayasu M, Ojika M, Wakamatsu K, Yamada K, Sugimura T. Okadaic acid: an additional non-phorbol-12-tetradecanoate-13-acetate-type tumor promoter. Proc Natl Acad Sci USA 1988; 85: 1768-1771.

3. Kiguchi K, Giometti C, Chubb CH, Fujiki H, Huberman E. Differentiation induction in human breast tumor cells by okadaic acid and related inhibitors of protein phosphatases 1 and 2A. Biochem Biophys Res Commun 1992; 189: 1261-1267.

4. Mumby MC, Walter G. Protein serine threonine phosphatases: Structure, regulation, and functions in cell growth. Physiol Rev 1993; 73: 673-699.

5. Nishizuka Y. Studies and perspective of protein kinase C. Science 1986; 233: 305-312.

6. Cohen P. The structure and regulation of protein phos--phatases. Annu Rev Biochem 1989; 58: 453-508.

7. Katagiri T, Takahashi N. Regulatory mechanisms of osteoblast and osteoclast differentiation. Oral Dis 2002; 8: 147-159.

8. Aubin JE, Turkesen K, Hererssche JN. Osteoblastic cell lineage. In: Cellular and Molecular Biology of Bone. Noda M. ed. Academic Press, London, 1993: pp 1-45.

9. Kahn AJ. Simmons DJ. Investigation of cell lineage in bone using a chimaera of chick and quail embryonic tissue. Nature 1975; 258: 325-327.

10. Lacey DL, Timms E, Tan HL, Kelley MJ, Dunstan CR, Burgess T, Elliot R, Colombero A, Elliot G, Scully S, Hsu H, Sullivan J, Hawkins N, Davy E, Capparelli C, Eli A, Qian YX, Kaufman S, Sarosi I, Shalhoub V, Senaldi G, Guo J, Delaney J, Boyle WJ. Osteoprotegerin ligand is a cytokine that regulates osteoclast differentiation and activation. Cell 1998; 93: 165-176.

11. Kitazawa R, Kitazawa S, Maeda S. Promoter structure of mouse RANKL/TRANCE/OPGL/ODF gene. Biochim Biophys Acta 1999; 1445: 134-141.

12. Suda T, Takahashi N, Martin TJ. Modulation of osteoclast differentiation: update 1995. Endocr Rev 1992; 13: 66-80.

13. Lee SK, Lorenzo JA. Parathyroid hormone stimulates TRANCE and inhibits osteoprotegerin messenger ribonucleic acid expression in murine bone marrow cultures: correlation with osteoclast-like cell formation. Endocrinology 1999; 140: 3552-3561.

14. Takami M, Takahashi N, Udagawa N, Miyaura C, Suda K, Woo JT, Martin J, Nagai K, Suda T. Intracellular calcium and protein kinase C mediate expression of receptor activator of nuclear factor-κB ligand and osteoprotegerin in osteoblasts. Endocrinology 2000; 141: 4711-4719.

15. Schreiber E, Matthias P, Muller MM, Schaffner W. Rapid detection of octamer binding proteins with 'mini-extracts', prepared from a small number of cells. Nucleic Acids Res 1989; 17: 6419.

16. Deyama Y, Takeyama S, Koshikawa M, Shirai Y, Yoshimura Y, Nishikawa M, Suzuki K, Matsumoto A.Osteoblast maturation suppressed osteoclastogenesis in coculture with bone marrow cells. Biochem Biophys Res Commun 2000; 274: 249-254.

17. O'Brien CA, Gubrijb I, Lin SC, Saylors RL, Manolagas SC. STAT3 activation in stromal osteoblastic cells is required for induction of the receptor activation of NF-κB ligand and stimulation of osteoclastogenesis by gp130-utilizing cytokines or interleukin-1 but not 1,25-dihydroxyvitamin $D_3$ or parathyroid hormone. J Biol Chem 1999; 274: 19301-19308.

18. Wera S, Hemmings BA. Serine/Threonine protein phosphatases. Biochem J 1995; 311: 17-29.

19. Komori T, Yagi H, Nomura S, Yamaguchi A, Sasaki K, Deguchi K, Shimizu Y, Bronson RT, Gao YH, Inada M, Sato M, Okamoto R, Kitamura Y, Yoshiki S, Kishimoto T. Targeted disruption of Cbfa1 results in a complete lack of bone formation owing to maturational arrest of osteoblasts. Cell 1997; 89: 755-764.

20. O'Brien CA, Kern B, Gubrij I, Karsenty G, Manolagas SC. Cbfa1 does not regulate RANKL gene activity in stromal/osteoblastic cells. Bone 2002; 30: 453-462.

21. Feyen JHM, Kuntzelmann GMM (1991) Inhibitory effect of okadaic acid on bone resorption in neonatal mouse calvaria in vitro. Biochem Biophys Res Commun 178:758-763.

22. Goad DL, Meurer EA, Voelkel EF, Petrou CP, Tashjian Jr AH. Protein phosphatase inhibitors and bone resorption: inhibition by okadaic acid and biphasic action of calyculin A. Endocrinology 1992; 130: 3402-3410.

23. Kim IS, Park RW, Sohn KY, Jo JS. Selective inhibition of collagen synthesis of okadaic acid in cultured human fibroblasts. Biochem Biophys Res Commun 1994; 199: 177-182.

24. Murata T, Shirakawa S, Takehara T, Kobayashi S, Haneji T. Protein phosphatase inhibitors, okadaic acid and calyculin A, induce alkaline phosphatase activity in osteoblastic cells derived from newborn mouse calvaria. Biochem Mol Biol Int 1995; 36: 365-372.

25. Kim HJ, Lee MH, Kim HJ, Shin HI, Choi JY, Ryoo HM. Okadaic acid stimulates osteopontin expression through de novo induction of AP-1. J Cell Biochem 2002; 87: 93-102.

26. Zakany R, Szucs K, Bako E, Felszeghy S, Czifra G, Biro T, Modis L, Gergely P. Protein phosphatase 2A is involved in the regulation of protein kinase A signaling pathway during in vitro chondrogenesis. Exp Cell Res 2002; 275: 1-8.

27. Watanabe Y, Kozawa O, Suzuki A, Kotoyori J, Ito Y, Oiso Y. Okadaic acid reverses the inhibitory effect of protein kinase C on alkaline phosphatase activity in osteoblast-like cells. Mol Cell Endocrinology 1994; 103: 115-118.

28. Morimoto Y, Ohba T, Kobayashi S, Haneji T. The protein phosphatase inhibitors okadaic acid and calyculin A induce apoptosis in human osteoblastic cells. Exp Cell Res 1997; 230: 181-186.

29. Morimoto H, Morimoto Y, Ohba T, Kido H, Kobayashi S, Haneji T. Inhibitors of protein synthesis and RNA synthesis protect against okadaic acid-induced apoptosis in human osteosarcoma cell line MG63 cells but not in Saos-2 cells. J Bone Miner Metab 1999; 17: 266-273.

30. Kito S, Shimizu K, Okamura H, Yoshida K, Morimoto H, Fujita M, Morimoto Y, Ohba T, Haneji T. Cleavage of nucleolin and argyrophilic nucleolar organizer region associated proteins in apoptosis-induced cells. Biochem Biophys Res Commun 2003; 300: 950-956.

**Correspondence to:**

Dr. Kaya Yoshida
Department of Histology and Oral Histology
School of Dentistry, The University of Tokushima
18-15, 3 Kuramoto-cho, Tokushima 770-8504
Japan

Phone: ++81-88-633-7322
Fax ++81-88-633-7342
e-mail: kaya@dent.tokushima-u.ac.jp

*Biomedical Research 2003; 14 (2): 133-137*

# Assessment of body fat in young Indian males and females by two and four skinfold methods

**Binit Kumar and Arun Kumar De**

Department of Physiology, Institute of Medical Sciences, Banaras Hindu University, Varanasi, India

**Key words:** Skinfold thickness, body fat percentage, Harpenden's caliper

*Accepted May 27, 2003*

## Abstract

**The estimation of percentage of total body fat had been conducted by measuring skinfold thickness (SFT) at two sites (2 SFT- triceps and subscapular) and four sites SFT (4SFT-biceps, triceps, subscapular and suprailiac) with the help of Harpenden's caliper. A total of 169 (M 106, F 63) young students with moderately sedentary lifestyle, age range varying between 17 to 25 years (Mean ± SD for M 19.31 ±1.91 for F 19.19 ±1.77) of Banaras Hindu University, India. Their height, weight, BMI were measured, calorie intake and physical activity pattern were estimated by questionnaire method. It was observed that distribution of fat at trunk region were more than the upper limb. Body fat percentage estimated either by 2SFT or 4SFT method was higher in females. Estimated mean percentage of body fat in females both by 2SFT and 4 SFT were 19.51± 2.59% and 26.46 ± 2.60 % respectively and in males 13.12± 2.60% and 14.81 ± 2.04 % respectively. Mean daily calorie intake in kilocalorie of females and males were 2034.83 ±618.80 respectively. The 4SFT of females in millimeter were 8.02±2.47, 15.62±3.41, 17.67 ± 3.61 and 21.02±4.69 respectively whereas for male the same were 4.77±1.39, 9.01± 2.98, 12.75 ± 3.93 and 16.03±5.63 respectively. It was concluded that for females 4 SFT was superior method but for males both methods may be used for the age range covered in the study for estimation of body fat percentage.**

## Introduction

The importance of assessment of fat content of human body lies in both disease and health including appraisal of physical fitness level. The percentage of body fat may influence morbidity and mortality and also play an important role during alteration of environmental temperature as well as during starvation. Moreover, certain extra quantity of fat is helpful for sportsman participating in swimming (helps in buoyancy) especially in cold water channel swimming (helps in buoyancy and body temperature maintenance), and in body contact games like wrestling football etc. whereas little lower percentage of body fat helps in better performance in gymnastics, short distance run, kho-kho, badminton etc. The excess body fat in physically less active persons predisposes many diseases like coronary ailments, hypertension, diabetes mellitus, exacerbation of osteoarthritis etc. The low fat content however, is noted during insufficient intake of nutrients in individual with predominantly ectomorphic hereditary character, suffering from chronic diseases including severe debilitating diseases and in anorexia nervosa. Though a moderately satisfactory estimate of body fat may be roughly assessed from height and weight and compared with the standard norms but for precise evaluation several methods are employed to portray a reasonably accurate measure of total body fat. Most of such methods are based on assumption that the body may be considered to consist of two compartments [1] body fat which includes the entire contents of chemical fat and lipids [2]. Fat free mass (FFM) which includes the rest of body tissues apart from fat.

The fat compartment is anhydrous, contains no potassium with a fairly constant density of about 0.90 x $10^3$ Kg/$m^3$. The fat free compartment on the other hand, presumably has a fairly constant density of about 1.10 x $10^3$ Kg/$m^3$ with potassium content of approximately 68 meq/Kg in males and about 10% less in females and water content of

approximately 720 gm/Kg. Therefore, by measuring body density or total body water and subsequently body fat and FFM can be calculated. However, relatively high and low proportion of bone development in an individual may under- or overestimate the fat content by these methods as bone has a low water and potassium content but having high density compared with rest of FFM. The above methods of estimation require complex, costly laboratory equipments and therefore, a comparatively simple technique has been tried by several research workers. Durnin and Rahman [1] reported that relationship between body density and skinfold thickness (SFT) noted to be sufficiently uniform and regression equation as well as tables could be constructed to calculate individual's total body fat. However, Gray et al [2] observed that body fat and SFT equation as well as bio electrical impedance tended to be under-estimated when compared with total body fat calculated from underwater weighing including total body water content in most obese subjects. It is however, noted regarding body fat content that several influencing factors like age, sex, occupation, physical activity, environmental conditions, socio-economic status, types of food predominantly taken also come into picture. Therefore, the generalized equation for assessing the fatness is extremely difficult. There are other methods also to assess the body fat percentage like bio electrical impedance technique and dual energy x-ray absorptiometry.

However, easier, cheaper, less time consuming SFT at various sites have become more popular for estimation of fatness. The data of SFT and body fat percentage in Indian population groups from various parts of the country are not easily available [3,4].

The present pilot study was therefore, undertaken to assess the body fat percentage by measuring SFT at two sites (2SFT-triceps and subscapular) and four sites (4 SFT-biceps, triceps, subscapular and suprailiac) were compared with earlier studies [5,6].

## Methodology

The present study was conducted with prior consent on a total of 169 (M 106, F63) young students, age varying between 17-25 years of Banaras Hindu University, India. It included MBBS students (n-84; M 73, F 11), Bachelor of Ayurvedic Medicine and surgery (BAMS) (n 49; M 33, F16), Home science students (HSS) (n 12; all females) and nursing course students (NCS) (n 21, all females).

The height was measured with a precision of 0.5 cm in standing posture and head in Frankfurt's plane. The weight was measured by weighing machine having standard platform type (The India Machinery Company Ltd. Dassnagar, Howrah, India) and recorded to the nearest of 0.1 Kg with minimum clothing and without footwear. The skin SFT was measured by Harpenden's caliper (Holtain Ltd. Bryberian, U.K.) with a consistent and uniform pressure of 10gm/mm$^2$ with contact area of 0.1 mm at the following four sites biceps, triceps, subscapular and suprailiac at the right side of the body. All SFT were measured within four seconds of application of calipers, to avoid the displacement of subcutaneous interstitial water causing underestimation of SFT [7]. Biceps SFT was measured at the midpoint of the belly of biceps muscle, while the right arm pendant. Triceps SFT was measured at the level of midway between acromion process of scapula and olecranon process and subscapular SFT at about 20 mm below the tip of scapula at an angle of 45 degree towards lateral side of body i.e. skinfold directing downward and outwards like ribs. Suprailiac SFT was measured at approximately 20 mm above right iliac crest at mid axillary line so that the skinfold runs forward and slightly downward.

The percentage of body fat was calculated by using two methods (I) 4SFT method (Table by Deurenberg et al 1990[6]) (biceps, triceps, subscapular and suprailiac) (2) 2SFT method (McArdle et al 1996[8]. The following equations were used for calculation by 2 SFT method.

For young woman between 17 to 26 years, % body fat = 0.55 (A) + 0.31 (B) + 6.13 for young man between 17 to 26 years, % body fat = 0.43 (A) + 0.58 (B) + 1.47 Where A = triceps SFT (mm) B= Subscapular SFT (mm)

## Results

The boys had significantly higher weight and BMI than girls (P<0.001). The SFT at all four sites as well as percentage of body fat were significantly (p<0.001) higher in girls than boys. Total daily calorie intake was significantly higher (p<0.001) in boys than girls (Table I)). Both the groups were sedentary as per guidelines by Indian Council of Medical Research (ICMR).

***Table I: Physical characteristics, skinfold thickness, percentage of body fat and daily total calorie intake of healthy subjects of both sexes***

| | Girls (n=63) | Boys (n=106) | 'p' value |
|---|---|---|---|
| Age (year) | 19.31 ± 1.91 | 19.92 ± 1.77 | < 0.001 |
| Height (cm) | 155.19 ± 5.88 | 170.85 ± 5.89 | < 0.001 |
| Weight (Kg) | 48.42 ± 5.91 | 61.18 ± 5.92 | < 0.001 |
| BMI (Kg/m$^2$) | 20.11±2.89 | 20.97±2.44 | >0.05 |
| **SFT (mm)** | | | |
| Biceps | 8.02 ± 2.47 | 4.77 ± 1.39 | < 0.001 |
| Triceps | 15.62 ± 3.41 | 9.01 ± 2.98 | < 0.001 |
| Subscapular | 17.67 ± 3.61 | 12.75 ± 3.93 | < 0.001 |
| Suprailiac | 21.02 ± 4.69 | 16.03 ± 5.63 | < 0.001 |
| Sum of 4 SFT | 60.07± 12.66 | 40.88 ± 10.02 | < 0.001 |
| Percentage of Body fat by 2 SFT | 19.51 ± 2.59 | 13.12 ± 3.27 | < 0.001 |
| Percentage of Body fat 4 SFT | 26.46 ± 2.60 | 14.81 ± 2.04 | < 0.001 |
| Total Calorie intake (Kcal/day) | 2034.83±489.89 | 2655.91±618.80 | < 0.001 |

*All the subjects were moderately sedentary*

*Table 2: Height, weight, SFTs and Body fat percentage reported by different authors*

| Author/Year/Country | Sex | Age | n | Height (cm) | Weight | Biceps (mm) | Triceps (mm) | SC | SI | % of body fat |
|---|---|---|---|---|---|---|---|---|---|---|
| y, JN 1974 Chandigarh, a | Male | 18 | 774 | - | - | - | 14.2 | 17.4 | 9.4 | |
| | Male | 19 | 383 | - | - | - | 23.4 | 33.6 | 34.0 | |
| | Male | 23 | 51 | - | - | - | 12.6 | 28.2 | 15.6 | |
| in & Womersley 1974, UK | Male | 17-19 | 24 | 178±0.08 | 73.1±16.1 | 4.6±3.0 | 11.0±7.0 | 11.0±6.5 | 14.0±12.0 | 15.0±7.0 |
| | Male | 20-29 | 92 | 177±0.69 | 70.1±12.2 | 4.8±4.2 | 9.8±5.8 | 12.0±8.9 | 16.0±12.0 | 15.0±7.0 |
| | Female | 16-19 | 29 | 163±5.6 | 57.8±10.9 | 8.7±5.4 | 16.0±8.0 | 14.0±9.4 | 16.0±9.3 | 26.0±7.8 |
| | Female | 20-29 | 100 | 163±6.1 | 61.3±14.4 | 11±7.5 | 21.0±10.0 | 18.0±11.0 | 18.0±12.0 | 29.0±10.0 |
| renberg et al 1990, erlands | Male | 17.5±0.39 | 21 | 180.5±1.1 | 72.3±2.33 | 5.6±0.7 | 10.5±1.11 | 9.7±0.94 | 14.2±1.92 | 13.9±0.98 |
| | Female | 16.8±0.36 | 24 | 169.7±11.5 | 61.7±1.47 | 7.7±0.65 | 15.9±0.89 | 10.7±0.79 | 15.0±1.20 | 21.7±1.11 |
| | Male | 23.65 ± 4.4 | 51 | - | 74.57±11.7 | - | 13.2±4.7 | 15.3±6.2 | - | - |
| 1986 USA | Female | 24.84± 5.30 | 44 | - | 56.44±7.96 | - | 17.5±5.0 | 14.5±6.3 | - | - |
| eja et al 2001 New Delhi, a | Male | 28.2±11.9 | 86 | 166.4±23 | 62.4±11.33 | 8.33±5.8 | 14.6±7.8 | 18.8±8.8 | 21.3±10.6 | 21.3±7.6 |
| | Female | 33.9±12.9 | 37 | 158.6±23.2 | 56.9±11.6 | 14.0±6.6 | 21.1±6.7 | 23.4±8.5 | 24.6±7.0 | 35.4±5.0 |
| ent Study | Male | 19.92±1.77 | 106 | 170.85±5.89 | 61.18±5.92 | 4.77±1.39 | 9.01±2.98 | 12.75±3.9 3 | 16.03±5.63 | 14.81±2.04 |
| | Female | 19.31±1.91 | 63 | 155.19±5.88 | 48.42±5.91 | 8.02±2.47 | 15.62±3.4 1 | 17.67±3.6 1 | 21.02±4.69 | 26.46±2.6 |

**In blank space corresponding data was not available.*

*Table 3: Distribution of Subjects according to their BMI(Kg/m$^2$ by Asian and WHO criteria*

| | | Under weight (< 18.5) | Normal weight (18.5-22.9) | Over weight (23.-24.9) | Obese (≥ 25) |
|---|---|---|---|---|---|
| Asian Criteria | Males (n=106) | 12 | 77 | 13 | 4 |
| | Females (n=63) | 17 | 39 | 5 | 2 |
| | | Under weight (< 18.5) | Normal wt. (18.5-24.9) | Over wt. (25-29.9) | Obese (≥ 30) |
| | Males (n=106) | 12 | 90 | 3 | 1 |
| WHO Criteria | Females (n=63) | 17 | 44 | 1 | 0 |

## Discussion

From above observations it was revealed that in both sexes, suprailiac SFT was highest followed by subscapular, triceps and biceps in decreasing order (Table 1)

Females had significantly higher ($p<0.001$) SFT at all above four sites as well as calculated percentage of body fat. Such observation was also reported earlier [4,5, Table 2]. As it is well known that in females, there is predominance of estrogen which favors the fatness. Further, females had lower surface area and overall lower physical activity pattern than males.

When SFT measurements of present male group were compared with those reported by Deurenberg et al 1990 [6], it was observed that SFTs of present group at biceps and triceps were lower than the above study. (Table 2) However, SFTs at subscapular and suprailiac of present study were significantly ($p<0.05$) higher than those of postpubertal boys of above study from Netherlands. Females of present study had approximately similar SFT at biceps and triceps as reported in above study. The SFT at subscapular and suprailiac in females were significantly higher ($p<0.05$) than those of reported study. Such findings were probably because of increasing trend in deposition of fat over the trunk region with increase in age. Moreover, percentage of body fat was also significantly higher ($p<0.05$). SFT of present subjects when compared with male subjects of similar age group from Glassgow (Durnin and Womersley, 1974[5]), it was observed that in male biceps SFT was almost similar whereas at triceps it was higher than present group. Further, lower SFTs were noted at subscapular and suprailiac regions in Glassgow study though the difference was not significant ($p>0.05$). Percentage of body fat however, was noted to be similar in both the studies (Table 2). In females, SFTs at biceps and triceps were almost similar to present study but at trunk region i.e. subscapular and suprailiac, lower SFTs were reported. Difference however, was not significant ($p>0.05$) indicating at similar age group distribution and percent of body fat in subjects of both the countries were approximately similar.

SFTs of present study when compared with those from New Delhi people of age range 18 to 75 years [4], it was observed that all the four sites SFT were higher in males and females than those of present study. Such finding was probably due to higher mean age group as well as higher nutrition status.

Further, SFTs at present study when compared with males of different age groups from Chandigarh [3] it was noted that 18 year age group male had higher triceps and subscapular but lower suprailiac SFT than male subjects of present study. In 19 year age group, higher SFT at all the three sites (Triceps, Subscapular and suprailiac) were noted whereas 23 year age group males of Chandigarh had higher triceps and subscapular SFTs but lower suprailiac SFT (15.6). Such trend of increase in distribution of body fat further substantiated that with the gradual increase in age, trunkal fat was also increasing. While considering the percentage of body fat calculated by 4 SFT and same calculated by 2SFT and then compared it was observed that fat percentage estimated by 4SFT in female was significantly higher than 2 SFT method. Further, percentage of body fat estimated by 4 SFT were comparable with the data of similar age group with moderately sedentary habits like our subjects as reported by Durnin and Womersley [5]. However, the body fat percentage in postpubertal school girls with lower mean age (F $16.8 \pm 0.36$) by Deurenberg et al 1990[6] was lower than present study. The subjects of higher age group had shown higher fatness as also noted by Dudeja et al [4] indicating more accumulation of fat with the increase of age. It was interesting to note in present study that 4SFT fat estimation when compared, it was observed that females had shown higher 4SFT mean value ($26.46 \pm 2.6$) than 2SFT ($19.51 \pm 2.59$) showing a significantly lower value ($p<0.001$). Between the two methods of fat estimation, it was therefore concluded that for females 4SFT was superior method and therefore, may be used for the age range covered in the study.

Triceps and subscapular SFT when compared with those of the study of Shaw [9] in Houston USA covering higher age group, it was observed that male subjects of present study had lower SFT than above study indicating lower fat percent in our subjects. In females, present study whereas had lower SFT at triceps but higher at subcapular region than the subjects of above study indicating less distribution of fat in upper limbs and more in trunk region in our subjects.

The mean values of percentage of body fat either by 2SFT or by 4SFT and BMI may be used for identifying underweight, normal weight, overweight or obese. However, both the values of an individual are to be compared and correlated. In the present study out of 106 males 4 had shown obesity (BMI $\geq 25$, Asian criteria [10] Table 3) but body fat percent calculated by 4SFT had shown only one obese male (Fat % $\geq 20\%$) and out of 69 females according to BMI, 2 were obese whereas 4SFT method showed 5 obese (Fat % $\geq 30\%$). Therefore estimation of fatness in males by only BMI, obesity was overestimated whereas in female obesity was underestimated.

## References

1. Durnin JVGA, Rahman MM. Relationship between body density and skinfold thickness. Br J Nutr 1967; 21: 681.

2. Gray DS, Bray GA, Bauer M, Kaplan K, Gemayel N, Wood R., Greenway F, Kirk S. Skin-fold thickness measurements in obese subjects. Am J Clin Nutr 1990; 51: 571-577.

3. Berry JN. Use of Skinfold Thickness for Estimation of Body Fat. Indian J Med Res1974; 62: 233-239.

4. Dudeja V, Misra A, Pandey RM, Devina G, Kumar G, Vikram NK. BMI does not accurately predict overweight in Asian Indians in Northern India: British Journal of Nutrition 2001; 86: 105-112.

5. Durnin JVGA, Womersley J. Body fat assessed from total body density and its estimation from skinfold thickness: meaurements on 481 men and women aged from 16 to 72 years. *Br J Nutr* 1974; 32: 77-97.

6. Deurenberg P, Pieters JJL, Hautvast JGAJ. The assessment of the body fat percentage by skinfold thickness measurements in childhood and young adolescence. British Journal of Nutrition 1990; 63: 293-303.

7. Becque DM. Time course of skin-plus-fat compression in males and females. Hum Biol1986; 58: 33.

8. McArdle WD, Katch FI, Katch VL. Exercise physiology-Energy, nutrition and human performance. 1996 Fourth edition. Baltimore, Williams & Wilkins.

9. Shaw W. Vickie: The accuracy of two training methods of skin-fold assessment. Research Quarterly for Exercise and Sport 1986; 57: 85-90.

10. Jaslin Diabetes Center: Best body mass for Asians (accessed on 28-8-2002 at http//www.jaslin.narvarel.edu/ api/ bodymass.html).

**Correspondence to:**

Professor A.K. De
Incharge, Sports Medicine
Department of Physiology
Institute of Medical Sciences
Banaras Hindu University
Varanasi 221 005
India

e-mail : binit_bhu@yahoo.com

*Biomedical Research 2003; 14 (2): 138-146*

# Expression and distribution of aromatase mRNA in developing mouse brain

**Lan Xiao and Wen-qin Cai**

Department of Histology and Embryology, Third Military Medical University, Chongqing, 400038, P. R. China

**Key words:** Aromatase, distribution, development, brain, mouse

*Accepted April 27 2003*

## Abstract

**The expression and distribution of aromatase cytochrome P450 in the brain of the developing mouse were investigated with techniques of RNA Dot-Blotting and in situ hybridization. These methods were employed male mouse tissue by using a Digoxingin-labeling (DIG-labeling) cRNA probe that was transcribed in vitro from the human placental aromatase cDNA. The results revealed: (1) Aromatase specific mRNA was presented in the brain tissue from embryonic day 16 (E16) to postnatal day 300 (P300), with higher level at the fist two postnatal weeks and the highest level at postnatal 6 days (P6), the lowest level emerged at adulthood and old age. (2) The location of the aromatase mRNA was confined to neuron cell bodies and their processes. The mainly distribution of aromatase mRNA were detected in the regions of the cerebral cortex, hippocampus, thalamus, hypothalamus and large part of nucleus in limbic system. Many heavily labeled cells were found in the layer of pyramidal cells of cerebral cortex, pyramidal layer of hippocampus, medial preoptic area, medial septal nucleus, amygdaloid nuclei, cingulate cortex, piriform cortex and periamygdaloid cortex. The moderate dense signals presented in several thalamic and hypothalamic nuclei such as ventromedial nucleus, ventrolateral nucleus, laterodorsal thalamic nucleus, paraventricular nucleus, and etc. These data indicate that aromatase mRNA revealed an ontogenestically regulated pattern of expression. The first two postnatal weeks may be a key stage for sex differences of brain, especially of hippocampal plasticity and function. High levels of aromatase expression in regions of cerebral cortex and hippocampus may deal with the modulation of sex dimorphism in memory and cognition function.**

## Introduction

Aromatase, named estrogen synthase, is the last key enzyme to catalyze the conversion of androgen to estrogen. It is a member of the P450 cytochrome family encoded by gene CYP19(15q21.1) [1]. The aromatase cDNA has been cloned in humans and several other species with high homology (>80%) with human and mouse. Aromatase gene contains ten exons, the coding region of the transcripts spans nine exons beginning with exon II, and is associated with an untranslated first exon ( exon I) that varies among different tissues, which results in the same protein being finally expressed in all tissues (ovary, placenta, brain, liver, skin, fibroblasts, adipose tissues and ect.) [2,3,4]. The tissue-specific regulation of aromatase transcription is due to the existence of tissue-specific promoters exon I. In the past 30 years, Naftolin et al created and confirmed the foundation for the brain aromatization hypothesis that many of the effects of androgens on neural cell differentiation are mediated by the local formation of estrogens by the aromatase enzyme [5,6]. During the development of central nerve system, local estrogen formation influences the sexual differentiation of neural structures and modulates neuroendocrine/reproductive functions and sexual behavior [7-10]. In recent years, it has been found that estrogen is involved in the control of motor and cognitive functions or acts as a protective factor for neurodegenerative disorders [11-13]. Studies of the distribution and the effects of brain aromatase gene expression have led to a new perspective on the control of brain function [14].

Aromatase activity was found in many regions of the rat brain. In vitro enzyme activity assays have demonstrated high level of aromatase activity in the bed nucleus of the stria terminalis (BNST), the medial preoptic area (MPO), and the medial and cortical amygdaloid nuclei (mAMY

and CoAMY). Intermediate level of aromatase activity was found in the anterior hypothalamus and the ventromedial hypothalamic nucleus (VMN). In other regions such as caudate-putamen, hippocampus, and parietal cortex, the aromatase activity is not been detected [15]. However, it is difficult to measure the aromatase activity in vivo for the limitation to identification of neurons expressing aromatase. Several reports have described the localization of cells containing aromatase immunoreactivity in the rat brain, but the distribution of aromatase immunoreactivity differed dramatically depending on the antibody used and, in general, did not correlate well with the distribution of aromatase activity in early records [16-19].

Aromatase mRNA level has been primarily examined in the brain during development and showed sexual differentiation, with a higher level in males [10,20]. The relevant reports on the localization of aromatase mRNA in the brain used to employ technique of in situ hybridization with a radioactive isotope labelled probe [21-23]. The results showed some variation because it was difficult to detect the positive cells in the brain clearly.

In present study, techniques of RNA Dot-Blotting and in situ hybridization were used to examine the expression of specific aromatase mRNA in the developing brain tissues and define the distribution of aromatase mRNA expression at cellular levels.

## Materials and Methods

### *Animals*

Kun-Min mice were bred under a controlled light/dark cycle (12h: 12h) with a standard diet and water available. The day detected vaginal plugs was defined as embryonic day 0 (E0), the day of birth was defined as postnatal 0 day (P0). Except E16, male mice were selected for the study according to the presence of testes. 26 animals from E16 to P300 were divided into 7 groups according to age: E16, P1, P6, P12, P30, P60 and P300 (n=3). Aromatase mRNA was detected in all of the groups where RNA Dot-Bloting was used, the distribution of aromatase mRNA in the brain was detected by using in situ hybridization with 5 male mice between P6 to P12.

### *Probe preparation*

The human placental aromatase cDNA is a 2.4kb fragment inserted into plasmid pBluescripte SK(+/-). The cDNA was linearized with Sph□. Then $T_3$ polymerase was used to transcribe in vitro using the digoxigenin (DIG) labeling system (BoEhringer Mannheim, BM.) to transcribe the DIG-labeling antisense RNA (cRNA) probe and $T_7$ polymerase was used to transcribe the DIG-labeling sense RNA probe. The cRNA probe was 1200bp in length and was complementary to the region of the sequence encoding the hemachrome-binding region of the aromatase gene.

### *RNA Dot –Blotting*

RNA Dot–Blotting was performed according to the procedure described by the BM. Company. Total RNA was isolated from 100mg brain tissue with TriPure™ isolation Kit. The isolated RNA has an A260/A280 ratio of 1.7--2.0. The RNA sample was diluted in RNA dilution buffer with a final concentration of 500ng/μl. 2μl of the RNA sample was dropped onto a dry nylon membrane and fixed by baking in an oven at +120 °C for 30 min. The membrane was placed in a hybridization bag containing 2ml prehybridization buffer per 10cm$^2$ of membrane surface area and prehybridized at 45 °C for 1h. Then hybridization was carried out at 45°C for 16h (with a concentration of 800μg/ml of aromatase cRNA probe). After hybridization, washed the membranes twice, 15 min per wash, in 0.1×wash solution (0.1×SSC containing 0.1% SDS) at +68 °C. For detection, the membrane was incubated in a solution with anti-DIG-alkaline phosphatase (1:4000 dilution) for 30 min at 37 °C. Discard the antibody solution, washed the membrane twice, 15 min per wash, in buffer1 (100mM maleic acid, 150mM NaCl, pH 7.5) to remove unbound antibody. Equilibrate the membrane in 20ml buffer 2 (100mM Tris-HCl, pH 9.5; 100mM NaCl, 50mM $MgCl_2$)for 2min. Finally, incubated the membrane in freshly prepared color solution (mix 45μl NBT solution and 35μl X-phosphate (BCIP) in 10ml of buffer 3 in dark box. Once the desired spots have been detected, washed the membrane with buffer 1 for 5 min to stop the reaction. Control experiments were run in parallel with sense-transcript probe of aromatase.

For semiquantitative analysis about the intensity of aromatase mRNA in each group animal, the optic density (OD) (means ± SEM) of the staining dots were detected with the image analysis software of Tiger System.

### *In situ hybridization*

In situ hybridization was performed as described previously [24]. Briefly, 25μm thick frost sections fixed in 4% paraformaldehyde were prehybridized at 43 °C for 2h in 100μl of hybridization buffer (4×SSC, 10% dextran sulfate, 1×Denhardt's solution, 2mM EDTA 50% deionized formamid, 500ug/ml herring sperm DNA). The sections were then hybridized with 100 μl of hybridization buffer containing 5ng/μl anti-sense aromatase specific riboprobes, prior to a 20 h incubation at 43 °C in humid chamber. Following hybridization, a series of post-hybridization steps were performed, including RNase treatment to digest all unhybridized RNA, and stringency washes: once for 15 min in 2×SSC at 37°C, three times for 5 min each in 0.5×SSC and once for 5 min in 100 mM Tris-HCl (pH7.5), 150mM NaCl at room temperature (RT). The sections were then incubated in alkaline phosphatase conjugated anti-DIG antibody (1:1000) dilution for 1h at 37 °C and washed further two times for 10min each in 100mM Tris-HCl (pH7.5), 150 mM NaCl at RT. The detection of alkaline phosphatase was performed by incubating the treated sec-

tions in the detection buffer containing 0.18mg/ml BCIP, 0.34mg/ml NBT and 240mg/ml levamisole in dark box at RT. Once the desired signal has been detected, the staining reaction was stopped by washing the sections in 10 mM Tris-HCl(pH 8.0), 1mM EDTA for 5 min. Control experiments were run in parallel with sense-transcript probe of aromatase.

For analysis of the results, all sections were observed under the microscope at a final magnification of 40× to 400×. A sketch map of the distribution of aromatase mRNA was drawn with the help of image analysis at a magnification 40× and the exact anatomical localization of the labeled structures was confirmed with the help of the adjacent Nissl-stainінged sections. A summary of the distribution of the labeled cells was then prepared on semi-schematic drawings of Nissl-stainінged sections. Different symbols were used in these drawings to indicate the intensity of the aromatase mRNA expression from weak to strong.

## Results

### *Expression of Aromatase-mRNA in the brain of the developing mouse*

Fig. 1 (A,B) show the results of RNA Dot-Blotting and the semiquantitative analysis of aromatase mRNA expression in each group animal. The staining dots represent the expression of aromatase mRNA. The aromatase mRNA was detected in the brain tissue with different expression levels during the period from E16 to P300. The intensity of the dot staining is strong at the stage from birth (postnatal 1day, P1) to postnatal 12 days (P12), with the strongest intensity at postnatal 6 days (P6) and the lightest intensity

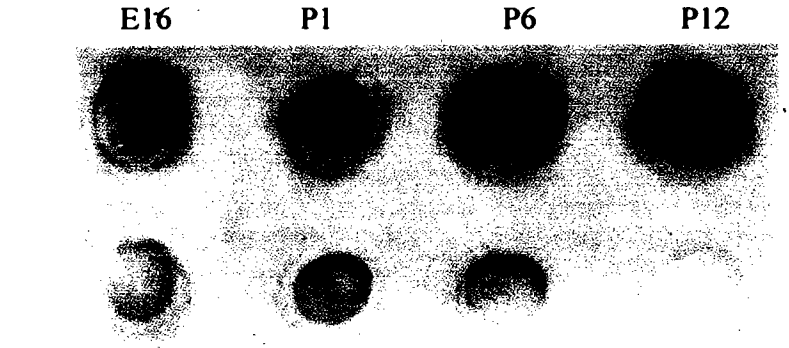


Fig1-A

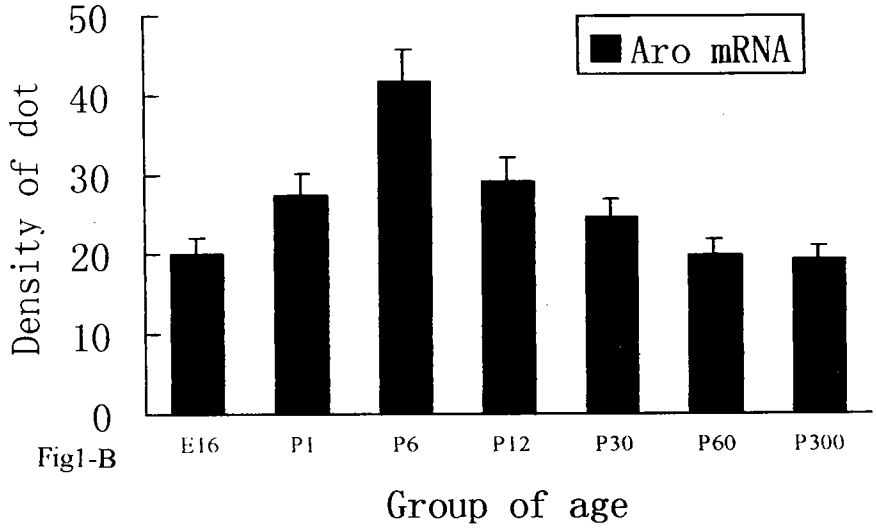


Fig1-B

***Fig1 (A, B): Expression of Aromatase mRNA in the brain of developing mouse.***

*A. Result of RNA Dot-Blotting.*

*B. Image analysis of aromatase mRNA expression during brain development. The X-axis represent the group of animals and the Y-axis represent the optic density (OD) of staining dot. The density represent the content of aromatase mRNA. It showed that the highest level of aromatase mRNA is at postnatal day 6 (P6), and the lowest level is at adulthood*

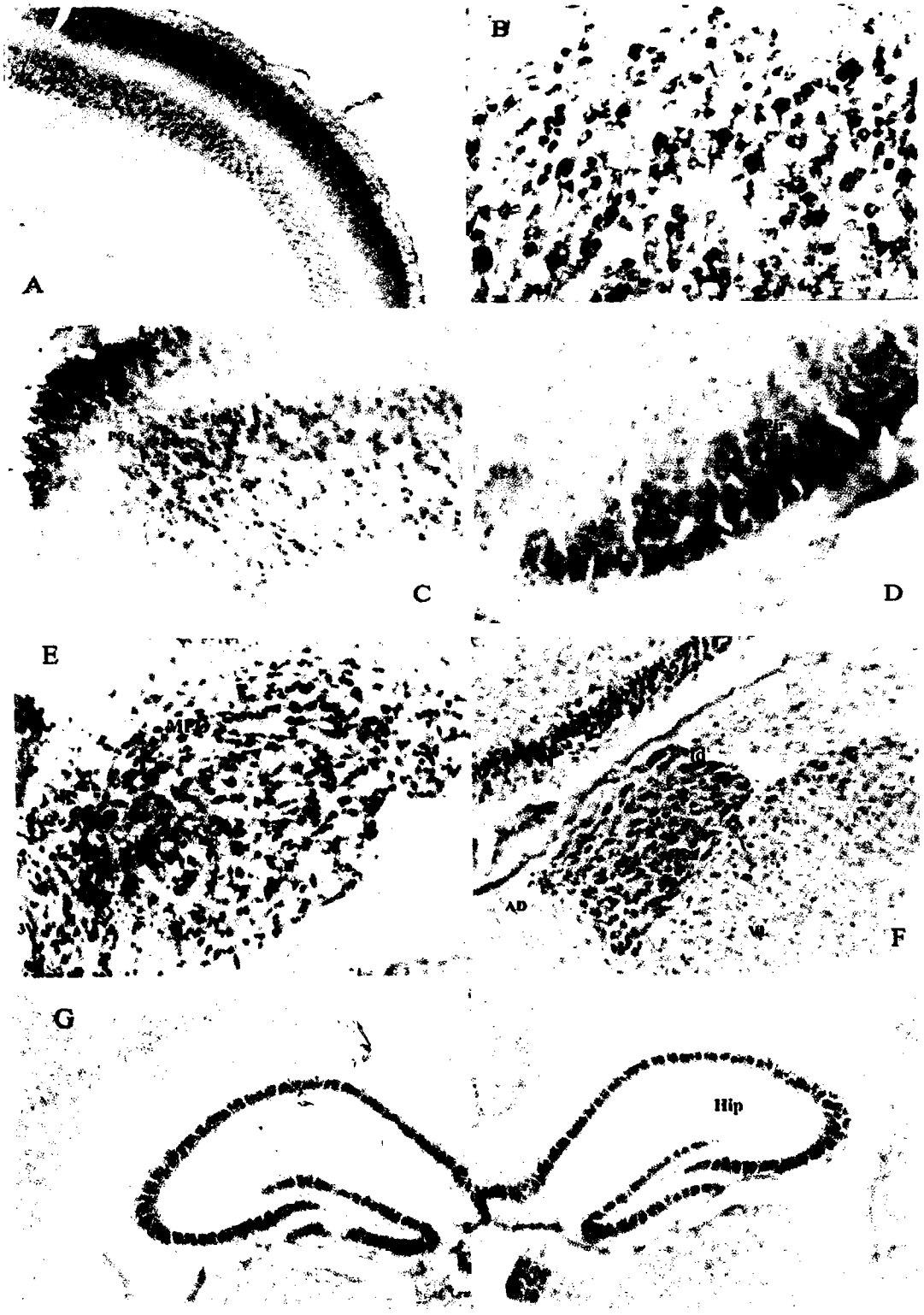


*Fig. 2 (A-G). Microphotographs of Aromatase mRNA localization in mouse brain regions at early postnatal stage (P6-P12). A. Low magnification showing the distribution of positive cells in cerebra cortex. ×40. B. Higher magnification of these cells illustrating the positive deposition of Aromatase mRNA in the perikarya and cell processes ×200. C. Heavily labeled cells in posterior cingulated cortex (PCg) ×100. D. Heavily labeled cells in prepirifom cortex (Pir), posterior part (×100). E. Heavily labeled cells in medial preoptic area (MPO). ×200. F. Moderately labeled cells in laterodorsalis thalamic nucleus (ld) ×100. G. Heavily labeled cells in pyramidal layer of hippocampus (CA1, CA2, CA3 and dentate gyrus) ×40.*

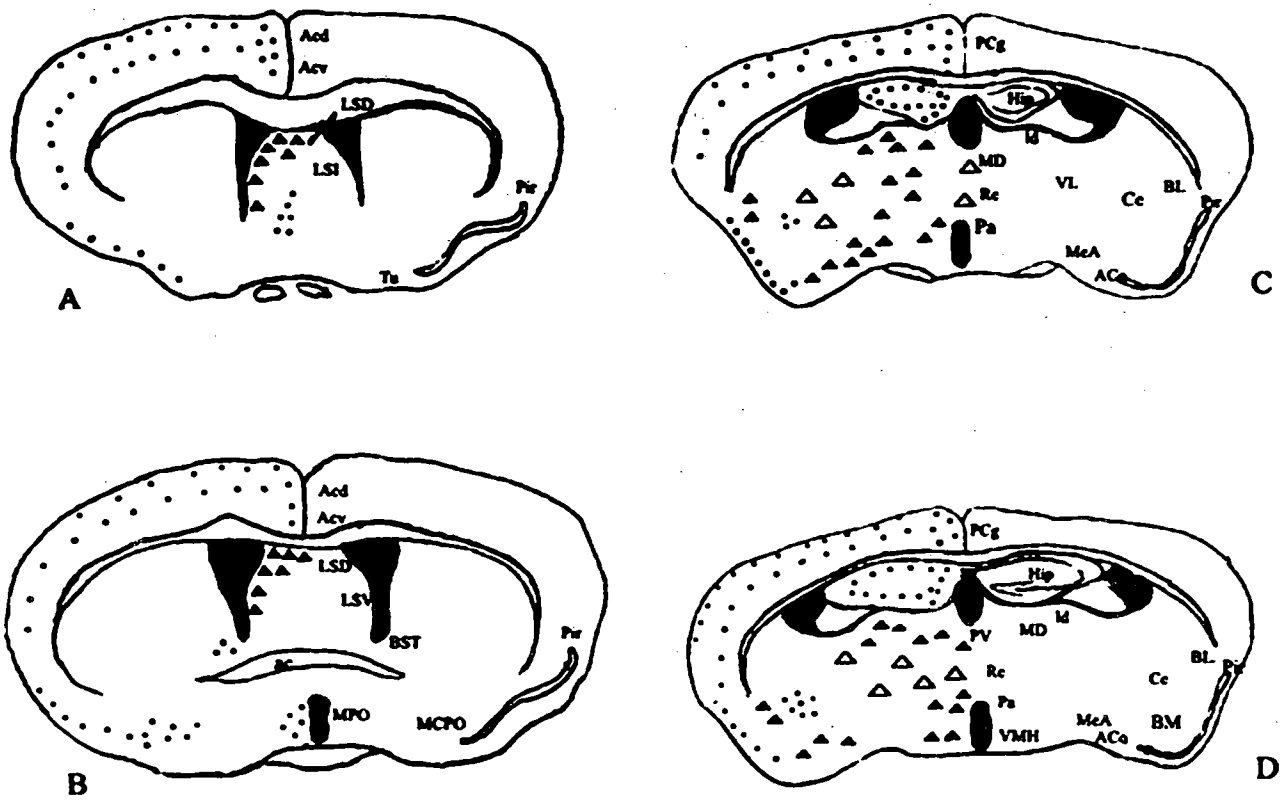


Fig3(A-D)

*Fig. 3: (A-D), The schematic drawing of four representative cross-sections through the medial septal nucleus and hipocampus showing the distribution of aromatase mRNA expressing cells in analysed brain region. Regions containing Aromatase mRNA cells are presented to the reaction intensity: strong (●), medium (▲) or weak (Δ). ac Anterior commissure; ACd anterior cingulated cortex, dorsal part; Acv anterior cingulated cortex, ventral part; Aco anterior cortical amygdaloid nucleus; BL basolateral amygdaloid nucleus; BM basomedial amygdaloid nucleus; Ce central amygaloid nucleus; Hip hippocampus; ld laterodorsal thalamic nucleus; LSD lateral septal nucleus, dorsal part; LSI lateral septal nucleus, intermediate part; MCPO magnocellular preoptic nucleus; MD mediodorsal thalamic nucleus; MeA medial amygdaloid nucleus, anterior part; MPO medial preoptic area; Pa paraventricular hypothamlamic nucleus; PCg posterior cingulated cortex; Pir piriform cortex; PV paraventricular thalamic nucleus; Re reuniens thalamic nucleus; VL ventrolateral thalamic nucleus; VMH ventral posterolateral thalamic nucleus.*

at adult (P60) and old age (P300). The same results were repeated 3 times. No staining reaction was detected in control experiment.

***Distribution of aromatase mRNA in the mouse brain at postnatal early stage***

According to the result of RNA Dot-Blotting, the high level of aromatase mRNA emerged at stage from postnatal 6 days to postnatal 12 days. So male mice at this stage (between P6 to P12) (n=5) were used to detect the aromatase mRNA distribution in the brain with in situ hybridization technique.

Figure 2 (A-G) and Fig 3 show the results about the distribution of aromatase mRNA and its schematic map.

The positive reaction for aromatase mRNA showed blue deposition in the perikarya and cell process with varying densities, cell nuclei were always devoid of staining. The positive cells were confirmed mainly as neurons on the basis of nissl-staining of adjacent sections. Main distribution of aromatase mRNA was detected in the regions of

cerebral cortex, hippocampus, thalamus, hypothalamus and large part of nucleus in limbic system.

***Thalamus and hypothalamus***

The aromatase mRNA contain cells were widely distributed. Many heavily labeled cells were found in medial septal nucleus, the medial preoptic area with varying density and many small neurites (Fig. 2-E). The moderately strong signal was present in several nuclei such as mediodorsal thalamic nucleus, laterodorsal thalamic nucleus, paraventricular hypothaloamic nucleus, ventromedial hypothalamic nucleus and etc. (Fig. 2-F). In addition, some weakly labeled cells were present in small numbers in the ventrolateral thalamic nucleus and at the edge of the adjacent reticular nucleus and some others covered an area extending from the central anterior hypothalamic area to the lateral hypothalamic and the anterior hypothalamic area.

***Limbic system***

In hippocampus, the pyramidal layer of field CA1 to CA3 of Ammon's horn and granular layer of the dentate gyrus showed a strong staining (Fig. 2-G). Many labeled cells were also detected in most parts of amygdala region, which extended laterally from the medial amygdaloid nucleus to the cortex-amygdala transition zone. The central amygdaloid nucleus showed stronger staining than the others.

Otherwise, some lightly labeled cells were detected in the island of Calleja and the caudate putamen. No positive signal was detected in the control experiment.

## Discussion

In present study, DIG-labeled aromatase riboprobe was employed in nucleic acid molecular hybridization to examine the aromatase mRNA and get some information about the pattern of aromatase gene expression during the brain development. The DIG system is one kind of comprehensive, convenient and effective systems for the labeling and detection of DNA, RNA and oligonucleoitide. It provides a more secure method for the detection and localization of nucleic acid at the cellular level than other labeling system such as the isotope labeling system. The details of the localization of aromatase mRNA and the distribution of aromatase mRNA positive cells were much more clearly shown in this study than early reports.

Nucleic acid Dot-Blotting is one kind of techniques to detect RNA or DNA quickly and simply, but it is not easy to locate and quantify. In order to get a semi-quantitative re sult, the amount of brain RNA in each group animal was fixed for detection of the aromatase mRNA. The expression of aromatase mRNA was detected with higher level at

the stage of the first two postnatal weeks, and the highest level at postnatal 6 days (P6). Then it decreased to the lowest level in adult and old animals. These data are in agreement with other reports, which showed that the level of aromatase gene expression is significantly higher during development than in adulthood [10,20]. However, there are some differences in the time of the highest level of brain aromatase mRNA expression between our results and others. For example, some reports have shown that the highest level of aromatase mRNA in the mouse brain was at postnatal 3 days and another report showed that the higher level of aromatase expression in mouse hypothalamus was at postnatal 15 days [25,26]. These differences may simply be due to the differences in method and tissue preparation in different studies. Nevertheless, recently, one report showed, by using semiquantitative reverse transcriptase polymerase chain reaction (RT-PCR) analysis, the aromatase mRNA is expressed prenatally in the mouse hippocampus of both sexes, aromatase mRNA increased during the first two postnatal weeks and decreased to lower levels in adult [27]. This data is very in agreement with our present result. With these data, we might presume that aromatase mRNA in hippocampus may be a main part of the aromatase mRNA in brain during the early stage of postnatal development and it may provide some important effort unknowable during this stage, the first two postnatal weeks.

With regard to the results of aromatase mRNA distribution in present study, aromatase mRNA positive individual cells were clearly demonstrated and large parts of them are identified to be neurons. Many cells with highly aromatase mRNA expression were found in the cerebral cortex, hippocampus, thalamus, hypothalamus and other regions of limbic system. These data agree well with measurements of enzyme activity that have been previously reported [10]. For example, in brain regions with high level of aromatase activity, such as the medial preoptic nucleus (MPO) and medial amygdala (mAMY), many cells expressing high level of aromatase mRNA were detected. In regions with relatively lower level of activity (e.g. VMN, CoAMY and some nuclei of the hypothalamus), cells with medium levels of aromatase mRNA expression were detected. However, there are some differences in the expression of aromatase mRNA and activity in some brain regions. For example, some brain regions, such as the mediodorsal thalamus and the cingulated cortex, are not yet known to contain aromatase activity, but they contained many cells expressing high levels of aromatase mRNA. In this regard, the results of the present study, agree with the reports of Wagner et al [22], may indicate new regions previously dismissed as possible areas of estrogen production.

More interestingly, the present in situ hybridization procedure has visualized large numbers of cells with high level of aromatase mRNA in some regions such as hippocampus (mostly the pyramidal layer) and various parts of the cortex, include neocortex, which was found with lower level of aromatase mRNA and weak enzymatic activity in rat and mouse by some reports [21-23], and no aromatase mRNA was indicated in monkey by other reports [28]. These differences may be due to the different sensitivity of the techniques used, or different probes and procedures

used. In addition, there may be differences in animal variety. In earlier studies, although in situ hybridization was used to examine aromatase mRNA in the brain, the probe used in each experiment was quite different. Where Lauber et al used $^{33}$P-labelled oligo nucleotides directed at both the 5' and 3' ends [21]; Wagner used $^{35}$S-labelled riboprobe transcribed from rat ovarian aromatase cDNA and the studied animal was rat [22] . The present study employed DIG-labelling riboprobe transcribed from human placental aromatase cDNA directed at the 3' end of the mRNA and immersion staining method was used, and the studied animals are mouse. So our present result demonstrated aromatase mRNA in some brain regions that were not positive in other studies. Yamada et al [29] revealed that a relatively high level of the aromatase mRNA existed in the cerebral cortex (CC) of the rat, where the aromatase activity was reported to be weak or absent. Further study found that this cortical type mRNA variant lacked exons I-III in the adult rat brain and seemed to be widely distributed in other tissues. So the aromatase mRNA detected in these regions (CC, hippocampus) might be this cortical type of mRNA. Foidar et al [30] reported that many strong aromatase immunoreactive cells were found in the pyramidal cell layer of the hippocampus and it proved that there is indeed aromatase synthesis in these regions.

Recently, knowledge of how estrogen interferes with mammalian brain function and development has broadened substantially. In the brain, estrogen is not only involved in the neuroendocrine feedback regulation at the hypothalamic and pituitary level but also in the control of motor and cognitive functions [11-13]. Cerebral cortex and hippocampus are known to be regions concerned with learning and memory. It has been reported that sex difference showed in the developing hippocampus, such as higher GAD expression and increased levels of GABA, glutamate, and aspartate in males [31,32]. On the other hand, cholinergic enzyme activities are higher in females. Gender-related differences in cell morphology and function in adult hippocampus have also been reported, including mossy fiber synapses, the dendritic morphology of granules and pyramidal neurons, the regulation of axon sprouting and proligeratin of hippocampal cells, hippocampal-dependent learning tasks as well as differences in the strategies that male and femal rats use to solve spatial navigation problems [33-36]. So the result of the present study, corresponding others [26], demonstrate that the high level of expression of aromatase in hippocampus likely to be one pathway involved in the masculinization of hippocampal structure and function.

In summary, our present work establishes that aromatase mRNA revealed an ontogenestically regulated pattern of expression. The data that higher level of aromatase mRNA emerged in the stage between P6 and P12 and distributed in regions of hippocampus and cerebral cortex suggest that the first two postnatal weeks may be a key stage for sex differences of brain, especially of hippocampal plasticity and function. Aromatase in these regions may deal with the modulation of memory and cognitive functions. Still, it is essential in future studies to understand the real physiological mechanisms.

## Acknowledgements

The authors thank Prof. Shiuan Chen, Beckman Research Institute of the City of Hope, Duarte, CA, USA for providing the plasimd pBluescripte SK (+/-) containing human placental aromatase cDNA. This research was supported by a grant of National Natural Science Foundation of China (No.39870724).

## References

1 Chen SA, Besman MJ, Sparkes RS, Zollman S, Klisak I, Mohandas T, Hall PF, Shively JE. Human aromatase: cDNA cloning, Southern blot analysis, and assignment of the gene to chromosome 15. DNA 1988; 7: 27-38.

2 Harada N, Utsumi T, Takagi Y. Tissue-specific expression of the human aromatase cytochrome P-450 gene by alternative use of multiple exons 1 and promoters, and switching of tissue-specific exons 1 in carcinogenesis. Proc Natl Acad Sci U S A 1993; 90: 11312-11316.

3 Honda SI, Harada N, Takagi Y. Novel exon 1 of the aromatase gene specific for aromatase transcripts in human brain. Biochm. Biophy Res Comm 1994; 198: 1153-1156.

4 Honda SI, Harada N, Takagi Y. The alternative exons 1 of the mouse aromatase cytochrome P-450 gene. Biochimica et Biophysica Acta 1996; 1305: 145-150.

5 Naftolin F and Maclusky NJ. Aromatization hypothesis revisited. In M. Serio (Ed.), Differentiation: basic and Clinical Aspects. Raven Press New York 1984 pp79-91.

6 Naftolin F. Brain aromatization of androgens. J Reprod Med. 1994; 39: 257-261.

7 Naftolin F, Maclusky NJ, Leranth CZ, Sakamoto HS, Garcia-Segura LM. The cellular effects of extrogens on neuroendocrine tissues. J Steroid Biochem 1988; 30: 195-207.

8 Naftolin F, Garcia-Segura LM, Keefe D, Leranth C, Maclusky NJ, Brawer JR. Estrogen effects on the synaptology and neural membranes of the rat hypothalamic arcuate nucleus. Biol Reprod 1990; 42: 21-28.

9 Hutchison JB, Beyer C, Green S and Wozniak A. Brain formation of oestrogen in the mouse: sex di-

morphism in aromatase development. J Steroid Biochem Mol Biol 1994; 49: 407-415.

10 Lephart ED. A review of brain aromatase cytochrome P450. Brain Res Rev 1996; 22: 1-26.

11 Hutchison JB. Aromatase: neuromodulator in the control of behavior. J Steroid Biochem Mol Biol 1993; 44: 509-520.

12 Fink G, Sumner BE, Rosie R, Grace O, Quinn JP. Estrogen control of central neurotransmission: effect on mood, mental state,and memory. Cell Mol Neurobiol 1996; 16: 325-344.

13 McEwen BS, Alves SE, Bulloch K and Weiland NG. Ovarian steroids and the brain: implications for cognition and aging. Neurology. 1997; 48: S8-15.

14 Balthazart J and Ball DF. New insights into the regulation and function of brain estrogen synthase (aromatase). Review, Tins. 1998; 21: 243-249.

15 Roselli CE, Horton LE and Resko JA. Distribution and regulation of aromatase activity in rat hypothalamus and limbic system. Endocrinology. 1985; 117: 2471-2477.

16 Shinoda K, Yagi H, Fujita H, Osawa Y and Shiotani Y. Screening of aromatase-xontaining neurons in rat forbrain: An immunohistochemical study with antibody against the human poancental antigen X-$P_2$ (hPAX-$P_2$). J Comp Neurol 1989; 290: 502-515.

17 Sanghera MK, Simpson ER, McPhaul MJ, Kozlowski G and Conley AJ. Immunocytochemical distribution of aromatase cytochrome P450 in the rat brain using peptide-generated polyclonal antibodies. Endocrinology 1991; 129: 2834-2844.

18 Jakab RL, Harada N and Naftolin F. Aromatase (estrogen synthetase) immunoreactive neuronsin th erat septal area. A light and electron microscopic study. Brain Res 1994; 664: 85-93.

19 Tsuruo Y, Ishimura K, Fujita H and Osawa Y. Immunocytochemical localization of aromatase-containing neurons in the rat brain during pre- and postnatal development. Cell Tissue Res 1994; 278: 29-39.

20 Lephart ED, Simpson ER, Mcphaul MJ, Kilgore MVV, Wilson JD and Ojeda SR. Brain aromatase cytochrome P450 messenger mRNA levels and emzyme actiity during prenatal and perinatal development in the rat. Mol Brain Res.1992; 16: 187-192.

21 Lauber ME, Lichtensteiger W.. Pre- and Postnatal ontogeny of aromatase cytochrome P450 messenger ribonucleic acid expression in the male rat brain studied by in situ hybridization. 1994; 135: 1661-1670.

22 Wagner CK and Morrell JT. Neuroanatomical distribution of aromatase mRNA in the rat brain: indications of regional regulation. J. Steroid Biochem. Molec Biol 1997; 61: 207-314.

23 Roselli CE, Abdelgadir SE, Ronnekleiv OK, Klosterman SA. Anatomic distribution and regulation of aromatase gene expression in the rat brain. Biol Reprod 1998; 58: 79-87.

24 Cai WQ, Wang BY. Practical Immunocytochemistry and Nucleic Acid hybridiaztion Techniques, Sichuan Science and Technique Publisheing house, Chendu, P.R. China, 1994 (in chinese).

25 Karolczak M, Kuppers E, Beyer C. Developmental expression and regulation of aromatase and 5alpha-reductase type I mRNA in the male and female mouse hypothalamus. J neuroendocrinol 1998; 10: 267-272.

26 Harada N, Yamada K. Ontogeny of aromatase messenger ribonucleic acid in mouse brain: fluorometrical quantitation by polymerase chain reaction. Endocrinology 1992; 131: 2306-2312.

27 Ivanova T. and Beyer C. Ontogenetic expression and sex differences of aromatase and estrogen receptor-mRNA in the mouse hippocampus. Cell Tissue Res 2000; 300: 231-237.

28 Abdelgadir SE, Roselli CE, Choate JV and Resko A. Distribution of aromatase cytochrome P450 messenger ribonucleic acid in adult rhesus monkey brains. Biol Reprod 1997; 57: 727-7.

29 Yamada MN, Hirata S, Kato J and Hoshi K. Expression and distribution of cortical type aromatase mRNA variant in the adult rat brain. J Steroid Biochem Mol Biol 1997; 60: 325-329.

30 Foidart A, Harada N and Balthazart J. Aromatase-immunoreactive cells are present in mouse brain areas that are known to express high levels of aromatase activity. Cell Tissue Res 1995; 280: 561-574.

31 Davis AM, Grattan DR, Selmanoff M, McCarthy MM. Sex differences in glutamic decarboxylaxe mRNA in neonatal rat brain: implications for sexual differentiation. Horm Behav 1996; 30: 538-552.

32 Davis AM, Ward SC, Selmanoff M, Herbison AE, McCarthy MM Developmental sex differences in amino acid neurotransmitter levels in hypothalamic and limbic areas of rat brain. Neuroscience 1999; 90: 1471-1482.

33 Madeira MD, Sousa N, Paula- Barbosa MM. Sexual dimorphism in the mossy fiber synapses of the rat hippocampus. Exp Brain Res 1991; 87: 537-545.

34 Juraska JM, Fitch JM, Washburne DL. The dendritic morphology of pyramidal neurons in the rat hippocampal CA3 area II. Effects of gender and the environment. Brain Res. 1989; 479: 115-119.

35 Tanapat P, Hastings NB, Reeves AJ, Gould E. Estroge stimulates a transient increase in the number of new neurons in the dentate gyrus of the adult female rat. J Neurosci 1999; 19: 5792-5801.

36 McEwen BS, Gould E, Orchinik M, Weiland NG, Woolley CS. Oestrogens and the structural and functional plasticity of neurons: implications of memory, ageing and neurodegenerative processes. Ciba Found Symp. 1995, 191: 52-66; discussion 66-73.

**Correspondence:**

Dr. Wen-qin Cai
Department of Histology and Embryology
Third Military Medical University
Chongqing, 400038
P. R. China

Fax: ++86-23-6531-8230
e-mail: wenqin@public.cta.cq.cn

*Biomed Res 2003; 14 (2): 147-150*

# Fluorescence study of motor neurons of mylohyoid muscle

**Amin A. Rufai**

Department of Anatomy, College of Medicine, King Saud University, Riyadh, Saudi Arabia.

**Key words:** Mesencephalic, trigeminal motor nucleus, fluorescence microscopy, retrograde tracer.

## Abstract

**The somatotopic organization of lower motor neurons of the mylohyoid muscle in the motor trigeminal nucleus has been determined by fluorescence microscopy and Nissl staining at Neuro-histological laboratory, College of Medicine, King Saud University, Riyadh, Kingdom of Saudi Arabia.**

**The mylohyoid muscle in twenty albino rats were injected with retrogradely transported fluorescent material DAPI-Pr. Fluorescence microscopy was performed, followed by subsequent staining of these sections with the Nissl stain, thionine.**

**The fluorescent cells were found to occupy the rostro-medial part of the ipsilateral motor trigeminal nucleus. Subsequent staining of the sections with the Nissl stain thionine confirmed the rostromedial location of the labeled cells. The entire lot of cells in this "rostro-medial subgroup" was found labeled, representing the domain area of the lower motor neurons of the mylohyoid muscle.**

**The rostro-medial subgroup of the trigeminal motor nucleus is the only one to supply the mylohyoid muscle.**

## Introduction

The motor nucleus of trigeminal nerve cytoarchitecturally is composed of dorsolateral and ventromedial divisions [1-2]. the former extending craniocaudally almost the whole extent of the nucleus while the latter localized to caudal two thirds of the nucleus [3]. The ventromedial division of the motor trigeminal nucleus along its whole craniocaudal extent provides innervation to the mylohoid muscle [4-6]. Gromysz et al [7] shift this innervation of the mylohyoid muscle to the neurons in the intermediate part of the nucleus in the rabbit. The medial position of the mylohoid motor neurons is intermingling with those described for the anterior belly of the digastric, temporalis and masseter muscles [6,8-10] Chen et al. [6] (1998) found ventromedial location for the lateral pterygoid and ventromedial part of the rostral two thirds of the motor trigeminal nucleus for the medial pterygoid muscle of the rabbit. Apart from the area for the tensor tympani muscle, very little of the motor trigeminal nucleus is exclusive for one muscle [11-12]. Do the stem neurons of the mylohyoid muscle occupy the entire medial extent of the motor trigeminal nuleus? The adopted technique shows the exact location of the motor neurons supplying the mylohyoid muscle and shows also the unlabelled cells. This is the first study of its kind carried out in the kingdom of Saudi Arabia for identification of the musculotopic organization of lower motor neurons of the mylohyoid muscle.

## Materials and Methods

The left mylohoid muscle of twenty adult Wistar albino rats was injected slowly at three different places by means of Hamilton syringe mounted on a micro-drive machine, with 10-50µl of DAPI-Pr (25% of 4'6-Diamidino-2-phenyl indole-2-HCL added to equal amounts of 5% Primuline), after resection of the anterior belly of the digastric muscle under anesthesia. Forty-eight hours after injection, the tissue was fixed in situ by perfusion through the aorta with 10% buffered formalin. The brains were removed after decapitation and kept in the buffered formalin made up with 30 % sucrose solution. The control side of the brain-stems were marked with a nick and kept for a few days in the same solution. The hindbrains were cut transversely on the freezing microtome into 8µ thick sections. All the

pontine sections were collected, mounted on gelatinized slides and examined without cover-slips under the fluorescence microscope which was fitted with an excitation filter of 365 μ wave length and showed only the fluorescing cells. All these labeled cells were immediately photographed.

In order to show the entire area of these labeled cells among the unlabeled ones, all sections containing them were charted sequentially, stained with 1% thionine, cover-slipped and photographed. The labeled cells were singled-out from the rest by virtue of their charted places and their overall shapes. This technique revealed the exact place as well as the number of the labeled versus the unlabeled cells. Level and place of the labeled cells were identified with reference to photos made of alternating Nissl (1% thionine) stained sections displaying the entire extent of the motor trigeminal nucleus.

## Results

Following injection of the mylohyoid muscle with the different amounts (10-50μl) of DAPI-Pr, only two places in the brainstem showed labeled cells, the mesencephalic trigeminal nucleus and the motor trigeminal nucleus. The ipsilateral motor trigeminal nucleus displayed a labeling pattern of its own as revealed by the successive cranio-caudal transverse sections containing these labeled cells (Fig. 1, sections H through A). As seen through the fluorescence microscope, the labeled nerve cells were filled with small granules that sparkled with a white color against a deep blue background. Except for the nucleus of the cell, the whole of the perikaryon was filled with these shiny fluorescing granules. They filled the processes of the motor cells to a variable distance, particularly the proximal segments of these processes. Microscopy revealed only those retrogradely labeled cells having their axons intact and contacting the area receiving the injected dye. Some hazy and less sparkling cells were also intermingled with the rest. No other element of the neuropil was visible.

At the level where mesencephalic trigeminal nucleus took a large dimension, the cellular mass of the medial group of the motor trigeminal nucleus was reduced. All cells of the medial patch were labeled. This indicates that the stem cells of the mylohyoid extend rostrally as far as there is still a medial group. Caudal to this level (at G in Fig. 1) the nucleus is large and the medial group became more distinct. It extended with a smaller part laterally into the ventral portion of the intermediate group. Again at this level, all cells of the medial group were labeled.

The entire cellular lot of the medial division of the nucleus at the middle third of the nucleus (corresponding to E-F of Fig. 1) is labeled following the injection of the mylohyoid muscle. No cell is spared, which would otherwise, indicate a possible overlap of this area by stem cells of other muscles occupying the medial motor division. At the level of the locus Ceruleus, which corresponds to (D and E in Fig. 1) and where the mesencephalic trigeminal nucleus starts


*Fig. 1: 1% thionine stained sections of the rat hindbrain (X10), displaying the entire extent of the motor trigeminal nucleus. The photograph shows only one half of the transverse sections only, to avoid eventual asymmetry. 1–motor trigeminal nucleus, 2–sensory trigeminal nucleus, 3–internal loop of the facial nerve, 4–fourth ventricle, 5–locus ceruleus, 6–mesencephalic trigeminal nucleus, 7-internal genu of the facial nerve, 8-reticular formation, 9-cerebellum, 10-flocculonodular lobe, 11-cochlear nucleus, 12-middle cerebellar peduncle, 13-inferior cerebellar peduncle, 14-corticospinal tract, 15-deep cerebellar nuclei, 16-abducent nerve.*

to appear, the trigeminal motor nucleus is well developed, with an appreciable size and its medial subgroup is quite distinct. This "medial subgroup" seems to be entirely specific for the mylohyoid stem cells as revealed by its the fluorescent staining material. All the cells comprising the medially located "subgroup" at the above-mentioned level i.e., at the middle of the rostro-caudal extent of the nucleus, took up the dye, leaving no cells unlabeled. The medial cellular patch of the motor trigeminal nucleus at this level represents the absolute territorial domain of the mylohyoid muscle, no other muscle is sharing or overlapping this area of the nucleus.

The most caudal level of the trigeminal motor nucleus, which showed labeled cells following the injection of the ipsilateral mylohyoid muscle, corresponds to sections C and D of Fig. 1. The motor cells lie besides the internal loop of the facial nerve. In addition to the presence of this loop, the caudality is confirmed by the exclusion of any part of the mesencephalic trigeminal nucleus that starts to appear more rostrally. The cells of the motor nucleus that appear at this level are only those of the medial "subgroup". Other cells are not quite distinct from the surrounding reticular formation. Yet under the light microscope, some cells found dorsolateral to the medial "subgroup" resemble, to an extent, those comprising this medial "subgroup", and are assumed to be the caudal part of the intermediate motor part. The medial "subgroup" is less developed than the situation at more rostral levels.

## Discussion

The fluorescence technique employed in the present study singles-out the lower motor neurons of the injected mylohyoid muscle from the rest of the motor trigeminal nucleus, and by comparison with the Nissl stain of the same sections, one can determine what proportion of the cells took up the dye. The boundaries of the "subgroup" allocated to a particular muscle are dependent on the presence or absence of spaces that separate any motor cell group from another similar group of neighboring motor cells. Contrary to other studies, which found the ventrolateral cells of the motor trigeminal nucleus labeled by retrograde injection of horseradish peroxidase into the mylohyoid [2,13-14], the present study showed it to be the medial group. The medial part of the ipsilateral motor trigeminal nucleus was identifiable by a gap free of motor cells from the rest. It looked like a circumscribed patch of cells that was known not to extend as much rostrally as the other "subgroups" of the motor nucleus [3]. The rostral part of this medial subgroup was found to be composed entirely of labeled cells, after injection of the mylohyoid with DAPI-Pr. The labeling of all cells in this group could not be due to simultaneous contamination of neighboring muscles, because the adjacent muscles, liable to contamination occupy other places within the motor trigeminal nucleus, which were found empty of labeled cells. The immediate impression is that all cells of the rostromedial patch are reserved for the mylohyoid muscle. This was confirmed by comparison with the Nissl stained photos, which showed the presence of only the labeled cells. Therefore, the stated overlap [8-9] was not substantiated by the present study, for at least the rostro-medial part of this "subgroup", and which was found entirely devoted to the mylohyoid muscle. This also confirmed the subgrouping of the trigeminal motor nucleus 1,14-16]. The two mylohyoid muscles are inseparable by virtue of their midline fusion. Their stem cells are shown to occupy the most medial aspect of their respective motor trigeminal nuclei, a fact that renders bilateral communication easier and more economical [1,17,18]. The rostral occupation of the stem cells within the medial part of the motor trigeminal nucleus is also justified. Because the two bellies of the digastric muscle, with which the mylohyoid is most associated, are the ones that shall occupy the caudal position within this medial part of the nucleus, as implied by the dual innervation of the digastric muscle by the more caudally lying facial nerve. The presented results show no contralateral labeling, which means that no contamination of the other side took place during the injection of the one side of the mylohyoid muscle. The spreading of the injected dye did not affect the underlying anterior belly of the digastric muscle because that muscle was resected, and no cells were found labeled in the caudal part of the nucleus (the domain area of the digastric muscle).

## Conclusion

The rostro-medial subgroup of the trigeminal motor nucleus is the only one to supply lower motor neurons to the mylohyoid muscle.

## References

1. Nolte J. (ed). The human brain, an introduction to its functional anatomy. 4th Ed. St. Louis: Mosby. p. 283-309, 1999.

2. Crossman AR, Neary D. (eds). Neuroanatomy, an illustrated colour text. 2nd Ed. Edinburgh: Chuchill Livingstone. p. 103-116, 2000.

3. Mizuno N, Konishi A, Sato M. Localization of the masticatory motoneurons in the cat and rat by means of retrograde axonal transport of horseradish peroxidase. J Comp Neurol 1975; 164: 105-115.

4. Sasamoto K. Nuclear representation of masticatory muscles in the rat. Jpn J physiol 1979; 29: 739-747.

5. Terashima T, Kishimoto Y, Ochiishi T. Musculotopic organization in the motor trigeminal nucleus of the reeler mutant mouse. Brain Res 1994; 666: 31-42.

6. Chen KN, Wen CY, Shieh J, Tseng TM. The somatotopy of the masticatory neurons in the rat trigeminal motor nucleus as revealed by HRP Study. Proc Natl

7. Gromysz H, Karczewski WA, Kosmal A, Kukwa A. Horseradish peroxidase localization of the mylohyoid motoneurons in the rabbit. Acta Neurobiol Exp (Warsz), 1993; 53: 421-424.

8. Uemura-Sumi M, Satoda T, Tashiro T, Matushima R, Mizuno N. Re-examination of the topographical distribution of the motoneurons innervating the digastric muscle in the rabbit and guinea pig. Anat Anz 1991; 173: 9-16.

9. Lev-Tov A, Tal M. The organization and activity pattern of the anterior and posterior head of guinea pig digastric muscle. J Neurophysiol 1987; 58: 496-509.

10. Mong FS, Chen YC, Lu CH. Dendritic ramification of trigeminal motor neurons innervating jaw-closing muscles of rats. J Neurol Sci 1988; 86: 251-264.

11. Kitamura S, Nagase Y, Nishiguchi T, Shigenaga Y. An HRP study of the location of the motoneurons supplying the tensor veli palatini muscle of rabbit. Anat Anz 1992; 174: 353-356.

12. Gannon PJ, Eden AR. The innervation of the tensor tympani muscle of the middle ear in Macaca fascicularies (cynomolgus monkey) was studied using the horseradish peroxidase (HRP) neural tracing technique. Brain Res 1987; 404: 257-262.

13. Zeman W, Maitland-Innes JR. Craigie's Neuroanatomy of the rat (Revised and expanded). Academic press London 1963.

14. Weijs WA. Functional somatotopic organization of motoneutrons supplying the rabbit masseter muscle. J Comp Neurol 1996; 364: 279-289.

15. Saad M, Dubuc R, Widmer CG, Westberg KG, Lund JP. Anatomical organization of efferent neurons innervating various regions of the rabbit masseter muscle. J Comp Neurol 1997; 383: 428-438.

16. Roste GK. None-motoneutrons in the facial and motor trigeminal nuclei projecting to the cerebellar flocculus in the cat. A fluorescent double labeling and WGA-HRP study. Exp Brain Res 1989; 75: 295-305.

17. Nicholls JG, Martin AR, Wallace BG. From neuron to brain: a cellular and molecular approach to the function of the nervous system. 3rd Edition Sinauer Associates, Sunderland Massachusetts 1992.

18. Yoshida A, Fukami H, Nagase Y et al. Quantitative analysis of synaptic contacts made between functionally identified oralis neurons and trigeminal motoneurons in cats. J Neurosci 2001; 21: 6298-6307.

**Correspondence**

Dr. Amin A. Rufai
Department of Anatomy
College of Medicine
King Saud University
P.O. Box-2925 (28), Riyadh-11461
Saudi Arabia

Phone: +9661-4672545
Fax: +9661-4671300 e
e-mail: aminu_rufai@hotmail.com

*Biomedical Research 2003; 14 (2): 151-156*

# Light microscopical details of perineuronal nets in the cerebellar cortex of the mouse revealed by means of methylene blue labeling

**Thomas Müller**

Institute for Anatomy, University of Mainz, D-55099 Mainz, Germany

**Key words:** Cerebellum, cationic dye, redox dye, extracellular substance, proteoglycans, collagenous elements, glycoproteins, surface coats

*Accepted: August 4; 2003*

## Abstract

**Light microscopic results regarding the morphology of perineuronal nets in the cerebellar cortex of the mouse achieved by means of methylene blue supravital staining are shown. Within the paraffin sections obtained from the dye-perfused tissue, an intense staining of the extracellular matrix of the molecular layer could be identified. In the granular layer, bundles of extracellular fibrillary elements were seen; they formed perineuronal nets around the Purkinje cells. These structures were also found in contact to blood capillaries. A putative association of them with glial cell perikarya could not absolutely be clarified, but appeared to be likely. The existence of perineuronal nets in the central nervous system supports some aspects of the old reticulum theory without contradicting the neuron theory, i.e. a reticular formation of extracellular matrix connects glial with nerve cells and is also associated via ankyrin and spectrin with the intracellular cytoskeleton of the cells. In conclusion, due to its selectivity for perineuronal nets, the technique used here supplement histochemistry in a helpful manner; moreover, regarding morphological details it appears to be superior compared with common histochemical procedures.**

## Introduction

Using his own silver impregnation technique, Golgi [1] described at first a delicate covering, mainly reticular in structure, which surrounds the cell bodies of nerve cells and expands along their dendrites. Later, this pericellular coat was also found by means of supravital methylene blue staining [2, 3]. In the end of the 19th century, the central point of discussion was, whether these perineuronal nets represent delicate axonal networks or nonneuronal structures; in this context, it has to be referred to an excellent review given by Celio et al [4]. In later studies applying Golgi`s silver impregnation technique, these nets were interpreted to be identical with thin processes orginating from glial cells [5]. Using the PAS-reaction for carbohydrate residues, it could be shown that these perineuronal glia nets are associated with anionic residues, i.e. carboxyl groups of acidic proteins or glycoproteins [6].

In the last decade of the 20th century, these molecules were investigated more in detail by means of lectin histochemistry and immunohistochemistry which led to a differentiation of two extracellulary located types of perineuronal nets: one of these is composed of glial cell , i.e. astrocyte, processes, whereas the other one consists of extracellular matrix molecules interposed between the tiny endfeet at the neuronal surface [4]. Manifold functions have been attributed to the perineuronal nets of extracellular matrix which include stabilization of synapses, concentration of growth factors around certain neurons, the generation of a polyanionic ion-buffering microenvironment, the formation of a link with the intracellular cytoskeleton via ankyrin and spectrin etc [4].

Regarding perineuronal nets in the cerebellum, two studies are very important: Steindler and Cooper [7] could visualize glial glycoconjugates in the cerebelum of the mouse by the application of lectin histochemistry; using different histochemical staining techniques, Mabuchi et al [8] demonstrated unequivocally the existence of perineuronal nets of proteoglycans around Purkinje cells in the cerebellar cortex of the cat.

Müller [9] introduced a new modification of the supravital methylene blue staining technique and published the first photographs of perineuronal nets of extracellular matrix around hippocampal non-pyramidal cells in mice. In a further study, the methylene blue method was combined with various other histochemical techniques for the detection of perineuronal nets [10].

The aim of the present study was to apply methylene blue labeling to the cerebellar cortex of the mouse for the detection of perineuronal nets. The results were compared with findings published using other staining methods. In addition, more details on the morphology of the stained material should be elucidated.

## Materials and Methods

General principles of animal care were applied throughout the experiments and all experiments and procedures complied with the German law on the protection of animals. Adult mice (Mus Musculus) were killed with tribromethanol. Further treatment of the tissues was carried out as described previously [9]:

Immediately after death, about 2 ml of an aqueous, 37°C warm dye solution (MB med. puriss., C.I. 52015; Chroma, Köngen, Germany) were injected into the left cardiac ventricle until the skin became blue. The dye was administered at a concentration of 20%.

After 1 h at room temperature (20°C), the cerebelli were removed, cut into approximately 1 mm-thick slices with a razor blade, and exposed to air in a moist chamber for 1 hour at room temperature (20°C). This led to a blueing of the specimens, i.e. oxidation of leuco-MB, since the dye had been primarily reduced to its colourless form in situ.

The first fixation was performed at 4°C (refrigerator) for 5 h (stock solution: 100 ml of 9% aqueous ammonium heptamolybdate solution with the addition of 9 drops of 25% hydrochloric acid and 0.9 ml 30% hydrogen peroxide). After a short rinse in distilled water, a second fixation took place for 2 h 30 min at 4°C [stock solution: 100ml of 2% paraformaldehyde and 2.5% glutaraldehyde in 0.1M phosphate buffer (pH 7.4) containing 1.8% phosphomolybdic acid and 0.1% hydrogen peroxide (final pH 5.0)]. Subsequently, the specimens were washed overnight in distilled water.

The tissues were dehydrated in 100% tertiary butanol (melting point: 25°C) for 48 h. The first alcohol change was performed after 15 min, the second after 1 h and the third after 7 h. For these three preliminary dehydration steps, phophomolybdic acid was added to the alcohol in a concentration of 0.05%. The tissues were then transferred into pure tertiary butanol. After dehydration, they were stored for 1 h in a mixture of 8 parts decahydronaphthalene (Dekalin®; Chroma, Köngen, Germany) and 2 parts methyl benzoate. Before being embedded in paraffin, they were immersed for another hour in 100% decahydronaphthalene.

20 µm-thick microtome sections were mounted on glass slides. After drying, they were deparaffinized in xylene and coverslipped with DePeX® (Serva, Heidelberg, Germany). Due to the thickness of the paraffin sections combined with the 3-dimensional structure of the perineuronal nets, it was focused and photographed in different planes. Therefore, the production of photomontages got necessary.

## Results

In the deeper regions of the slices (more than 200 µm distant from the cut surface), a selective staining of components of the extracellular matrix could be achieved (Figs. 1-5).

In the molecular layer, the extracellular matrix was found to be intensely labeled, whereas in the granular layer bundles of fibril-like structures were seen between the unstained granule cells (Fig. 1). These extracellular fibrils were observed getting contact with the Purkinje cells forming a delicate network, i.e. perineuronal net, around them. These nets could be studied in different planes (Figs. 2 and 3). Only a few small perikarya were detected to be intensely stained within the granule cell layer and white matter (Fig. 4). It could not doubtlessly be claryfied, whether the extracellular fibrillary structures were in fact associated with these cells. Moreover, the extracellular fibrils were also seen contacting blood capillaries (Fig. 5).

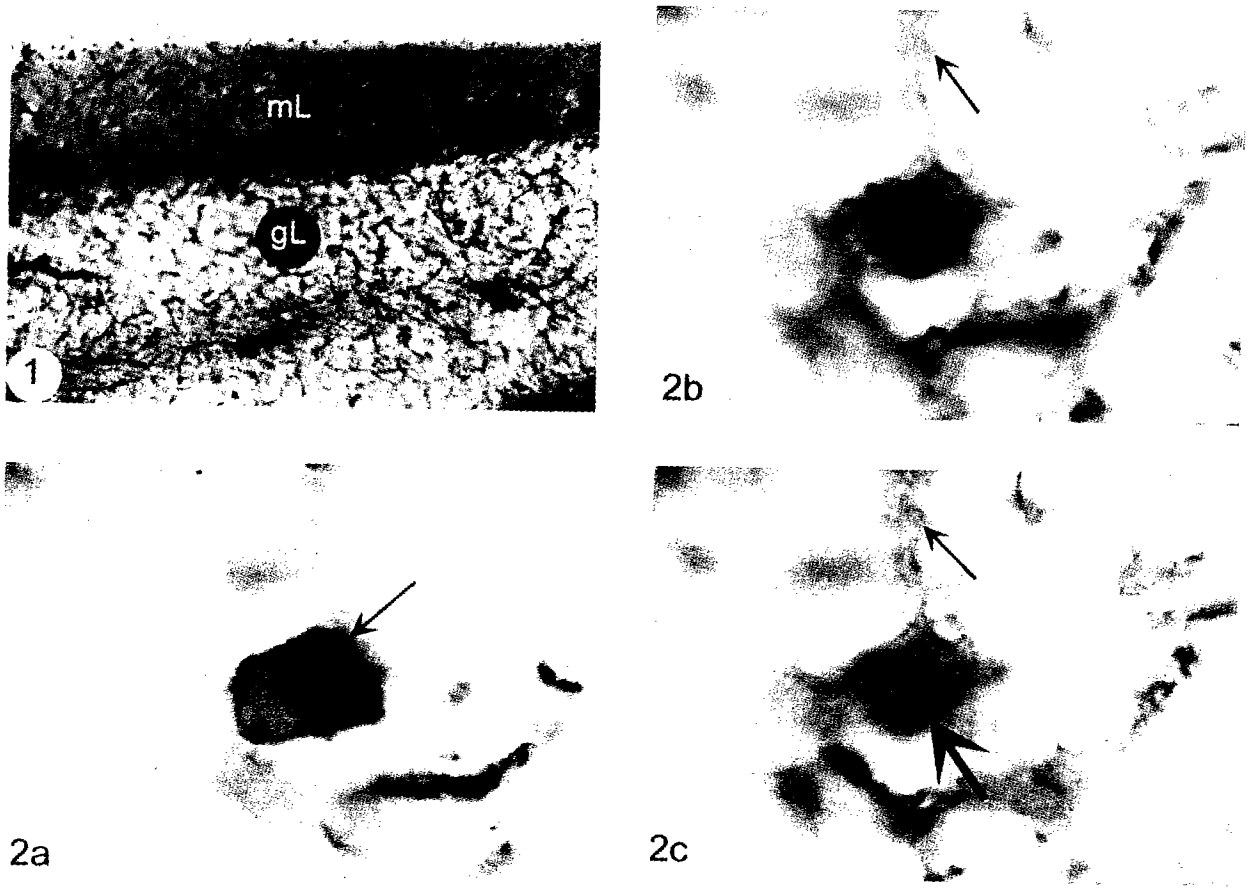


*Fig. 1*: *The overview shows the dye distribution in the molecular layer (ml) and the granular layer (gl); note that the molecular layer (ml) appears to be more intensely stained, whereas the granular layer (gl) exhibits only an inhomogenous staining caused by a labeling of fibril-like structures. x 80*

*Fig. 2a*: *A strong dye accumulation is visible in contact with the plasma membrane of a Purkinje cell (arrow). x 800*

*Fig. 2b*: *Focused in another plane, the dye accumulation is found to be connected with a bundle of fibril-like structures (arrow). x 800*

*Fig. 2c*: *Focused in a further different plane, it is verified that the dye accumulation represents a network (thick arrow) which is in continuity with the bundle of fibril-like elements (arrow) . x 800*

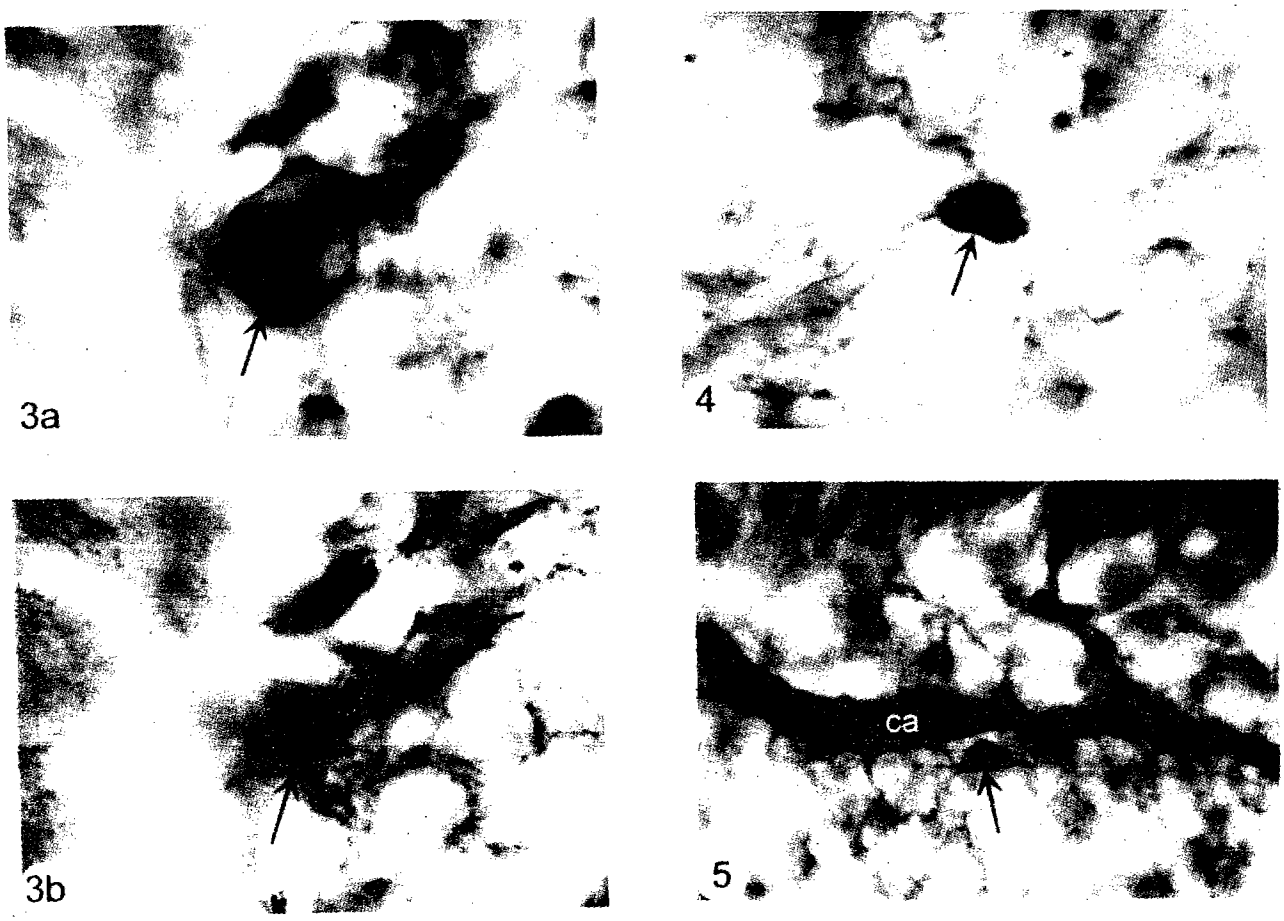


*Fig. 3a: A single Purkinje cell soma exhibits a strong labeling in the region of the plasma membrane (arrow). x 900*

*Fig. 3b: Focused in a different plane, the staining of the outer membrane represents in fact a staining of a delicate network of fibril-like structures surrounding the perikaryon (arrow). x 900.*

*Fig. 4: A small single perikaryon (arrow) within the granule cell layer appears to be associated the extracellular fibrillary elements. x 900*

*Fig. 5: Extracellular fibrils were seen contacting a blood capillary (ca) within the granular layer; note also an intensely stained small cell (arrow). x 400*

## Discussion

An important observation of the present study was the finding that perineuronal nets were not only found covering Purkinje cell bodies but were also observed extending via the intercellular spaces into the granular layer and down to the white matter.

A further interesting result was the observation that the extracellular space of the molecular layer showed a relatively intense staining; this phenomenon points to functional differences between the layers with special regard to the arrangement and composition of the extracellular matrix.

A point of special interest represents also the detected fibril-like structure of the labeled extracellular matrix. This was more clearly shown in the demonstrated methylene blue preparations than visualized by common histochemical techniques in a recent study in the cat [8]. In this context, it has to be contradicted to the opinion of Mabuchi et al [8] that in mice perineuronal nets are so thin and coarse that they cannot be sufficiently visualized under the light microscope.

Regarding the staining mechanism, the opinions differ: There is some evidence that methylene blue is reduced to its uncharged colourless lipophilic leucoform immediately before passing the blood brain-barrier followed by a subsequent reoxidation to the blue positively charged, i.e. cationic, form. This phenomenon leads to two possible binding mechanisms of the dye: Since perineuronal nets of extracellular matrix are known to be rich in strong anionic residues; these negatively-charged groups might attract the dye in its cationic form after reoxidation. The alternative would be that the perineuronal nets themselves represent sites of reoxidation, where the leucoform is oxidized to the blue form; this would mean that the perineuronal nets fulfil redox-functions. Both putative mechanism would be in accordance with the assumed neuroprotective tasks of the extracellular matrix [for review see 9]. It has to be emphasized that according to the investigations of Murakami et al [10] ligand-proteoglycans which connect the perineuronal proteoglycan surface coat with cell surface glycoproteins are considered to be the targets of the dye.

Furthermore, the observation that a subpopulation of small perikarya, probably glial cells, appear in continuity with the perineuronal nets supports the findings of Brauer et al [5]. In addition, this phenomenon is in full accordance with the results of Derouiche et al [11] achieved using lectin histochemistry combined with antiglutamine synthetase

immunohistochemistry; these findings demonstrated that N-acetylgalactosamine-containing extracellular matrix molecules and astrocytic processes are topically associated to a high degree which led to the conclusion that distal glial processes by themselves may form net-like contacts on neurons.

Moreover, it has to be pointed out that the existence of perineuronal nets in the central nervous system supports in a certain kind of manner the old reticulum theory without contradicting the neuron theory, i.e. a reticular formation of extracellular matrix connects glial with nerve cells and is also associated via ankyrin and spectrin with the intracellular cytoskeleton of the cells. However, this does not mean that axons and dendrites anastomose in a continuous network. Therefore, from the present point of view the opinion of the moderate reticularist Bethe [12] has to be confirmed; in contrast to Meyer [3], Bethe did not interpret perineuronal nets as delicate axon terminals, he attributed other properties and functions to these structures.

In conclusion, the MB-method used in the present study is highly selective, easy to handle, and visualises morphological details. In contrast to common histochemical techniques, the staining method can also successfully be applied to the mouse cerebellum. When histochemical reactivity for a specific marker or several markers is absent, the methylene blue-method may give the decisive answer whether perineuronal nets are really present or not. Therefore, this technique represents a helpful supplement to histochemistry in neuroanatomical research.

## Acknowledgement

The author is grateful to Mrs. A. de Cuvry, Institute for Anatomy, University of Mainz, for her skilled technical assistance.

## References

1. Golgi C. Sulla struttura della sostanza grigia del cervello. Gazzetta Med Ital-Lomb 1873; 6: 244-246.

2. Ramon Y Cajal S. La red superficial de las células nerviosas centrales. Rev Trim Micrográf 1897; 3: 199-204.

3. Meyer S. Ueber centrale Neuritenendigungen. Arch Mikrosk Anat 1899, 54: 296-311.

4. Celio MR, Spreafico R, De Biasi S, Vitellaro-Zuccarello L. Perineuronal nets: past and present. Trends Neurosci 1998; 21, 510-515.

5. Brauer K, Werner L, Leibnitz L. Perineuronal nets of Glia. J Hirnforsch 1982; 23: 701-708.

6. Brückner G, Gogala M, Zei M, Biesold D. Histochemical detection of anionic components in the cephalopod brain. Acta Histochem 1984, 74: 91-102.

7. Steindler DA, Cooper NG. Wheat germ agglutinin binding sites in the adult mouse cerebellum: Light and electron microscopic studies. J Comp Neurol 1986; 249: 170-185.

8. Mabuchi M, Murakami S, Taguchi T, Ohtsuka A, Murakami T. Purkinje cells in the adult cat cerebellar cortex possess a perineuronal net of proteoglycans. Arch Histol Cytol 2001, 64: 203-209.

9. Müller T. Methylene blue supravital staining: an evaluation of its applicability to the mammalian brain and pineal gland. Histol Histopathol 1998; 13: 1019-1026.

10. Murakami T, Murakami T, Sato H, Mubarak WA, Ohtsuka A, Abe K. Perineuronal nets of proteoglycans in the adult mouse brain, with special refererence to their reactions to Gömöri's ammoniacal silver and Ehrlich's methylene blue. Arch Histol Cytol 1999; 62: 71-81.

11. Derouiche A, Härtig W, Brauer K, Brückner G. Spatial relationship of lectin-labelled extracellular matrix and glutamine synthetase-immunoreactive astrocytes in rat cortical forebrain regions. J Anat 1996; 189: 363-372.

12. Bethe A. Über die Neurofibrillen in den Ganglienzellen von Wirbelthieren und ihre Beziehungen zu den Golginetzen. Arch Mikrosk Anat 1900, 55: 513-558.

**Correspondence**
PD Dr. Thomas Müller
Anatomisches Institut, Universität Mainz
Postfach 3980, Saarstr. 19-21
D-55099 Mainz
Federal Republic of Germany

Fax: + 49 6131 3925401
e-mail: tmueller@mail.uni-mainz.de

*Biomedical Research 2003; 14 (2): 157-160*

# Effect of lead acetate on wound contraction in Wistar rats

**Salah Eldin O. Elsayed**

Department of Anatomy, College of Medicine& King Khalid University Hospital, King Saud University, Riyadh, Saudi Arabia

**Keywords**: Wistar rats, Lead acetate, wound contraction, wound-healing.

*Accepted July 13, 2003*

## Abstract

**The aim of this study was to investigate the effect of lead acetate on wound contraction in male Wistar rats. A total of 30 male Witar rats were used. The experimental /test group (15-Male rats) were allowed to drink aqueous lead acetate at a concentration of 125 mg% for six months. The control group (15-Male rats) were allowed to drink aqueous sodium acetate at the same concentration for the same period. At the end of the 6 months period, serum lead concentration was measured in both groups and a full thickness skin wound of an area of one $cm^2$ was made on the flanks of the rats in the two groups. The wounds were photographed postoperatively on day one, day seven and day fourteen. The surface area of the wounds was measured using a planimeter and the results were analyzed statistically using the student's t-test.**

**At the end of the 6-month period the experimental group of rats showed a statistically significant loss of weight ($P<0.5$). The lead serum level was significantly higher in the experimental group ($P<0.5$) compared to the control group. The measurement of the wound surface areas showed that lead delayed significantly ($P<0.5$)wound contraction in the test group at day-7 and day-14 compared to the control group.**

**Lead exposure in rats can lead to loss of weight and retards wound contraction and hence delays wound healing.**

## Introduction

Widespread contamination of the environment by lead (Pb) may have an impact on human health through the constant and persistant exposure to small doses over long periods of time [1]. Lead toxicity may take various forms depending on the degree of exposure. This study was undertaken to reveal the effect of lead on wound healing. A review of the available literature showed no report on the relationship between lead toxicity and wound healing.

Lead is known to be one of the famous environmental pollutants. It is found in soil, grown food produce [2] and in drinking water in some areas [3]. Environmental exposure to toxic levels of lead occurs in a number of industries [4]. In Saudi Arabia, it was shown that the primary source of lead pollution is the motor vehicle emissions [5].

Lead in rats can suppress spermatogenesis [6] and if given simultaneously with N-nitrosodiethylamine can cause cancer of the kidney [7]. In humans lead overdose can lead to neuropathies [8].

Wound contraction is an essential component of woung healing. Its measurement is used as a method of assessing wound healing [9]. Wound contraction is mediated by myofibroblasts (specialized fibroblasts) that appear in large numbers as the wound matures and when resistance to contractile forces increases [10]. Some researchers nevertheless think that fibroblasts, not myofibroblasts, are responsible for wound contraction [11]. In rats the presence of the panniculus carnosus was found to be important for wound contraction [12].

In general, delay in wound healing due to lead toxicity, in accidental or iatrogenic wounds, can be a burden on the economies of poor countries, by lowering the output of the individuals through absence from work, specially if there is a superimposed wound infection.

## Materials and Methods

The effect of lead on wound contraction was investigated in 30 male Wistar rats weighing between 180-350 grams. The animals were housed in two groups (Test and control groups, 15 rats each) at a constant temperature of 23 degrees centigrade. They were provided with food (Number 1 maintenance diet B.P.) and water *ad libitum*, containing lead acetate for the test rats and sodium acetate for the control rats. The concentration of lead in the water was 125mg in 100 mls of water. This regime was followed daily for six months.

### *Measurements of lead concenteration in rat venous blood*

After dosing all the rats (both test and control groups) with lead orally for six months and before making the wounds, venous blood was taken from the rat tails and the concenteration of lead was measured by atomic absorption spectrophotometry [13].

### *Surgical procedure*

After six months of drinking water containing lead acetate (Test group) or sodium acetate (Control group), while rats were under general anaesthesia induced by inhalation of ether, hair was electrically clipped off from the skin of one flank, selected randomly. The shaved area was then cleaned with an alcohol- based bactericide (Hibitane). The area to be removed was first marked out with a template, and a square excised lesion, area 1 $cm^2$, was made through the flank skin with sterile, blunt-nosed, plastic surgery scissors. The lesion extended deep to the panniculus carnosus.

### *Photography*

Immediately after the surgical procedture, the wounds were photographed (Day 1) and then on the 7$^{th}$ (Day 7) and 14$^{th}$ (Day 14) day for both test and control groups. Using a New Tamaya Digital Planimeter ( Planix 7P. Tamaya Technics Incorporation), the surface area of each wound was measured three times and the average was calculated.

### *Weighing of the rats*

The two groups of rats (both test and control) were weighed at the start of the experiment and before making the wounds (i.e after 6 months).

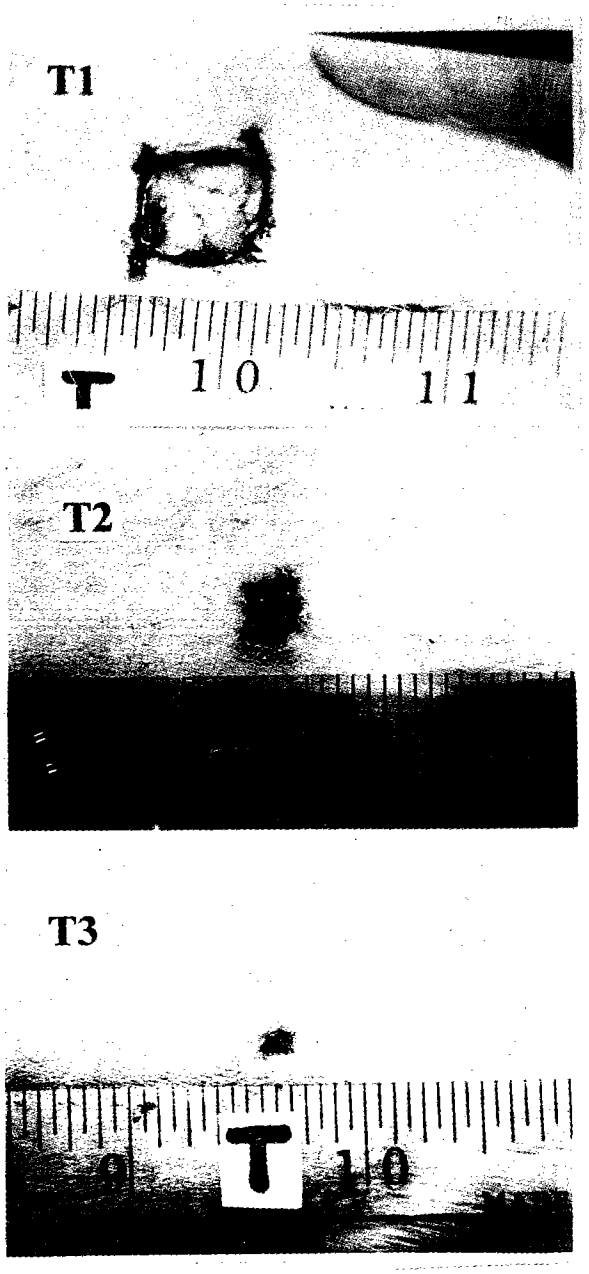


*Fig 1: Photograph showing the wound in the lead-treated rat. Day 1= T1; Day 7= T2; Day 14= T3*
*The scale shows the extent of the wound*

## Results

### *Measurements of the venous blood lead levels*

These measurements confirmed that lead level in the venous blood of the test group was higher ((P<0.5) compared to that of the control group. Mean lead venous blood level in the test rats was (1.24 =/- 0.23) micromol/L and ( 0.47+ /- 0.12) micromol/L in the control rats.

### *weighing of rats*

At the end of the six month of oral lead, the test rats looked cachexic and lethargic and there was a statistically significant loss of weight. There were also small reddish pinhead size swellings in the skin of test rats but not in the control rats. Specimens were taken for further histological investigation.

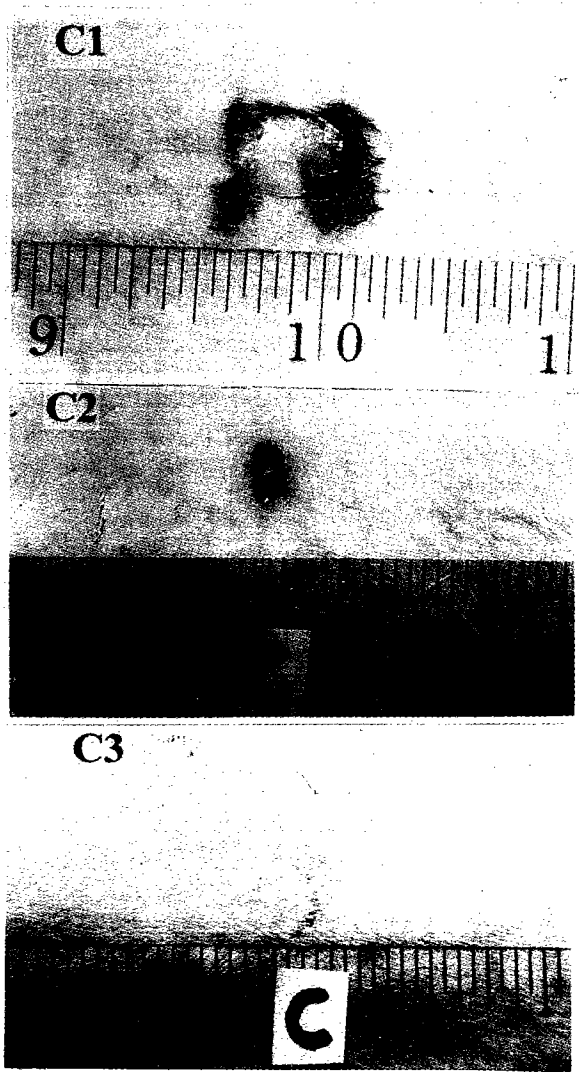


*Fig 2: Photograph showing the wound in the control rat.Day 1=C1; Day 7=C2; Day 14=C3 The scale shows the extent of the wound*

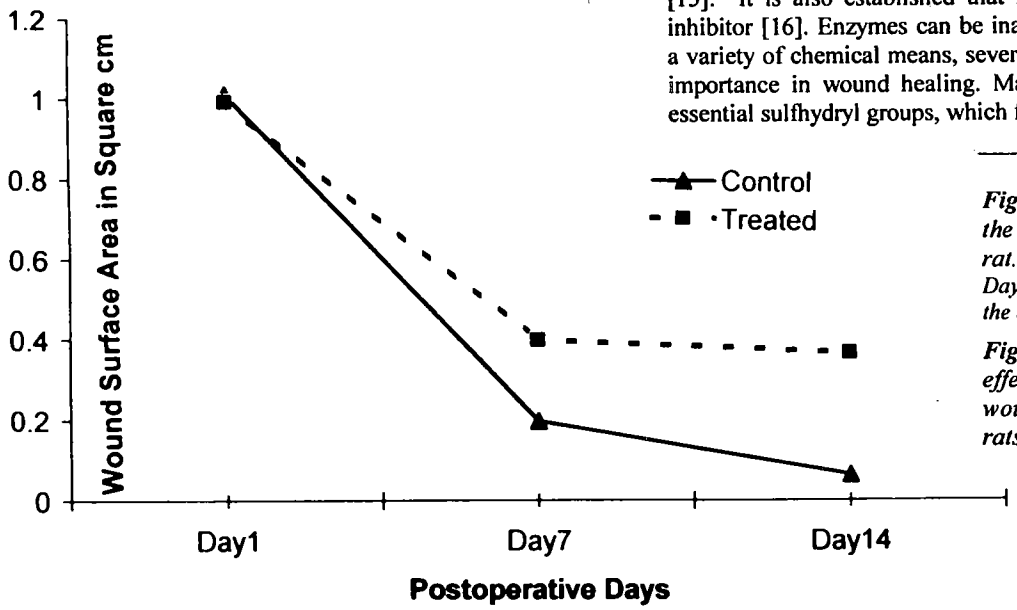


*Fig 3: Graph showing the effect of lead acetate on woundcontraction in Wistar rats*

***Measurement of surface area of wounds***

It was observed that the decrease in the surface area of the wounds of the test group was slower than the control group (Fig 1-3) at day 7 and day 14, and the difference was statistically signicant ($P<0.5$).

## Discussion

Lead compounds are mostly insoluble in water and therefore it may pollute the environment in the absence of preventive measures. About 90% of lead in the atmosphere is produced by combustion of lead containing gasoline [5]. Lead enters the body by inhalation or ingestion of contaminated material and crosses the placental barrier and poses a hazard to the developing fetus; cases of stillbirths and abortions have been reported [4]

The effect of lead poisoning on wound healing received no attention in medical research. The present study is therefore the first report in this subject and it revealed that oral exposure of lead acetate delayed wound contraction and healing in experimental rats. To verify adequate intestinal absorption of lead following oral administration of aqueous lead acetate to rats, venous blood levels of lead were measured. A surgical skin wound was then made as described earlier. It was evident that the delay in wound healing was statistically significant.

Healing of wounds is a complex process involving epidermal regeneration, fibroblast regeneration, neovascularization, synthesis and remodeling of extracellular matrix components [14]. The mechanism by which lead delays wound healing is not fully understood but it is known that the main target of lead (Pb) toxicity is the red blood cell [15]. It is also established that lead is a strong enzyme inhibitor [16]. Enzymes can be inactivated or denatured by a variety of chemical means, several of which have clinical importance in wound healing. Many enzymes depend on essential sulfhydryl groups, which form tight covalent

bonds with various heavy metals. For this reason lead can be extremely toxic. Although individual clinical cases of lead poisoning may be treated, preventive measures to minimize pollution should be undertaken to protect the population at large. Further research is required to elucidate the exact mechanism operative at molecular level, responsible for delayed wound healing caused by lead exposure.

## Acknowledgements

I would like to thank Professor Harold Amonoo-Kuofi, Dr Amin Rufai, Dr Mohammed Saeed and Dr Shakil Sadig for their technical help; Mr Akram and Mr Jameel for photography and Dr Mohammed Abdalla for reviewing this manuscript.

## References

1. Needleman HL, Bellinger D, Leviton E and Allred EN.The long-term effects of exposure to low doses of lead in childhood. The New England J Medicine 1990; 322: 83-88.

2. Counter SA, Buchanan LH, Ortega F, Amarasiriwardena C and Hu H. Environmental lead contamination and paediatric lead intoxication in an Andean Ecuadorian village. Int J Occup Environ Health 2000; 6: 169-176.

3. Kessler M, Durand PY, Hestin D, Cao Huu D, Renoult E, Prenat E, Chanliau J, Kaminski M and Duc M. Elevated body lead burden from drinking water in end-stage chronic renal failure. Nephrol Dial Transplant 1995; 10: 1648-1653.

4. Albert N and Moore K. Lead poisoning. New England Journal of Medicine 1990; 325: 1533-1537.

5. Al Saleh I. Sources of lead in Saudi Arabia. R C Bull 1992; 4: 4-12.

6. Sokol RZ. Hormonal effects of lead acetate in the male rat. Biol Reprod 1987; 37: 1135-1138.

7. Nogueira E. Rat renal carcinogenesis after chronic simultaneous exposture to lead acetate and N-nitrosodiethylamine. Virchows Arch B cell Pathol Incl Mol Pathol 1987; 53: 365-374.

8. Kajiyama K, Doi R, Sawada J, Hashimoto K, Hazama T, Nakata S, Hirata M, Yoshida T and Miyajima K. Significance of subclinical entrapment of nerves in in Lead neuropathy. Environ Res 1993; 60: 248-253.

9. Nedelec B, Shen YJ, Ghahary AScott PG and Tredget EE. The effect of interferon alpha 2b on the expression of cytoskeletal proteins in an *in vitro* model of wound contraction. J Lab Clin Med 1995; 126: 474-784.

10. Arora PD, Narani N and Mculloch CA. The compliance of collagen gel regulates transforming growth factor-beta induction of alpha-smooth muscle actin in fibroblasts. Am J Pathol 1999; 154: 871-882.

11. Ehrlich HP, Keefer KA, Myers RL, Passaniti A. Vandate and the absence of myofibroblasts in wound contraction. Arch Surg 1999; 134: 494-501.

12. Bakheit MA. An experimental study of wound contraction in wistar rats, with particular reference to the role of the panniculus carnosus (PhD thesis 1984).

13. Lubran M. Determination of Lead by Atomic Absorption Spectrophotometry. In: Laboratory diagnosis of diseases caused toxic agents.: Adam Hilger Sunderman FW and Sunderman FW Jr, eds. London; 1970; 360-365.

14. Pessa ME, Bland KI. Copeland EM III. Growth factors and determinants of wound repair. J Surg Res 1987; 42: 207-217.

15. Taupeau C, Poupon J, Nome F and Lefevre B. Lead accumulation in the mouse ovary after treatment-induced follicular atresia. Reprod Toxicol 2001; 15: 385-391.

16. Singh SP. Enzymes and Isoenzymes. In: A textbook of Biochemistry, 1st ed. Delhi (India): Satish Kumar Jain for CBS Publishers & Distributors 1993; 127-144.

**Correspondence:**

Dr. Salah Elsayed
Department of Anatomy
King Khalid University Hospital
P.O. Box-2925, Riyadh-11461
Saudi Arabia

Phone: +9661-4671301
Fax: +9661 4671300
e-mail: elsayed9@hotmail.com

*Biomedical Research 2003; 14 (1): 161-165*

# Quality of nutrition in critically ill patients

**Mojtaba Mojtahedzadeh[1], Hossein Khalili[1], Mohammad Reza Oveisi[2], Firoozeh Tavakolli[1], Mohammad Abdollahi[3]**

[1] Department of Pharmacotherapy, Faculty of Pharmacy, Tehran University of Medical Science, Tehran, Iran
[2] Department of Bromatology, Faculty of Pharmacy, Tehran University of Medical Science, Tehran, Iran
[3] Department of Toxicology and Pharmacology, Faculty of Pharmacy, Tehran University of Medical Science, Tehran, Iran.

**Key words:** Nutrition, ICU patients, APACHE, Mortality risk

*Accepted January 21 2003*

## Abstract

**Adequate nutritional support can reduce morbidity and mortality risks associated with nderlying diseases. Due to complexity of care and severity of illnesses, the critically ill patients are more susceptible to malnourishment than other patients. The objective of this study was to examine the nutritional status of patients admitted to the ICU of Sina university referral hospital in Tehran.**

**Thirty patients ( mean age of 60.08 years) were evaluated in a cross-sectional study. The amounts of calorie and macronutrients including carbohydrate, lipid, and protein given by parenteral and/or enteral route over a 14-day period were calculated. The exact need of calorie and macronutrients of patients were also determined. The acute physiology and chronic health evaluation (APACHE) score II was used to evaluate the physiologic parameters and to calculate mortality risk of patients.**

**Significant differences (P<0.001) between needed and received calorie and protein were observed. No significant difference was observed between received calorie and protein between enteral and parenteral groups. Mortality rates and risks were not influenced by the amount of calorie and protein received between surviving and non-surviving patients. Although patients in the ICU were not adequately fed there was no association with increased mortality.**

## Introduction

Although the importance of nutritional support has been knowledge for two decades, malnutrition remains one of the most serious problems in hospitalized patients. Incidence of malnutrition is about 30 to 60 percent [1]. It has been reported that almost all critically ill patients who needed mechanical ventilatory supports suffer from malnutrition. In this report, even with 14 days post hospitalization and initiation of nutritional support, 94% of patients showed some degree of nutritional deficiencies [2].

Adequate nutrition of patients in Intensive Care Unite (ICU) is very important because both under- and overfeeding in terms of macronutrients, carbohydrates, fats and protein can cause several complications. Overfeeding can lead to hyperglycemia, elevated blood urea nitrogen concentration, elevated $CO_2$ production resulting in delayed weaning from mechanical ventilation, leukopenia, reticuloendothelial system dysfunction, and decreased bacterial clearance. Underfeeding may cause increased protein turnover, increased risk for decubitus, muscle degradation, decreased resistance to infection and increased mortality in patients with Multi Organ Failure (MOF). Furthermore, inadequate administration of electrolytes, trace elements and vitamins can lead to specific problems. [3-5]

In an ICU, especially-ventilated patients need to be artificially fed by parenteral and/or enteral route. It is mostly recommended to use enteral route. Enteral Nutrition (EN) is claimed to be less expensive, safer, and more physiologically advantageous as it preserves gut barrier function. [6-8]

Calorie, protein and mineral contents of used EN solutions in the studied hospital are not specifically determined thus they can be categorized as non-standard nutritional solutions. In addition, Parenteral Nutrition (PN) solutions are expensive and not easily available. This study evaluates the nutritional status of critically ill patients admitted to the ICU.

## Methods

This was a cross-sectional study. Thirty adults ICU patients admitted to the Sina referral University hospital from mar 2001 to mar2002, who were not able to feed orally, not contraindicated for nasogastric intubation and a minimum hospital stay of 14 days, were enrolled in this study. All relevant information, patient's characteristics, history of comorbidities, reasons for ICU admission, laboratory tests and physiologic variables were recorded. The Harris-Benedict equation was used to determine patients basal energy expenditure (BEE) [9].

BEE (men) = (66.47+13.75W+5H–6.76A)
BEE (women) = (655.10+9.56W+1.85H-4.68A
Where W, H, A represent weight (kg), height (cm), and age (year)
Total energy expenditure (TEE) was calculated by multiplying BEE with stress factor:
TEE= BEE *Stress factor

The values for stress factors used were:
1-mild starvation
1.05-postoparative without complication
1.25-peritonotis
1.55-sever infection
1.45-cancer [10]

To establish the amounts of needed carbohydrates and fat, the published guidelines of American consensus statement on EN and PN were used. It is recommended that 30-50% of the amount of energy provided as carbohydrates with a maximum of 5 g/kg/24h and 50-70% in the form of fat [11]. The amount of protein intake that permit anabolism in non-stressed patients is set between 1.2-1.5g/kg/d, and in the absence of significant hepatic or renal disease this remains the goal. In the critically ill patients the optimal protein intake is approximately 1 5g/kg/d [12].

In order to determine the carbohydrate, lipid and protein contents of gavage solutions administered enterally, samples were randomly obtained from the gavage containers. To estimate actual protein content of gavage solutions, Kjeldahl method [13] was used while Soxhlet method [14] was applied for actual lipid quantifications. For carbohydrate portion, the method of Lane-Eynon was used [15]. The severity of disease was measured according to APACHE score II. To calculate the mortality risk, the following equation was considered: Ln(R/1-R) =-3.517+(APACHE II score×0.146)+(0.603 only if post emergency surgery)+ (diagnostic category weight). [16]

Ln= Logarithm neperian
R= the risk of hospital death.

Student t-test, and Pearson correlation tests were used for statistical determination of differences and correlation between variables respectively.

## Results

Baseline characteristics of the study patients are presented in Table 1. Fifty percent of patients received a combination of EN+ PN, whereas 16.6% and 33.4% of patients received only PN and EN respectively. Compared to the calculated amounts of energy per individual, all patients received less calories. In 26.7% of patients, the amount of calorie received was 25-50% of calorie needed and only 13.3% of patients received 80-95% of calorie needed. There was a significant difference between calorie need and intake ($P<0.001$).

The mean protein need of patients was 69.23±2.34 g but the mean amount received was 42.48±2.00 g. There was a significant difference between protein need and intake ($P<0.001$). Most patients received less protein than needed and only 23.3% of patients received 75-90% of protein needed. Patients on EN received more calorie and protein than parenteral route, but differences were not significant. Survived patients received more calorie and protein than non-survived, but there were not significant differences. Table 2 summarizes nutritional status of patients.

There was no correlation between percent of calorie received and APACHE difference (APACHE1-APACHE2) ($r=0.145$, $P=0.445$) or percent of protein received and APACHE difference ($r=0.043$, $P=0.820$).

Mortality risk at admission (mortality risk1) and 2 weeks later (mortality risk2) were 48.07±4.24% and 45.10±5.75% respectively. There was not correlation between percent of calorie received and mortality risk difference (mortality risk2-mortality risk1) ($r=0.004$, $P=0.984$) and percent of protein received and mortality risk difference ($r=0.048$, $P=0.801$).

## Discussion

This study showed that all patients warded at ICU were underfed . Patients received only 59.7% of calorie and 57.5% of protein needed. The mean calorie required was 35 kcal/kg whereas the mean amount of intake was 20 kcal/kg.

In the present study the Harris-Benedict calculation was used for measurement of calorie need. It has been reported that in 28% of patients, the calculated amount of energy by Harris-Benedict was lower than the measured energy expenditure by indirect colorimetry. [5]

According to another report, total energy expenditure of critically ill patients rises from 25 and 31 kcal/kg/d in the first week to 47 and 59 kcal/kg/d in the second week in sepsis and trauma respectively [17].

Concerning physiology, economic and mortality, EN is thought a preferred route of nutrition delivery [18-19].

*Table 1. Baseline characteristics of study population (n=30)*

| Characteristic | Frequency | Percent | Mean (range) |
|---|---|---|---|
| Age (years) | - | - | 60.03 (18-88) |
| Sex (female) | 10 | 33.3 | - |
| Hight (cm) | - | - | 171 (150-190) |
| Weight (kg) | - | - | 71 (60-90) |
| APACHE II at admission | - | - | 25 (18-32) |
| APACHE II 2 weeks later | - | - | 23 (10-39) |
| Mortality risk at admission | - | - | 48.07 (13-91) |
| Mortality risk 2 wees later | - | - | 45.10 (6-96) |
| Reason for admittance: | | | |
| Surgical | 12 | 40 | - |
| Medical | 18 | 60 | - |
| Comorbidity | | | |
| CVA | 10 | 33.3 | - |
| Trauma | 5 | 16.7 | - |
| Endocrine | 3 | 10 | - |
| COPD/Asthma | 2 | 6.7 | - |
| GI | 3 | 10 | - |
| Neurological | 5 | 16.7 | - |
| Cardiac | 1 | 3.3 | - |
| Lymphoma | 1 | 3.3 | - |

*Table 2: Nutritional status of patients*

| Parameters | Requirement | Intake |
|---|---|---|
| *All patients (n=30)* | | |
| Calorie | | |
| Carbohydrate | 2346.33±81.23 kcal | 1401.33±11.10 kcal |
| Lipid | 474.23±25.48 g | 261.60±20.63 g |
| Protein | 80.70±3.90 g | 65.14±3.49 g |
| | 69.23±2.34 g | 42.48±2.00 g |
| *EN group (10 patients)* | | |
| Calorie | 2232.50±98.91 kcal | 1452.81±47.41 kcal |
| Carbohydrate | 436.00±29.52 g | 251.40±15.07 g |
| Lipid | 83.15±5.14 g | 62.73±5.93 g |
| Protein | 72.50±2.38 g | 45.96±3.05 g |
| *PN group (5 patients)* | | |
| Calorie | 2193.00±164.90kcal | 995.00±173.49 kcal |
| Carbohydrate | 453.20±61.58 g | 163.20±38.02 g |
| Lipid | 75.80±9.40 g | 46.80±9.70 g |
| Protein | 69.20±3.48 g | 37.60±6.40 g |
| *EN+PN group (15 patients)* | | |
| Calorie | 2473.33±136.84kcal | 1503.13±77.70 kcal |
| Carbohydrate | 512.73±41.71 g | 301.20±34.37 g |
| Lipid | 80.70±6.52 g | 54.86±4.73 g |
| Protein | 67.06±4.27 g | 41.80±2.75 g |
| *Survived patients* | | |
| Calorie | 2348.68±117.63kcal | 1447.00±119.37kcal |
| Carbohydrate | 470.89±32.13 g | 267.47±29.87 g |
| Lipid | 82.70±4.95 g | 59.06±4.77 g |
| Protein | 67.68±3.40 g | 40.12±2.63 g |
| *Not-survived patients* | | |
| Calorie | 2342.27±95.00 kcal | 1322.45±86.07 kcal |
| Carbohydrate | 480.00±43.08 g | 251.45±24.00 g |
| Lipid | 77.22±6.50 g | 51.09±4.66 g |
| Protein | 71.90±2.48 g | 46.50±2.76 g |

*EN and PN represent enteral nutrition and parenteral nutrition respectively.*

It has been shown that EN reduces the nosocomial infection risk, hospital stay, risk of MOF and Systemic Inflammatory Response Syndrome (SIRS) [20]].

There is also evidence that the incidence of inadequate nutritional intake in EN patients is higher when compared with parenteral group (78% versus 25%) [21]. In this study patients given PN and EN received EN+PN received more calorie than those treated enteral or parenteral alone.

Using Therapeutic Intervention Scoring System (TISS) for determination of correlation between severity of illness and nutritional status in studied patients, it has been shown that on admission to ICU, 57% of patients are well-nourished and 43% malnourished. Mortality in well-nourished and malnourished patients is 20 and 31% respectively [22].

Patients who had greater APACHE and mortality risk scores also showed higher mortality rate. No significant relationship was found between nutrition status and mortality risk.

It has been shown that only depleted energy (but not other nutritional and anthropometrics parameters) indirectly relates with survival in ICU children [23].

The influence of nutrition on reducing mortality rate in patients with APACHE score between 10-15 has been reported [24]. Regarding patients outcome, adequacy of nutritional support had no benefit on reduction of illness severity.

A large difference was observed between needs and received calorie and protein, however with regard to the effects of non-nutritional factors, no significant relationship between calorie/protein and patients mortality were observed.

ICU patients are in hyper-metabolic state and would have much higher protein-calorie requirements. Since protein-rich formulations of parenteral solutions are expensive and are not easily available, dextrose solutions are solely used in most cases without supplementary protein for nitrogen balance purposes, thus patients on PN received less protein than EN group.

## Conclusions

For enteral nutrition, standard solutions with defined quantities of calorie, protein and micronutrients must be considered and present house- or hospital-made formulations do not seem to be appropriate for utilization in ICU. Calorie and protein amount of these solutions are not defined and they may be infected by microbes.

## References

1. Allison SP: Malnutrition, disease and outcome. Nutrition 2000; 16: 590-594.
2. Huang YC: Malnutrition in the critically ill patients. Nutrition 2001; 17: 745-746.
3. McMahen MM: Nutritional support of critically ill patients. Mayoclinic Proceedings 1993; 68: 911.
4. 25th Clinical Congress of American society for parenteral and enteral nutrition, January 21-24, 2001, Chicago, Illinois. Nutrition 2001; 17: 983-996.
5. Jansen MMPM, Heymer F, Leusink JA, deBoer A: The quality of nutrition at an intensive care unit. Nutr Res 2002; 22: 411-422.
6. Berger MM, Chiolero RL, A Pannatior, CayEux MC, Tappy LA: 10-year survey of nutritional support in a surgical ICU: 1986-95. Nutrition 1997; 13: 870-877.
7. Webster NR, Galley HF: Nutrition in critically ill patients. J. R. Coll. Surg. Edinb. 2000; 45: 373-381.
8. Frost P, Bihari D: The route of nutritional support in critically ill: physiological and echonomical considerations. Nutrition 1997; 13: 594-600.
9. Cheng CH, Chen CH, Wong Y, Lee BY, Kan MN, Huang YC: Measured versus estimated energy expenditure in mechanically ventilated critically ill patient. Clin Nutr 2002; 21: 165-172.
10. Rippe JM, Irwin RS, Alpert J, Fink MP: Intensive Care Medicine. 2nd ed. Little, Brown and Company USA 1991; 1669-1670.
11. Applied nutrition in ICU patients, a consensus statement of the American Collage of Chest Physicians. Chest 1997; 111: 769-778.
12. Grenvik A, Ayres S, Holbrook PR, Shoemaker WC: Textbook of Critical Care. 4th ed. W.B.Saunders Company, Philadelphia. 2000; 903-904.
13. Anglov T, Peterson IM, Kristiansen J: Uncertainly of nitrogen determination by Kjeldahl method. Accred Qual Assur 1999; 4: 504–510.
14. deCastro MDL, GarcõÂa-Ayuso LE: Soxhle extration of solid materials: an outdated technique with a promising innovative future. Anal Chim Acta 1998; 369: 1-10.
15. Sartini RP, Oliveira CC, Zagatto EAG, Filho HB: Determination of reducing sugars by flow injection gravimetry. Analytic Chemica Acta 1998; 366: 119-125.
16. Lemeshow S, Gall JR Le. Modeling the severity of illness of ICU patients. A system update. JAMA 1994; 272:1049-1055.

17. Griffiths RD: Nutrition in intensive care: give enough but choose the route wisely. Nutrition 2001, 17: 54-57.

18. Velasco N, Hernandez G, Wainstein C, Castillo L, Maiz A and et al: Influence of polymeric enteral nutrition supplemented with different doses of glutamine on gut permeability in critically ill patint. Nutrition 2001; 17: 907-911.

19. Finck C: Enteral versus parenteral nutrition in the critically ill patients. Nutrition 2000; 16: 393-394

20. McClave SA, Mallampalli A: Nutrition in ICU, part 1: enteral feeding, when and why? J. Crit. Illn. 2001, 16(4): 197-204.

21. Woodcock NP, Zeigler D, Plamer MD, Buckley P, Mitchell CJ, Macfic J: Enteral versus parenteral nutrition: a pragmatic study. Nutrition 2001, 17: 1-12.

22. Ginre M, Laviano A, Meguid MM, Gleason AR: In 1995 a correlation between malnutrition and poor outcome in critically ill patients still exist. Nutrition 1996; 12: 23.

23. Briassoulis G, Zavras N, Hatzis T: Malnutrition, nutritional indicces, and early enteral feeding in critically ill children. Nutrition 2001, 17: 548-557.

24. Galban C, Monteyo YC, Meseyo A, Marco P, Celaya S and.et al: An immnu-enhancing enteral diet reduces mortality rate and episodes of bacterimia in septic ICU patients. Crit. Care Med. 2000, 28: 643-648.

**Correspondence to:**

Dr. Hossein Khalili
Department of Pharmacotherapy
Faculty of Pharmacy
Tehran University of Medical Science
Tehran
Iran.

*Biomedical Research 2003; 14 (2): 166-170*

# The toxicity, mutagenicity and carcinogenicity of formaldehyde used in histology and histochemistry: A review

**A.A. Ngokere[1*] and P.M. Ofordile[2]**

[1]Department of Morbid Anatomy, University of Nigeria Teaching Hospital, Enugu, Nigeria

[2]Department of Medical Laboratory Sciences, College of Medicine, University of Nigeria Enugu Campus, Enugu, Nigeria

**Key words:** Formaldehyde, Toxicity, Mutagenicity, Carcinogenesis

*Accepted 07 May, 2003*

## Abstract

**Formaldehyde still remains the most widely used fixative for histological and histochemical work. This also remains the main component of embalming fluid. Unfortunately, formaldehyde is hazardous to health. It is, therefore, advisable to appropriately inform the users of this reagent regarding the recent findings bearing on its toxicity. In this review, a survey of published data on its toxic nature is presented.**

## Introduction

Formaldehyde is a gas, which is soluble in water to approximately 40 percent by weight. This saturated solution is available commercially as a 40 percent formaldehyde, or formalin. Formaldehyde prepared as 10 percent solution in physiological saline still remains the most widely used fixative for routine histological, cytological and histochemical work. However, formaldehyde compounds are harmful and therefore require careful handling.

It has been well established that formaldehyde reacts with the amino groups of proteins [1] in a pH dependent manner leading to the formation of cross-links between the molecules eventually via methylene bridges giving rise to an insoluble product. Formaldehyde has been shown to react rapidly with phosphatidyl ethanolamine causing degradation of the compound. Phospholipids, while not 'fixed' by formaldehyde, may be prevented from diffusing into the fixing fluid by the addition of calcium [2,3] or cobalt [4] without affecting their solubility in lipid solvents. Formaldehyde has little effect on free carbohydrates but it does fix glycoproteins. Formalin also favours the staining of acidic structures with basic dyes and diminishes the effect of acid dyes on basic structures [5].

Formaldehyde exposure is most common through gas-phase inhalation. However, it can also occur through liquid-phase skin absorption. Workers can be exposed during direct production, treatment of materials and producing of resins. Health care professionals, pathology and histology technicians and students who handle preserved specimens are potentially at high risk. At levels to which humans may be exposed adverse effects are most likely to be observed primarily following inhalation [7]. It has been shown experimentally that effects on humans are more closely related to concentration than to the accumulated total dose, this is due to the rapid metabolism, high reactivity and water solubility of formaldehyde [8]. Dermal exposure predominantly affects the skin itself and little, if any formaldehyde reaches the blood stream. There is a relatively large exposure to formaldehyde from ingestion of food, but most of it is present in a bound form [9].

Most books on histological and histochemical methods merely state that these reagents are 'toxic' to the skin, without stressing on their spectrum of harmful effects[6]. Most laboratory workers, mortuary staff and other users of formaldehyde and its mixtures are not informed about the dangers of exposure to these reagents. Aside from the previous work of Bulo [6], literature on the hazardous effects of formaldehyde and its mixtures is also scant or non-existent, particularly in this part of Nigeria.

In this paper, the authors intend to highlight the toxic, mutagenic and carcinogenic effects of formaldehyde.

***Review of toxic effects of formaldehyde***

Bulo [6] has shown that formalin has an irritant vapour which may injure the nasal mucosa and cause sinusitis. Dermatitis may be caused upon prolonged contact of skin with formaldehyde. Sugiura et al [10] succeeded in creating a uniform, reproducible hardened lens nucleus and an anterior capsule in a pig by injecting the lens with mixture of formalin and alcohol. Allergic dermatitis has been demonstrated from direct skin contact. In addition are varied forms of reactions ranging from simple erythema to maculopapular lesions, hyperesthesia, and angioneuretic edema. Inhalation causes varying degrees of interstitial inflammation of the lungs, thus, airborne formaldehyde is an irritant producing tissue damage and regenerative hyperplasia at the site of entry and it possesses genotoxic activity, inducing DNA protein cross links also at the site of entry. Focal chronic inflammatory changes develops in the heart and kidney depending on the length of exposure [11].

Shelley [12] reported that formaldehyde induces asthma in individuals that are well exposed to it. The investigator also reported photosensitivity in a 48 year old man who experienced pruritus, burning and redness of the skin within minutes of exposure to sunlight. In most studies, formaldehyde alone or in combination with other agents caused transient, reversible declines in lung function, but there was no evidence that formaldehyde induces chronic decrement in lung function. There are a few case reports of asthma-like symptoms caused by formaldehyde but none of these demonstrated a sensitization effect and the symptoms were considered to be due to irritation [13]. The works of Liden et al [14] did not support the hypothesis that specific IgE antibodies are active in the pathogenesis of contact sensitization.

In a previous work (unpublished data), we observed centrolobular necrosis and mononuclear cell infiltration of the liver parenchyma as well as renal tubular necrosis, hyalinization, glomerular loss due to severe necrosis and interstitial infiltration by mixed inflammatory cells in rabbits exposed to formaldehyde fumes for 30 days.

Discrimination between genotoxicity and cytotoxicity for the induction of DNA double-strand breaks in cells treated with aldehydes and diepoxides has been achieved [15]. These authors investigated the time-dependent dose response relationships for the induction of DNA double-strand breaks (DSB) assessed by pulsed-field gel electrophoresis (PFGE) and for viability in order to discriminate between genotoxic and cytotoxic mechanisms of DNA fragmentation. Volk et al treated cultured human lung epithelial cells (i) with formaldehyde and (ii) with the DNA-DNA interstrand crosslinkers melphalan, diepoxybutane or diepoxyoctane and DNA fragmentation was checked. It was suggested that formaldehyde treatment induced double strand break implicating the activation of DNA degrading enzymes.

Tang et al [16] have found that the DNA damage of human leukemia (HL–60) cells was caused by methyl tert- butyl ether (MTBE), a new gasoline additive, and its metabolites, tert-butyl alcohol (TBA), a hydroxyisobutyric acid (HIBA) and formaldehyde, with release of lactate dehydrogenase as an indicator for evaluating its cytotoxicity. Their results showed that MTBE, TBA and HIBA at levels of 1 to 30 mmol/L could cause DNA damage, in a dose-dependent pattern and that formaldehyde at level 5 mmol/L could cause DNA damage but at a higher level could decrease DNA migration. Dukes [17] found that formaldehyde may cause genotoxicity by a dual mechanism of directly damaging DNA and inhibiting repair of mutagenic and carcinogenic DNA lesions by other chemical and physical carcinogens. In addition to DNA protein cross-links, formaldehyde induces breaking of DNA single strand, chromosomal aberrations, sister chromatids exchange, gene mutations and cell transformation in human cells in vitro.

International Agency for Research on Cancer reported the possibility that formaldehyde induces pathological or cytogenic changes in the nasal mucosa which has been examined in people exposed in occupational settings like the laboratory, mortuary, and chemical industry resulting in squamous cell metaplasia and mild dysplasia of the respiratory epithelium and micronuclei in mucosal cells. The Agency, however, also reported that there were no conclusive data showing that formaldehyde is toxic to the reproductive system or to developing fetuses in humans. Contact uticaria has also, but rarely, been associated with exposure to formaldehyde. Cases have been reported in a nonatopic histology technician, and a worker in a pathology laboratory [18,19]. However, there are no conclusive data showing that, formaldehyde is toxic to the immune system. Pross et al [20] concluded that long-term exposure to formaldehyde had not affected the six immune parameters measured, but that short term acute exposure resulted in a minor immunological changes. No IgE mediated sensitization could be attributed to formaldehyde [21].

Formaldehyde in very high concentration has been reported as a potent carcinogen. Short term exposure can be fatal, symptoms are often more severe at the start of exposure than after minutes or hours, when they gradually diminish. However, the odour threshold is low enough that irritation of the eyes and mucous membranes will occur before these levels are achieved. Long term exposure to low levels of formaldehyde may cause respiratory difficulty, eczema and sensitization[8]. The cytotoxicity of formaldehyde, a monomer released from certain polymeric dental materials, has been studied in cultured human oral fibroblasts and epithelial cells [22]. The influences of growth conditions were evaluated for both cell types, as well as the role of the internal and external thiol states. The authors noted that a one-hour exposure to formaldehyde decreased the colony-forming efficiency (CFE) of both cell types in a concentration dependent manner, although the toxicity varied up to 100-fold with the conditions. It was

then concluded that the combined use of a controlled external milieu and the presumed target cell type may be advantageous in evaluations of oral toxicity mechanisms or the toxic potency of dental materials, particularly those which, like formaldehyde, may react with thoils or amines.

The effect of environmental pollutants, diesel exhaust particles (DEP) and formaldehyde (FA), on the production of pro-inflammatory cytokines by normal human dermal keratinocytes (HKCS) has been investigated [23]. Having incubated normal HKCS with various concentrations of DEP, the authors determined cytokine production by enzyme-linked immunosorbent assay (ELISA). They found that DEP (20μg/ml) induced 1L-β production without altering cell growth. They also observed that although FA alone did not stimulate the production of 1L- 1β or 1L- 8 and 1L – 1β production respectively, in cells stimulated with phorbol 12-myristate 13 acetate (PMA). Their findings suggest that environmental pollutants may act as modulating factors of cutaneous inflammation by affecting the ability of keratinocytes to release pro-inflammatory cytokines.

Di Felice and Lambardi[24] applied a paraformaldehyde preparation (Toxavit) to an inflamed and symptomatic pulp of the mandibular right first molar, in a 30-year-old woman. They noted that the leakage from the product was responsible for marked necrosis of the gingival and the alveolar cortical bone, which resulted in loss of the tooth, concluding that formaldehyde induced tooth decay.

*Mutagenic Effect of Formaldehyde*

The mutagenic effects of FA have been compared in DNA repair-proficient (heterokaryons of Neurospora crassa[25]. The data from their experiments with the DNA repair-deficient strain H-59 demonstrate that comparable concentrations of FA cause more pronounced inactivation of heterokaryotic conidia and, at the highest concentration tested, about a 35-fold higher frequency of adduct-3 mutations resulting from multilocus mutation in H-59 than in H-12. The workers concluded and it is this class of FA- induced adduct-3 that might be most expected to show deleterious heterozygous effects, adding that the implications of their experiments with Neurospora are that the mutagenic effect of FA might well vary in different human population subgroups. Several reports have shown that paraformaldehyde- containing zinc oxide-eugenol cements in particular, such as Endomethasone and $N_2$, are antibacterial. On the otherhand, it has been found that endodontic materials with strong antimicrobial activity are frequently mutagenic, i.e. primarily those which release formaldehyde. Geurtsen and his colleague have shown that, in general, formaldehyde-containing zinc oxide-eugenol cements are classified as extremely cytotoxic, whereas most calcium hydroxide ($Ca(Co)_2$ – based sealers are rated as possessing good or excellent cytocompatibility but warned that sealers with inferior biocompatibility, such as formaldehyde-releasing materials, should no longer be applied in practice because safer altermatives are available.

Chronic inhalation of toxic concentrations of MTBE has been shown to cause renal tubular cell neoplasms in male Fischer 344 rats and hepatocellular adenomas in female CD-1 Mice [26]. Mennear has observed that neither MTBE nor its metabolite, t-butyl alcohol, possess mutagenic potential in vitro and a second metabolite, FA, is mutagenic in vitro but in vivo results are equivocal. The 1980 report that inhaled formaldehyde induced nasal squamous cell carcinomas in rats and had a significant societal impact and resulting in an excessive research in the fields of rodent nasal pathology and human cancer risk assessment [27]. In the case of formaldehyde, Morgan recommended that low-concentration (< or = 2 ppm airborne exposure) extrapolation, where no tissue damage is observed, be uncoupled from the responses at high concentration (> or = 6 ppm), where epithelial degeneration, regenerative cell replication, and inflammation appear to be essential driving forces in formaldehyde carcinogenesis, stating that the presence of treatment- related nasal lesions in rats following exposure to chemicals should always be treated as an indication of a potential human, oral or dermal route.

Among methanol and its metabolites, formaldehyde has been found to have the strongest inactivating effect on the activity of alpha- antitrypsin preparation and inhibitor existing in blood serum [28]. Skrzydlewska and his colleague have shown that the influence of formaldehyde on the activity of serum alpha 1-antitrypsin is lower in comparison with purified inhibitor and that alpha 1-antitrypsin modified by formaldehyde inactivates the trypsin in its action on the BAPA to a smaller degree than on the hemoglobin. The effective formaldehyde concentration in the case of BAPA was found to be 64mM, and in the case of the hemoglobin was about 256 mM.

Chemicals including FA, and certain arsenic compounds have been shown to produce DNA-protein cross-links in human in vitro cell systems at high doses, such as those in the cytotoxic range [29]. Excluding paraformaldehyde and 2-furaldehyde treatments, significant increases in DNA-protein cross-links were observed by the authors at doses that resulted in complete cell death within 4d following dosing with FA. Their work demonstrates that DNA-protein cross-links can be formed in vitro following exposure to a variety of industrial compounds. Titenko-Holland et al [30] found that FA caused micronucleus formation and that the primary mechanism of micronucleus formation appeared to be chromosome breakage, concluding that this finding is consistent with known clastogenic properties of FA, the component of embalming fluid most likely responsible for micronucleus induction. Formaldehyde has been shown to produce metaplastic and dysplastic stages of the nasal epithelium as well as using starting values of cell proliferation to stimulate a tissue growth process [31]. Normal tissue renewal and progressive transitions between normality and hyperplasia after exposure to formaldehyde have been obtained [31].

***Precautionary measures***

For tissue fixation in histology laboratories and other embalming centers, staff should be made aware of the hazardous effects of FA as highlighted in the text. Formalin gives off an unpleasant vapour that causes irritation to the eyes and respiratory epithelium, particularly distressing to some individuals. For this reason, some system of forced ventilation should be a feature of any room used for the dissection of formalin-fixed tissues and all containers should be provided with well fitting, corrosion-resistant lids. In addition, rubber gloves or an efficient barrier cream should be worn when handling formalin-fixed material, for while some workers appear to be immune from its effects, others will suffer an 'unpleasant formalin dermatitis' after immersion of the hands in this solution. Concentrated acid formalin should not be treated with magnesium or calcium carbonate as the consequent release of carbondioxide has been shown to be responsible for a serious explosion in the laboratory.

Commercial formalin is usually acidic due to the formic acid content which is present either as an impurity or as a result of oxidation of the FA. For this reason, it should be made neutral or slightly alkaline prior to its use as a fixative which can be achieved by the use of calcium acetate. The use of neutral or slightly alkaline formalin fixatives results in a marked increase in the frequency with which ferric ion can be demonstrated and an almost complete absence of the formation of formalin pigment.

When preparing and handling aqueous padding emulsions incorporating Epikete 821, the usual precautionary measures recommended for using FA resin should be taken to minimize skin vapour contact. Goggles and face shields, rubber protective clothing and gloves are essential where there is possibility of contact with padding solutions or where accidental splashing may occur. The workroom should be kept clean, breathing of vapours should be avoided. Exhaust fans and air conditioners should be installed in cut-up, post mortem and embalmment rooms to remove excess formalin fumes in circulation. Be sure that FA solutions are clearly labeled with the chemical's name and hazards. As with any laboratory chemical, do not mouth pipette FA solutions. Do not eat, drink or smoke where FA is handled, processed or stored since it can be swallowed. Always wash hands thoroughly after its use, even if gloves are worn. Store FA in labeled, chemically compatible containers, away from heat and flame. Always place large volume containers on a low, protected shelf or in another location where they will not be accidentally spilled or knocked over.

Formaldehyde has been observed to be a potential mutagen and carcinogenic, hence it is necessary to ensure that the safcty precautions outlined above are strictly adhered to so as to minimize the rate and level of exposure to FA. Laboratory and mortuary workers should periodically be screened through cytological evaluation of nasal squamous epithelial cells for early detection of cancer.

## Acknowledgement

The authors gratefully acknowledge the secretarial assistance of Mr. Dan Ugwu.

## References

1 Calling CFA. Hand book of Histopathological and Histochemical Techniques: Reagents employed as fixatives. 3rd ed. London: Butherworth & co (Publishers) Ltd. 1974; P. 37.

2 Baker JR. Structure and chemical composition of Golgi Element. Quarterly Journal of Microscopical Science, 1944; 85: 1.

3. Lillie RD. In Histopathological Technic and practical Histochemistry. 3rd ed. New York: Blakiston, 1965.

4 McManus JF. A. Histological demonstration of mucin after periodic acid. Nature (London) 1946; 158: 202..

5 Drury RAB; Wallington EA. Cameron, R. Carleton's Histological Technique: Formaldehyde. 4th ed. London: Oxford University Press, 1976 pp. 35-36.

6 Bulo AN. The toxicity of some reagents used in electronmicroscopy and Histochemistry. Nig J Med Lab Tech 1974; 11: 19-22.

7 Main DM; Hogan TJ. Health effects of low level exposure to formaldehyde. Journal of occupational Medicine 1983; 25.

8 Bancroft JD; Stevens A. Theory and Practice of histological techniques. 4th ed. Churchhill Livingstone, New York. 585, 1996.

9 Restani P et al. Formaldehyde and hexamethylenetramine and food additives chemical interactions and toxicology. Food additives and contaminants. 1992; 9.

10 Suguira T; Kirosaka D, Uezuki Y, Eguchi D, Obata H, Takahashi T. Creating cataract in a pig eye. J Cataract Refract Surg 1999; 255: 615-621.

11 Coon RA et al. Animal inhalation studies on ammonia, Ethylene glycol, formaldehyde Dimethylamine and Ethanol. Toxicol Appl Pharmacol 1970; 16. 652 Academic Press, New York.

12 Shelley WB. Immediate Sunburn-like reaction in a patient with formaldehyde photosensitivity. Arch Dermatol 1982; 117.

13 WHO. Formaldehyde. Environmental Health Criteria. No 89. Geneva. 1989.

14 Liden S et al. Absence of specific IgE antibodies in allergic contact sensitivity to formaldehyde. Allergy 1993; 48.

15 Volk EH, Lutz WK, Hinskaya O, Vamvakas S. Discrimination between genotoxicity for the induction of DNA double-strand breaks in cells treated with aldehydes and diepoxides Mutat Res 1999; 441: 85-93.

16 Tang G, Wang J; Zhuang Z.Cytotoxicity and genotoxicity of methyl tert butyl ether and its metabolite to human leukemia cells. Chung Hua Fang 1 Hsueh Tsa Chih 1997; 31:334-337.

17 Dukes MNG. Meyler's side effects of drugs. 12th ed. Elsevier Amsterdan, London. 569, 1992.

18 Rappa Port BZ, Hoffman MM. Uticaria due to aliphatic aldehydes. J A M A 1941, 116.

19 Lindskov F. Contact Uticaria to formaldelyde contact dermatitis. 8, 1982.

20 Pross JF *et al.* Immunologic Studies of subjects with asthma exposed to formaldehyde and urea formaldehyde foam insulation of products. Journal of Altergy and Clin Immunol 1987; 79.

21 Kramps JA *et al.* Measurement of specific IgE antibodies in individuals exposed to formaldehyde. Clinical and Experimental Allergy 1989; 19.

22 Nilson JA, Zheng X. Sundqrist K, LiuY, Atzori L, Elfwing A; Arvidson K, Crafstrom RC. Toxicity of formaldehyde to human oral fibroblasts and epithelial cells: influences of Cultural conditions and role of thiole Status. J Dent Res 1998, 7711: 1896- 1903.

23 Ushio H; Nohara K, Fujimaki H. Effect of environmental Pollutants on the production of Pro-inflammatory cytokines by normal human dermal Keratinocytes. Toxicol Lett. 1999; 1051: 17-24..

24 Di Felice R, Lombardi T. Gingival and mandibular bone necrosis caused by a paraformaldelyde- containing paste. Endod Dent Traumatol1998; 144: 196-198.

25 De Serres FJ, Brockman HE. Comparison of the Spectra of genetic damage in formaldelyde-induced adduct – 3 mutations between DNA repair-Proficient and- deficient heterokaryons of Neurospara Crassa. Mutat. Res. 1999; 4372: 151- 163. Mennear JH. Carcinogenicity Studies on MTBE: Critical review and interpretation. Risk Anal 1997; 17: 673- 681.

26 Morgan KT. A brief review of formaldelyde carcinrgenesis in relation to rat nasal Pathology and human risk assessment. Toxicol. Pathol. 1997; 25: 291-307.

27 Skrydlewska E, Mielc Zarska J. Influence of Methanol and its metabitutes on the activity of alpha 1 – antitrypsin. Alcohol 1997; 14: 295-2995.

28 Costa M; Zhitkovich A, Harris M, Paustenbach D, Gargas, M. DNA- protein cross-links produced by various chemicals in cultured human lymphoma cells. J Toxicol Environ Health 1997; 50: 433-449.

29 Titenko-Holland N, Levine AJ, Smith MT, Quintana P. J, Boeniger M, Hayes R et al. Qualification of epithelial cell micronuclei by fluorescence in situ hybridization (FISH) in mortuary science students exposed to formaldehyde. Mutat Res 1996; 371: 237-248.

30 Clem CJ, Konig D, Rigant JP. A three- dimensional dynamic simulation model of epithelial tissue renewal. Anal Quant Cytol Histol 1997, 19; 174-184.

**Correspondence to:**

Dr. A.A. Ngokere
Department of Morbid Anatomy
University of Nigeria Teaching Hospital
Enugu,
Nigeria

*Biomedical Research 2003; 14 (2): 171-178*

# Morphometric analysis of the lumbar intervertebral foramina in Saudi population

**Amin A. Rufai**

Department of Anatomy, College of Medicine, King Saud University, Riyadh. Saudi Arabia

**Key words:** Lumbar spine, intervertebral canal, spinal nerve, anatomy

## Abstract

**Morphometric estimation of the vertical and transverse diameters of the lumbar intervertebral foramina (IVF) of normal Saudi population was done at King Khalid University Hospital, Riyadh, Saudi Arabia.**

**The plain anteroposterior radiographs of 600 lumbar spines of normal Saudi population were analyzed for measurements of vertical and horizontal diameter of intervertebral foramina with the help of a digitizing Tablet connected to a microcomputer.**

**The vertical diameters of lumbar intervertebral foramina varied from 26.2 mm to 17.2 mm in males and 25.6 mm to 16.3 mm in females, whereas the horizontal diameter was 17.5 mm to 9.2 mm in Saudi males and 16.1 mm to 8.1 mm in Saudi females. The least recorded vertical diameter was observed at $L_5/S_1$ in all age groups especially those above 50 years.**

**The vertical diameter of IVF increased rapidly at an early age in females as compared to males. The least vertical and horizontal diameters of IVF at $L_5/S_1$ level in +50 age group predisposes old people to the frequently observed symptoms of low back pain. The present study provides an insight to the Physicians, Surgeons, Anatomists and Physiotherapists about the anatomy of lumbar IVF, necessary for the interpretation and treatment of the low back pain, lumbar foraminectomy and reconstruction procedures employed for the burst fractures.**

## Introduction

The intervertebral foramen (IVF) is the principal route of entry and exit from the vertebral canal [1]. It is bound superiorly and inferiorly by the pedicles of the adjacent vertebrae, whereas the anterior boundary is formed by the posterior margin of the vertebral bodies and the intervertebral disc [2]. The posterior boundary consists of the pars interarticularis, ligamentum flavum and superior articular process of the vertebra below [3]. The lumbar intervertebral foramina are shaped like an inverted teardrop, and lie between the two principal lines of attachment of the psoas major muscle [4]. The walls of each foramen are covered throughout by the collagen of periosteal, perichondral, annular or capsular origin [2]. Each segmental spinal nerve is the chief content passing through the corresponding lumbar IVF and may be affected by trauma, prolapsed intervertebral disc, or the many disorders of the tissue bordering the foramen, i.e., the compact bone of pedicles, the capsules, synovial membranes, articular cartilages, fibroadipose meniscoids or fat pads of the synovial zygapophyseal joints [5]. Foraminal stenosis of the lumbar spine and compression of a spinal nerve within an IVF is one of the distant feature of the lateral spinal stenosis [5].

The dimensions of the intervertebral foramina, however, change constantly during daily activity [7-9]. Therefore the symptoms in patients with spinal stenosis are aggrevated or relieved by the posture of their lumbar spine [10=12]. Various methods has been employed in the past for estimation of the diameters of IVF and lumbar vertebral canal, however, radiographic estimation of interpedicular distance is considered to be a reliable technique [2,11]. As the age related and racial variations of intervertebral foraminal diameter have been documented by various authors [11-17], hence the present study was designed to present a brief report on the morphometric variations of the lumbar IVF in Saudi population.

## Materials and Methods

Plain antero-posterior radiographs of the lumbar spines of 600 subjects (300 males, 300 females) with ages ranging from 10 to 70 years, were studied. Radiographs were selected from the medical records of patients who had attended the Accident and Emergency unit of the King Khalid University Hospital, Riyadh, from January 2000 to December 2002, with history of suspected recent injury to the spine, and in whom no bony injury was found. A standardized technique was used in taking radiographs, using the same radiographic equipment and putting the patients in the recumbent position. The X-ray beam was centered on the 3rd lumbar vertebra and directed at 90 degrees to the film. An anode-film distance of 100 cm was maintained. The magnification resulting from the use of this technique was negligible. All films were screened for readability and certified to be free from spinal pathology by a diagnostic radiologist.

### *Selection of subjects*

Care was taken to exclude individuals with a history of back pain over the past 12-month period or patients receiving treatment for back pain. Other exclusion criteria included: (1) history of surgery for disorders related to the vertebral column; (2) history of growth disorders; (3) history of systemic bone disease; (4) history of chronic renal disease; (5) history of malabsorption; (6) evidence of scoliosis, kyphosis or other spinal pathology. Male and female subjects were grouped separately into 5 age groups. Each age group spanned 10 years. Subjects aged above 50 years were grouped together as 50+ years. The age and sex distribution of the sample are shown in Table 1.

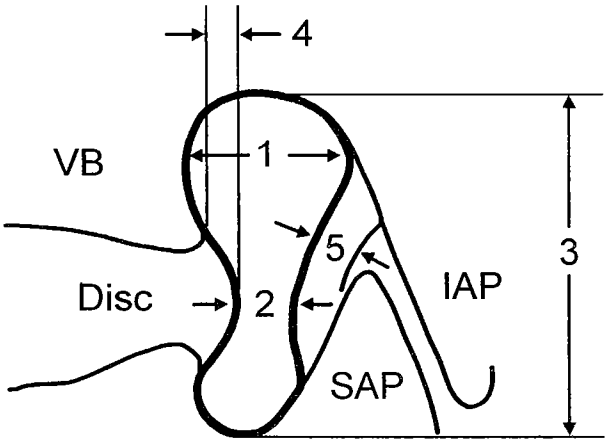


*Table 1: Distribution of sample according to age and sex.*

| Groups | Age (years) | Males (n) | Females (n) |
|---|---|---|---|
| A | 10-20 | 60 | 60 |
| B | >20-30 | 60 | 60 |
| C | >30-40 | 60 | 60 |
| D | >40-50 | 60 | 60 |
| E | >50+ | 60 | 60 |

*n-Number of subjects*

*Fig. 1: Schematic representation of the lumbar IVF showing landmarks used for measurements of the intervertebral foramen diameters: (1-Maximum Horizontal diameter; 2-MinimumHorizontal diameter; 3- Maximum vertical diameter; 4-Disc bulging; 5- Thickness of ligamentum flavum; IAP-inferior articular process of the vertebra above; SAP-superior articular process of the vertebra below; VB-vertebral body).*

### *Measurements*

Intervertebral foramen (IVF) diameters were measured in two mutually perpendicular planes, (1) and (3) (Fig.1). The vertical diameter (3) was taken as the maximum dimension of the IVF in the sagittal plane. At the lower lumbar levels, the plane of the vertical diameter was oblique, with the upper end nearer the midline than the lower. The horizontal diameter (1) was the maximum diameter in a plane at right angles to the vertical diameter. Pencil marks were first placed on the limits of the IVF. Distances were then measured by means of a digitizing Tablet connected to a microcomputer. All measurements were made by the author. Each radiograph was measured twice, at separate sittings, the second measurement serving as a check on the first. The right and left intervertebral foramina were measured at each vertebral level. The marks were completely erased from the films between measurement to avoid bias during the second reading.

### *Statistical analysis*

The mean (horizontal and vertical) diameters, standard errors of the means (SEM) and standard deviations (SD) of the diameters of the intervertebral foramens of all the lumbar vertebrae ($L_1$ to $L_5$) were calculated (separately for males and females) using the computer. Differences between the mean diameters of the intervertebral foramina of males and females belonging to the various age groups were tested by means of a 2-way analysis of variance (2 factor factorial ANOVA) in a completely randomized design, with vertebral level as a covariate. Multiple 2-tailed t- test was used in combination with ANOVA to test the differences between individual mean diameters. 95% confidence limits of the mean diameters were calculated for all age groups at all levels.

## Results

The mean vertical and horizontal diameters of the intervertebral foramina between $L_1$ and $S_1$ in Saudi population are tabulated in Tables 2-3. There were significant differences (P<0.001) between the mean diameters of the intervertebral foramen of males and females at all levels in most age groups (Tables 2,3).

***Table 2: Mean vertical diameter (mm) of the intervertebral foramina in Saudi population.***

| Level | Sex | Age groups (years) 10-20 | >20-30 | >30-40 | >40-50 | >50 |
|---|---|---|---|---|---|---|
| $L_1/L_2$ | M | 21.9 (2.75) | 24.7 (1.9) | 24.3 (0.4) | 24.3 (2.3) | 21.1 (1.1) |
| | F | 22.6 (2.5) | 20.8 (0.8) | 23.4 (1.6) | 22.9 (1.9) | 21.3 (2.7) |
| $L_2/L_3$ | M | 23.0 (1.3) | 25.4 (2.3) | 25.5 (1.6) | 25.2 (3.4) | 24.6 (1.7) |
| | F | 23.5 (2.4) | 22.9 (1.9) | 25.0 (1.4) | 24.4 (3.3) | 22.7 (2.3) |
| $L_3/L_4$ | M | 22.5 (2.5) | 25.5 (1.4) | 24.3 (1.4) | 25.6 (2.4) | 26.2 (1.7) |
| | F | 24.7(1.1) | 24.8 (2.4) | 25.6 (1.2) | 24.1 (2.0) | 22.4 (3.5) |
| $L_4/L_5$ | M | 21.0 (1.9) | 24.7 (1.9) | 25.0 (1.6) | 24.6 (1.6) | 22.1 (2.5) |
| | F | 23.4 (1.0) | 24.5 (1.5) | 25.4 (1.5) | 22.0 (1.0) | 20.4 (3.2) |
| $L_5/S_1$ | M | 17.2 (1.6) | 20.9 (2.3) | 20.2 (2.7) | 18.2 (1.6) | 18.2 (3.3) |
| | F | 22.4 (2.2) | 18.2 (1.7) | 22.2 (2.1) | 19.8 (1.4) | 16.3 (1.1) |

*Standard deviations in parentheses* *(P < 0.001)*

***Table 3: Mean horizontal diameter (mm) of the intervertebral foramina in Saudi population.***

| Level | Sex | Age groups (years) 10-20 | >20-30 | >30-40 | >40-50 | >50 |
|---|---|---|---|---|---|---|
| $L_1/L_2$ | M | 15.4(1.4) | 16.3(1.6) | 16.0(1.0) | 15.7(1.3) | 17.5(1.1) |
| | F | 15.0(1.7) | 15.3(0.6) | 14.9(1.2) | 16.1(1.3) | 14.9(1.1) |
| $L_2/L_3$ | M | 14.8(1.7) | 16.3(2.0) | 15.4(1.3) | 15.3(1.0) | 16.4(1.0) |
| | F | 14.6(1.1) | 13.6(1.1) | 15.6(1.3) | 15.4(1.5) | 14.9(1.0) |
| $L_3/L_4$ | M | 14.1(1.5) | 15.0(1.1) | 13.2(1.6) | 14.0(1.0) | 14.5(1.6) |
| | F | 12.9(1.4) | 12.5(1.1) | 15.4(1.3) | 13.9(1.5) | 13.8(1.0) |
| $L_4/L_5$ | M | 12.1(1.3) | 12.6(1.3) | 12.2(1.1) | 11.6(1.0) | 14.2(1.0) |
| | F | 12.7(1.0) | 12.5(1.6) | 13.9(1.6) | 11.9(1.7) | 11.1(1.6) |
| $L_5/S_1$ | M | 9.2(1.6) | 10.0(1.0) | 9.9(1.3) | 9.4(1.1) | 12.1(1.1) |
| | F | 10.7(1.0) | 10.6(1.3) | 10.3(1.2) | 10.9(1.4) | 8.1(3.3) |

*Standard deviations in parentheses(P < 0.001)*

### Vertical diameters

The vertical diameters of lumbar intervertebral foramina varied from 26.2 mm to 17.2 mm in males and 25.6 mm to 16.3 mm in females (Figs. 2-3). It was maximum at $L_2/L_3$ and $L_3/L_4$, however it decreased caudally in all age groups. The least recorded vertical diameter was observed at $L_5/S_1$. The vertical diameter of $L_5/S_1$ increased gradually to a maximum value in first three decades of life, however it was minimum in +50 years age group.

### Horizontal diameter

The horizontal diameter of lumbar intervertebral foramina varied from 17.5 mm to 9.2 mm in Saudi males and 16.1 mm to 8.1mm in Saudi females (Fig. 4-5). It increased with age up till the age of 30 years, remained almost constant in next two decades, and then slowly declined. The maximum horizontal diameter was recorded in upper two lumbar intervertebral foramina, whereas minimum values were found at $L_5/S_1$ level, in all age groups especially those over 50 years.

## Discussion

Each lumbar spinal nerve ensheathed in the dural sleeve traverses through an osteo-ligamentous tunnel, known as lumbar spinal nerve root canal, in the lateral recess of the vertebral canal [10-19]. This lumbar spinal nerve root canal or intervertebral canal has funnel shaped entrance and an oval exit foramen known as intervertebral foramen [19]. The IVF is the main route of exit of all spinal nerves, which might be irritated or compressed in various patholo-

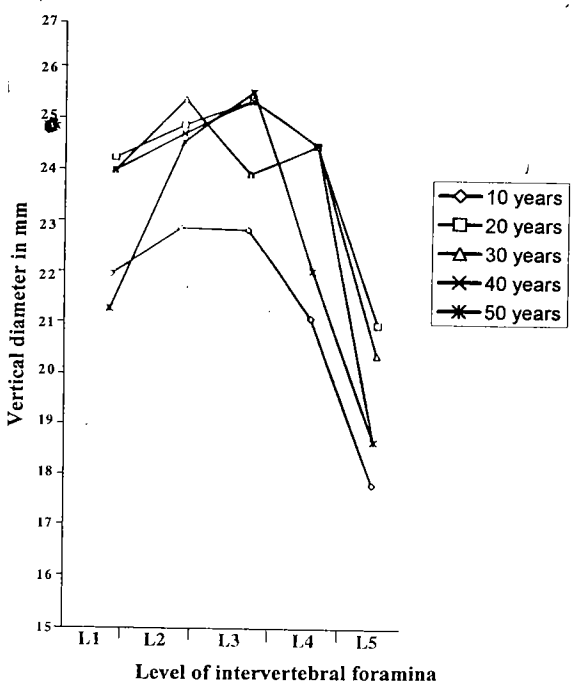


*Fig. 2: Age-related changes in the vertical diameter of the lumbar intervertebral foramina in Saudi males*

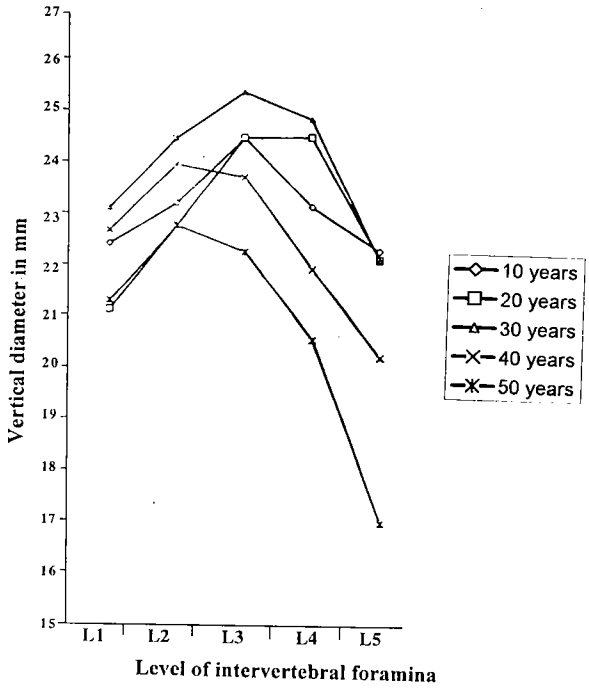


*Fig. 3: Age-related changes in the vertical diameter of the lumbar intervertebral foramina in Saudi f males*

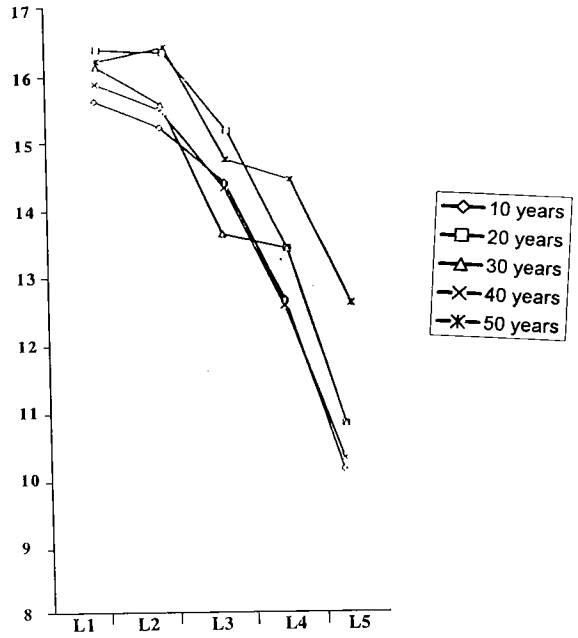


*Fig. 4: Age-related changes in the horizontal diameter of the lumbar intervertebral foramina in Saudi males*

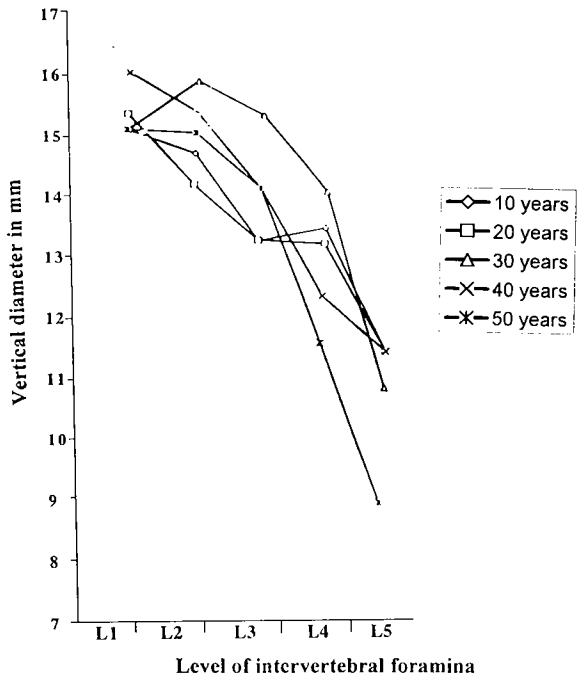


*Fig. 5: Age-related changes in the horizontal diameter of the lumbar intervertebral foramina in Saudi females*

gical conditions [20]. Although the space in the IVF foramen is normally adequate for the segmental spinal nerve [21], however various anatomical variations are possible in which adjacent nerve roots may be conjoined with an estimated incidence of 4-14% [22]. Such disproportionately thicker conjoint nerve roots may result in irritation or compression, leading to radicular symptoms [23].

Low back pain, a most common symptom, which affects 50-80% of the population [24], is always an expression of a disturbance of neurological function [25]. The dorsal root ganglia (DRG) are highly sensitive to mechanical pressure1. in the IVF [26]. Earlier studies have shown that DRG are an important anatomical factor in the patho-physiology of pain [27]. Two major factors are considered to be responsible for radicular symptoms: congenital or acquired abnormalities of nerves or nerve roots; bony and soft tissue derangements around nerve roots in IVF [18]. These anatomic abnormalities can be observed in contrast studies. The critical dimensions of lumbar foraminal stenosis are considered to be equal or more than 15mm for foraminal height [12], whereas the cross-sectional area of foramina decreases 15-23.2% during extension of lumber spine [8,9]. The critical dimensions of IVF may vary from level to level and individual to individual [12]. The status of intervertebral disc has been reported to be a major determinant of vertical height of IVF, in addition to fibrous and osseous changes in the boundaries of these foramina [20-29]. Degenerative changes in the intervertebral discs are always associated with osteophyte formation on vertebral bodies and remodeling in zygapophyseal joints [30-32]. These degenerative changes can lead to stenosis of intervertebral canal as well as that of spinal canal [33-34].

Among several imaging tools used to evaluate the configuration of lumbar intervertebral foramina, the radiological interpretation has been considered to be economic, quick and reliable [35]. The present study is the first of its kind in the kingdom of Saudi Arabia, to describe the morphometric evaluations of lumbar IVF in Saudi population. This study revealed that the vertical diameter (height) of IVF increased rapidly at an early age (10-20 years) in females as compared to males (20-30 years), possibly the indication of earlier growth spurt in the females under the influence of hormones. The least vertical as well as horizontal diameters of IVF at $L_5/S_1$ level in +50 age group might be the result of reduced vascularity, less bone density, degenerative changes in intervertebral discs and regression curve of sex steroid hormones [36-42]. This predisposes such senior citizens to frequent symptoms of low back pain due to compression / irritation of 5$^{th}$ lumbar spinal nerve or its DRG in the 5$^{th}$ lumbar IVF with least cross sectional area [36,43]. Our findings are consistent with frequently observed gradually increasing lumbar radicular symptoms from fourth to sixth decade, which reach a plateau after the sixth decade [44]. The present study provides an insight to the Physicians, Surgeons, Anatomists and Physiotherapists about the anatomy of lumbar IVF, necessary for the interpretation and treatment of the low back pain, lumbar foraminectomy, reconstruction and stabilization procedures frequently employed for the burst fractures.

## Acknowledgements

The author would like to thank the Director Accident and Emergency Department, King khalid University Hospital, Riyadh, for providing the material used in this study.

## References

1. Sinnatamby CS. (ed.), Last's Anatomy: Regional and applied. Edinburgh: Churchill Livingstone 1999; 414-431.

2. Williams PL, Warwick R, Bannister LH, Dyson M. (editors). Gray's Anatomy, 37$^{th}$ Ed. Edinburgh: Churchill Livingstone 1989; 315-324.

3. Romanes GJ. Cunningham's Textbook of Anatomy, 12$^{th}$ Edition. Oxford University Press 1981; 89-103.

4. Crock HV. Normal and pathological anatomy of the lumbar spinal nerve root canals. J bone Joint Surg (Br) 1981; 4: 487-490.

5. Giles LGF. Spinal and intervertebrtal canals. In: Giles LGF, Singer KP, eds. Clinical anatomy and management of low back pain. Oxford: Butterworth-Heinemann 1997; 97-113.

6. Gettey CJ, Johnson JR, Kirwan EO, et al. Partial undercutting facetectomy for bony entrapment of the lumbar nerve root. J Bone Joint Sur Br 1981; 63: 330-335.

7. Mayoux-Benhamou MA, Revel M, Aaron C, et al. A morphometric study of the lumbar foramen: Influence of flexion-extension movements and of isolated disc collapse. Surg Radiol Anat 1989; 11. 97-102.

8. Inufusa A, An HS, Lim TH, et al. Anatomic changes of the spinal canal and intervertebral foramen associated with flexion-extension movement. Spine 1996; 21: 2412-2420.

9. Schmid MR, Stucki G, Duewell S, et al. Changes in cross-sectional measurements of the spinal canal and intervertebral foramen as a function of body position: In vivo studies on an open-configuration MR system. AJR. 1999; 172: 1095-1102.

10. Hesagawa T, An HS, Haughton VM, et al. Lumbar foraminal stenosis: Critical heights of the intervertebral discs and foramina. A cryomicrotome study in cadavera. J Bone Joint Surg (Am) 1995; 77: 32-38.

11. Hesagawa T, Mikawa Y, Watanabe R, et al. Morphometric analysis of the lumbosacral nerve roots and

dorsal root ganglia by magnetic resonance imaging. Spine 1996; 21: 1005-1009.

12. Fujiwara A, An HS, Lim TH, Haughton VM. Morphological changes in the lumbar intervertebral foramen due to flexion-extension, lateral bending and axial rotation. Spine 2001; 26: 876-882.

13. Ericksen MF. Some aspects of aging in the lumbar spine. Am J Physical Anthropol 1976; 45: 575-580.

14. Ericksen MF. Aging in the lumbar spine. III. L5. Am J Physical Anthropol 1978; 46: 247-250.

15. Bogduk N, Twomey LT. Clinical anatomy of the lumbar spine. London: Churchill Livingstone 1987; 1-80.

16. Oda J, Tanaka H, Tsuzuki N. Intervertebral disc changes with aging human cervical vertebra. Neonate to eighty years. Spine 1988; 13: 1205-1211.

17. Amoono-Kuofi HS. Morphometric changes in the heights and anteroposterior diameters of the lumbar intervertebral discs with age. J Anat 1991; 175: 159-168.

18. Kikuchi S, Hasue M, Nishiyama K, Ito T. Anatomic and clinical studies of radicular symptoms. Spine 1984; 9: 23-30.

19. Lee CK, Rauschning W, Glenn W. Lateral lumbar spinal canal stenosis. Classification, pathologic anatomy and surgical decompression. Spine 1988; 13: 313-320.

20. Hu SJ, Xing JL. An experimental model for chronic compression of dorsal root ganglion produced by intervertebral foramen stenosis in the rat. Pain 1998; 77: 15-23.

21. Amoono-Kuofi HS, El-Badawi MGY. Ligaments related to the intervertebral canal and foramen. In: Giles LGF, Singer KP eds. Clinical anatomy and management of low back pain, Vol. 1. Oxford: Butterworth-Heinemann 1997; 114-133.

22. Kadish LJ and Simmons EH. Anomalies of the lumbosacral nerve roots. An anatomical investigation and myelographic study. J Bone Joint Surg 1984; 66: 411-416.

23. Rydevik B, Brown MD, Lundborg G, Pathoanatomy and pathophysiology of nerve root compression. Spine 1984; 9. 1-15.

24. White AA and Gordon SL. Synopsis: workshorp on idiopathic low back pain. Spine 1982; 7: 141-149.

25. Wyke BD. The neurology of low back pain. In: Jayson MIV (ed.), The lumbar spine and back pain, 3rd Ed. London: Churchill Livingstone 1987; 56-99.

26. Vanderlinden RG. Subarticular entrapment of the dorsal root ganglion as a cause of sciatic pain. Spine 1984; 9: 19-22.

27. Cohen MS, Wall EJ, Brown RA et al. Cauda equina anatomy II: Extrathecal nerve roots and dorsal root ganglia. Spine 1990; 15: 1248-1251.

28. Panjabi MM, Takata K, Goel VK. Kinematics of lumbar intervertebral foramen. Spine 1983; 8: 348-357.

29. Nowicki BH, Haughton VM, Schmidt TA, et al. Occult lumbar lateral spinal stenosis in neural foramina subjected to physiologic loading [see comments]. Am J Neuroradiol 1996; 17: 1605-1614.

30. Vernon-Roberts B, Pirie CJ. Degenerative changes in the intervertebral discs of the lumbar spine and their sequlae. Rheumatol rehabil 1977; 16: 13-21.

31. Ciric I. The lateral recess syndrome. J Neurosurg 1980; 53: 433-443.

32. Bullough PG, Boachie-Adjei O. Atlas of Spinal Diseases. J.B. Lippincott Philadelphia 1988; 84-97.

33. Kirkaldy-Willis WH, Heithoff KB, Tchang S, Bowen CVA, Cassidy JD, Shannon R. Lumbar spondylosis and stenosis. Correlation of pathological anatomy with high resolution computed tomographic scanning. In: Post MJD, ed. Computed Tomographic of the Spine. Baltimore: Williams and Wilkins 1984; 495-505.

34. Giles LGF, Kaveri MJP. Some osseous and soft tissue causes of human intervertebral canal (foramen) stenosis. J Rheumatol 1990; 17: 1474-1481.

35. Amoono-Kuofi HS. Morphometric changes in the height and anteroposterior diameters of the lumbar intervertebral discs with age. J Anatomy 1991; 175: 159- 168.

36. Sato K, Kikuchi S. An anatomic study of foraminal nerve root lesions in the lumbar spine. Spine 1993; 18: 2246-2251.

37. Amoono-Kuofi HS. Age related variations in the horizontal and vertical diameters of the pedicles of the lumbar spine. J Anatomy 1995; 186:321-328.

38. Tanaka N, Fujimoto Y, An HS et al. The anatomic relation among the nerve roots, intervertebral foram-

ina, and intervertebral discs of the cervical spine. Spine 2000; 25: 286-291.

39. Jenis LG. An HS. Spine update: Lumbar foraminal stenosis. Spine 2000; 25: 389-394.

40. Grimes PF, Massie JB, Garfin SR. Anatomic and biomechanical analysis of the lower lumbar foraminal ligaments. Spine 2000, 25: 2009-2014.

41. Willen J, Danielson B. The diagnostic effect from axial loading of the lumbar spine during computed tomography and MRI in patients with degenerative disorders. Spine 2001; 26: 2607-2614.

42. Panjabi MM, Kato Y, Hoffman H, Cholewicki J. Canal and intervertebral foramen enchroachments of a burst fracture. Spine 2001; 26:1231-1237.

43. Amoono-Kuofi HS, El-Badawi MG, Fatani JA, Butt MM. Extraspinal course of the fifth lumbar spinal nerve: An update of its topographical relationships. Clin Anat 1991; 4: 319-326.

44. Nagosa Y, Kikuchi S, Konno S. Epidemic study of lumbar canal stenosis. Presented at the annual meeting of the Japan Spine Research Society, Asahikawa, Japan, June 21-22, 1991.

**Correspondance:**

Dr. Amin A. Rufai
King Khalid University Hospital & College of Medicine
King Saud University
P.O.Box-2925, Riyadh 11461
Kingdom of Saudi Arabia

Phone: +9661 4671301
Fax: +9661 4671300.
e-mail: aminu_rufai@hotmail.com

*Biomedical Research 2003; 14 (2): 179-184*

# Ultrastructural aspects of chronic iron-sorbitol overload in rat liver

**Meltem Özgüner*, Özlem Dabak*, Nurşen Sayın****

*Süleyman Demirel University, Medical School, Department of Histology- Embryology, Isparta, Turkey.
**Ankara University, Medical School, Department of Histology- Embryology, Ankara, Turkey.

**Key words:** iron-sorbitol, chronic overload, ultrastructure, liver.

*Accepted August 17 2002*

## Abstract

**The liver is a major site of iron storage. Some patients took iron supplements for many years especially in chronic tranfusion therapy of syndromes including pure red cell aplasia, aplastic anemia and thalassemia. We aimed to investigate ultrastructural aspects of chronic iron-sorbitol overload in rat model relatively in a short period of time.**

**Ten Wistar albino rats (200-250gr) were divided into 2 groups in this study. Group I was administered saline (control group); Group II received iron-sorbitol (Jectofer, Eczacıbaşı Pharmaceutical) 2 days a week for 8 weeks at a dose of 400 mg/kg/day. Liver tissues were sectioned for electron microscopy, tissue blocks were embedded in Araldite, random sections were stained in uranyl acetate and lead citrate and scanned in Jeol JEM 1200 electron microscope.**

**Electron microscopic evaluation revealed visible ferritin particles in cytoplasm of paranchymal cells and iron-laden Kupffer cells. Also fibrillar agregattes which were thought to be collagen fibrilles were closely associated with the surface of hepatocytes.**

**In conclusion, our experimental study support the concept that parenteral iron overload may have a direct effect on stimulating collagen synthesis by hepatocytes, and we have observed that the only parenteral form of iron obtained in our country, iron-sorbitol, could produce some morphologic abnormalities alone in a relatively short period of time. This experimental model could be useful for parenteral iron overload investigations.**

## Introduction

Iron is an element essential for almost all living cells [1]. Tissue iron overload causes cell damage and organ dysfunction [2]. Hereditary or primary haemochromatosis is an inborn error of iron metabolism based on an increased intestinal absorption of iron from a normal diet that results in increased iron deposition in the heart, skin, liver and pancreas [2,3]. Transfussion related or secondary tissue iron overload occurs following the transfusion of approximately 100 units of blood without significant bleeding.Chronic transfusion therapy of syndromes including pure red cell aplasia, aplastic anemia and thalassemia result in transfusion-related iron overload [2].

Experimental primary haemochromatosis has been achieved by various dietary manipulations [4-10]. Also in experimental animal models, features of transfusional iron overload have been produced by parenteral administration of massive doses of iron chelates [4,11,12].

Using experimental animal model, we aimed to study ultrastructural aspects of chronic iron-sorbitol overload to determine if the only parenteral form of iron obtained in our country, iron-sorbitol, could produce some morphologic abnormalities alone.

## Materials and Methods

Ten Wistar albino rats (200-250g) were used in this study. They were fed a standart rat chow diet. The animals were divided into 2 groups. Group I was administered saline (control group); Group II received iron-sorbitol (Jectofer, Eczacıbaşı Pharmaceutical) by intramuscular injections 2 days a week for 8 weeks at a dose of 400 mg/kg/day. After completion of iron-sorbitol administration, rats were sacrificed by high dose ether anesthesia for histologic examination.

For electron microscopic examination, segments of liver from 5 ironloaded animals and 5 controls were fixed at

room temperature in 2% paraformaldehyde- 2,5% glutaraldehyde dissolved in 0.2 M phosphate buffer (pH 7.2). After a 1-2 h period of fixation, tissue blocks were washed in several changes of buffer and immersed for 60-120 min in 1% $OsO_4$. Tissue blocks were then washed in buffer and upon completion of dehydration in ethanol, tissue blocks were embedded in Araldite. At least eight blocks were obtained from each liver. Random sections from each block were stained in uranyl acetate and lead citrate and scanned in Jeol JEM 1200 electron microscope Areas of interest were photographed at original magnifications of x1900-4800.

## Results

Electron microscopic evaluation revealed ferritin visible as particles dispersed throughout the cytoplasm of parenchymal cells. The concentration of dispersed ferritin was greater in liver cells of animals from iron loaded group (Fig.1) as compared to controls (Fig.2).

Mitochondrial matrix demonstrated concentrated and mitochondrial volume was increased (Fig.3-4).

At x 3600 magnification, those lysosomal dense bodies in liver cells of experimental animals were suggested as siderosomes of iron-exposed cells. Unlike controls, iron-loaded rats frequently exhibited iron-laden macrophages dispersed throughout the space of Disse. The appearance and properties of these cells were identical to Kupffer cells (Fig. 3).

At intermediate magnifications, fibrillar aggregates were visible in the perisinusoidal space in the livers of obtained from iron-loaded rats (Fig.4). These fibrillar aggregates were absent from livers of control. The majority of collagen fibril bundles in iron-loaded rats were closely associated with the surface of hepatocytes (Fig.4).

No fibroblasts or inflammatory cells were seen to be associated the collagen fibril bundles in the intercellular space.

Lipocytes which were easily identified by accumulation of lipid droplets, were not seen adjacent to the fibrils (Fig.5). Electron dense ferritin molecules were not located in lipocyte cytoplasm, however well-developed Golgi apparatus was identified in cell cytoplasm. The ultrastructural features of endothelial cells of sinusoidal capillaries were essentially similar to those of controls and also siderosomes were not visible in cell cytoplasms

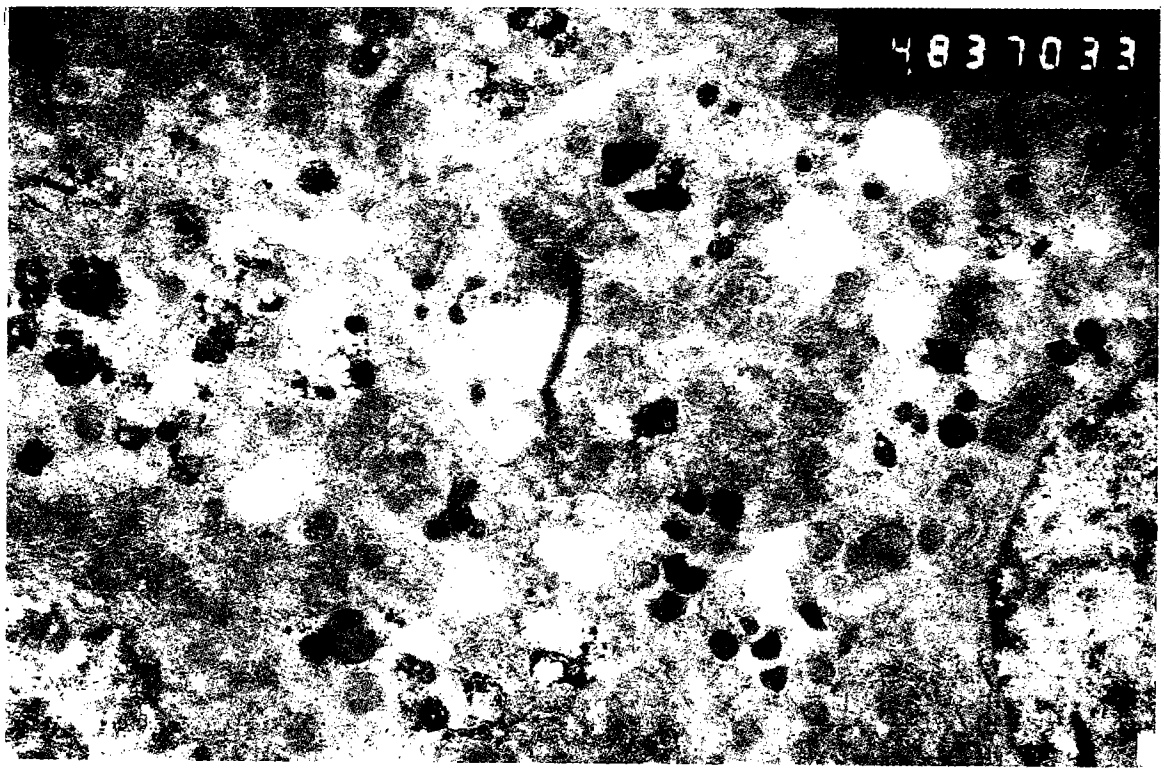

*Fig 1. Electron micrograph of the experimental group showing ferritin particles dispersed throughout the cytoplasm of parenchymal cells. Uranyl acetate-Lead citrate x4800.*

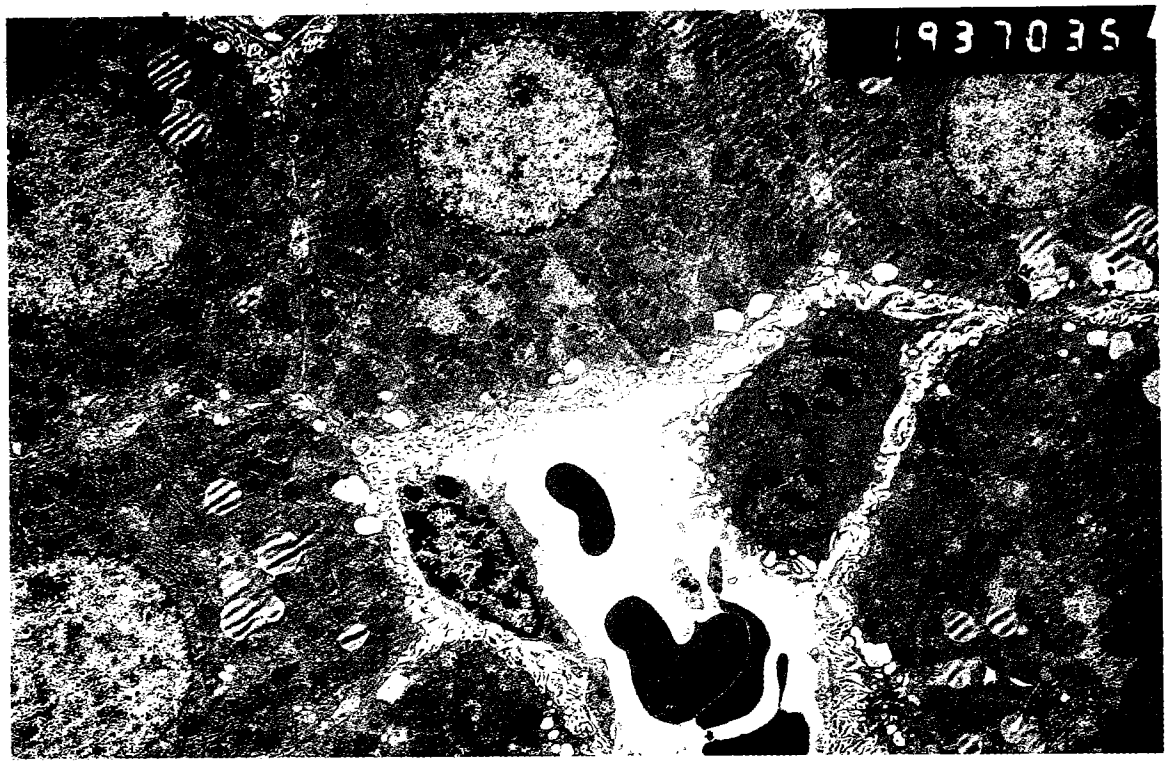

*Fig. 2. Electron micrograph of the control group. Kupffer cell and hepatocytes observed without ferritin particles in cell cytoplasms. Uranyl acetate-Lead citrate x1900.*

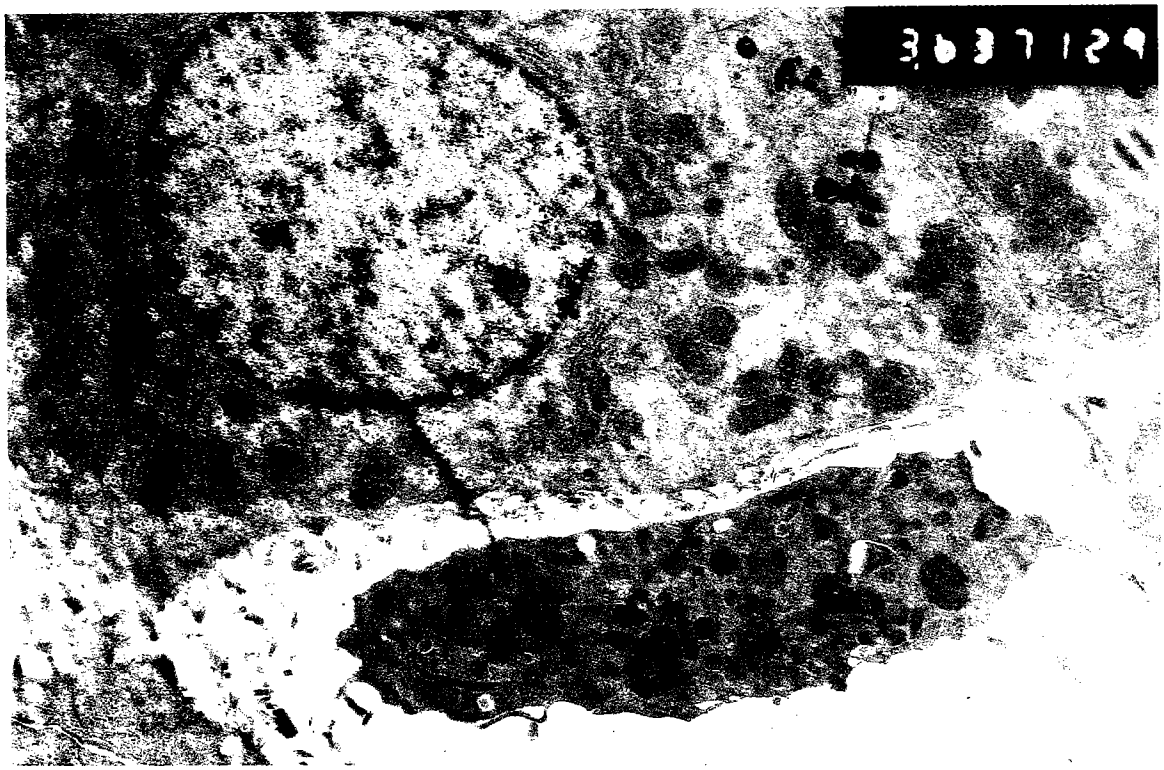

*Fig. 3. Electron micrograph of experimental group. Iron-ladden macrophages dispersed throughout the space of Disse. Uranyl acetate-Lead citrate x3600.*

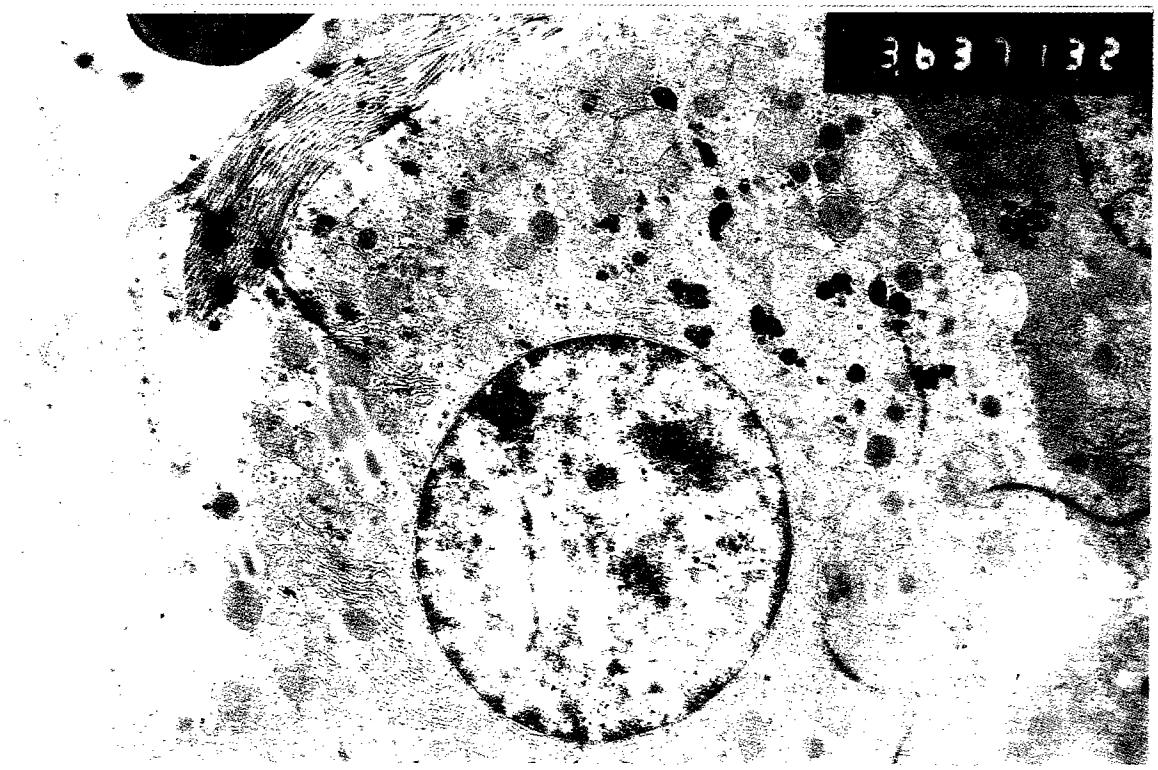

*Fig. 4. Electron micrograph of the experimental group showing collagen fibril bundles closely associated with the surface of hepatocytes. Uranyl acetate-Lead citrate x3600.*

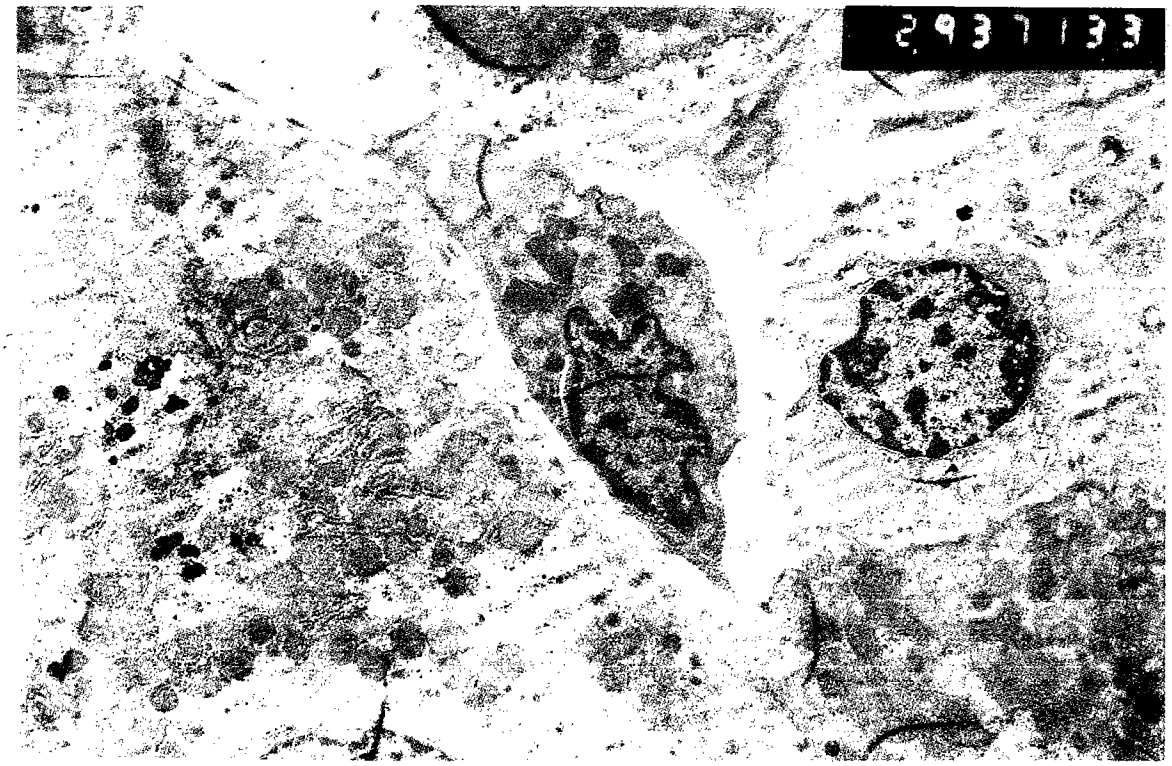

*Fig. 5. Electron micrograph of the experimental group. Lipocytes could easily be identified with lipid droplets in cell cytoplasms. Kupffer cell was also observed with siderosomes. uranyl acetate-Lead citrate x2900.*

## Discussion

Some patients took iron supplements for many years on the advice of a physician, and others took excessive amounts of iron of their own volition without an identifiable need. Several authors have reported hepatic iron was mainly localized into parenchymal cells in the enterally treated rats [3,4,9,10] and in reticuloendothelial cells in the parenterally treated rats [15,16]..

It is generally agreed that the presence of more than a few ferritin particles in the cytosol of cells, other than erytroid line precursors and macrophages, indicates iron overload.The presence of iron-containing lysosomes termed siderosomes and smaller and/or coalesced particles probably represent degraded ferritin forming hemosiderin. Repeated transfusions, hemodialysis, and iron injections into experimental animals have all been shown to increase storage iron (1). Transfusional iron overload is accepted mostly benign and well tolerated for many years[1].

Although all the molecular details have not been established, a growing body of evidence indicates that iron ex erts toxic effects by of its abbility: 1- to form highly reactive free radicals, especially from oxygen, and 2- to increase lysosomal instability [14]. Iron-catalyzed injury results in damage to cell constituents, including mitochondria, lysosomes, and the sarcolemmal membrane.It was reported that these mechanisms of iron-mediated damage are involved in the pathogenesis of organ dysfunction in primary hemochromatosis, transfusion-related iron overload, ischemia-reperfusion injury, and cardiac anthracycline toxicity [2].

In previous studies, features of transfusional iron overload have been produced by parenteral administration of massive doses of iron chelates and in these models hepatic fibrosis have been demonstrated after prolonged periods of heavy iron loading [11]. In our experimental model,by low dose iron-sorbitol administration up to 8 weeks could easily produce transfusional iron loaded animals but severe organ damage could not been observed after 8 weeks of parenteral iron sorbitol administration.

Brissot et al suggested that subhuman primates brings new evidence that iron per se has only a minor hepatic damaging effect [11]. As a consequence of the low bioavailability of carbonyl-iron, especially in already iron loaded animals, the chronic feeding of carbonyl-iron-enriched diet up to 9 months produced only a moderate iron overload in the rats [3]. However, the TMH-Ferrocene iron-loaded rats also did not show severe organ damage as typically found in hereditary haemochromatosis [3].

When iron overload becomes heavier, an insoluble compound of variable composition, called hemosiderin, occurs in hepatocytes and in other cells [14]. The present study has shown that most hemosiderin is found in secondary lysosomes called siderosomes in hepatocytes, which congregate around the biliary poles of hepatocytes.

Mitochondria are essential in the handling of iron within the cell and, therefore, they represent a primary target of oxidative liver injury during iron overload [13]. Bacon et al demonstrated no changes in mitochondrial function when iron as either ferritin or hemosiderin or as a combination was added in vitro to normal liver homogenates [10]. Galleanu et al suggested that lipid peroxidation occurs after mild iron overload even though the liver remains functional [12]. Mitochondrial changes in this experimental model was also in favour of oxidative injury hypothesis.

Park et al first demonstrated the production of hepatic fibrosis by chronic dietary iron overload [4]). Each individual cell of the hepatic lobule (hepatocyte, Kupffer's cell, endothelial cell, and fat-storing cell) may be actively involved in the fibrogenic process by either being directly responsible for collagen biosynthesis or contributing to the production of diffusible factors that are mediators of the fibrogenic process.It was reported that the cells responsible for enhanced collagen gene expression in the carbonyl iron rat model are indeed fat-storing cells [15] and some authors claimed fat storing cells in the mechanism of hepatic fibrosis in the gerbil in response to parenteral iron-dextran overload [19]. In our parenteral iron-sorbitol administration model, fat storing cells were not included in tissue pathology and also the results of our study was infavour of another study which indicate that hepatic reticuloendothelial cell iron overload is pathogenetically linked to the fibrogenic process when iron accumulation in these cells is secondary to hepatocellular necrosis (sideronecrosis) and is mainly caused by the phagocytic activity of necrotic or severely damaged iron-laden hepatocytes [15].

Iancu et al [18] note increased ferritin in 'secondary lysosomes whereas this finding did not seen in Weintraub et al. experimental study [16]. On our electron microscopic examination of this experimental model, lysosomal dense bodies in liver cells of iron-sorbitol loaded animals were seen.

Some investigators have speculated that accumulation of excess iron in hepatocyte lysosomes leads to destruction of these organelles and cell damage initiated by the released enzymes. However, in our electron microscopic studies and those of Iancu andWeintraub there was no evidence of cell or subcellular organelle membrane abnormalities despite the presence of fibrosis [16,18]

In an experimental model, animals were iron loaded by receiving intraperitoneal injections of iron-dextran and this experimental model suggested in view of the absence of any adjacent fibroblasts, reticuloendothelial cells or lipocytes, the location of the collagen fibrils indicate that they may have been synthesized by the hepatocytes [16]. Using electron microscopy, we were able to visualize structures which had the characteristics of collagen bundles immediately adjacent to the surface of hepatocytes of the

ironloaded animals and collagen fibrils were seen between paranchymal cells or in the space of Disse.The hepatic parenchymal cells from adult rats have been reported to produce type IV collagen (basement membrane collagen) as well as types I and III collagen (interstitial collagen) [17]. Our experimental study also support the concept that parenteral iron overload may have a direct effect on stimulating collagen synthesis by hepatocytes.

In conclusion, according to our knowledge this experimental model was the second iron-sorbitol administered study but the first study was the result of a 2-year study on baboons.Our experimental model seems to be suitable for transfusional iron overload in rats in a relatively short experimental period. We have mainly observed that the only parenteral form of iron obtained in our country, iron-sorbitol, could produce some morphologic abnormalities alone.

## References


1 Iancu CT. Biological and ultrastructural aspects of iron overload: An Overview.1990; 281-296.

2 Jesnefsky EJ. Tissue iron overload and mechanisms of iron-catalyzed oxidative injury.In: Free Radicals in Diagnostic Medicine. Armstrong D (ed.). New York: 1994; 129-146.

3 Nielsen P, Heinelt S, Düllmann J. Chronic feeding of carbonyl-iron and tmh-ferrocene in rats. Comparison of two iron-overload models with different iron absorbtion. Comp Biochem Physiol 1993; 106: 429-436.

4 Park HC, Bruce RB, Brittenham GM, Tavill AS. Pathology of dietary carbonyl iron overload in rats. Lab Invest 1987; 57: 555-563.

5 MacDonald RA. Experimental pigment cirrhosis: its production in rats by feeding a choline-deficient diet with excess iron. Am J Pathol 1960; 36: 499.

6 MacDonald RA, Pechet GS. Experimental hemochromatosis in rats. Am J Pathol 1965; 46: 85.

7 Richter GW. Effects of cyclic starvation-feeding and of splenectomy on the development of hemosiderosis in rat livers. Am J Pathol 1975; 74: 481-483.

8 Bates GW, Boyer J, Hegenauer JC, Saltman P. Facilitation of iron absorption by ferric fructose. Am J Clin Nutr. 1972; 25: 983-985.

9 Bacon BR, Healey JF, Brittenham GM, Park CH, Tavill AS, Bonkovsky HL. Hepatic microsomal function in rats with chronic dietary iron overload. Gastroenterology 1988; 90: 1844.

10 Bacon BR, Park CH, Brittenham GM, O'Neill R, Tavill AS. Hepatic mitochondrial oxidative metabolism in rats with chronic dietary iron overload. Hepatology 1985; 5:789-797.

11 Brissot P, Campion JP, Guillouzo A, Allain H, Messner M, Simon M, Ferrand B, Bourel M. Experimental hepatic iron overload in the Baboon: Results of a two year study. Digestive Diseases and Sciences 1983; 28: 616-624.

12 Galleano M, Puntarulo S. Hepatic chemiluminescence and lipid peroxidation in mild iron overload. Toxicology 1992; 76: 27-38.

13 Pietrangelo A,Borella F, Casalgrandi G, Montosi G, Ceccarelli D,Gallesi D, Giovannini F, Gasparetto A, Masini A.Antioxidant activity of silybin in vivo during long-term iron overload in rats. Gastroenterology 1995; 109: 1941-1949.

14 Bonkovsky HL. Iron and the liver. Am J Med Sci. 1991; 301: 32-43.

15 Gualdi R, Casalgrandi G, Montosi G, Ventura E, Pietrangelo A. Excess iron into hepatocytes is required for activation of collagen type I gene during experimental siderosis. Gastroenterology 1994; 107: 1118-1124.

16 Weintraub LR, Goral A,Grasso J, Franzblau C, Sullivan A, Sullivan S. Pathogenesis of hepatic fibrosis in experimental iron overload. British J Haem 1985; 59: 321-331.

17 Diegelmann RF, Guzelian PS. Collagen formation by the hepatocyte in primary monolayer culture and in vivo. Science 1983; 219:1343-1345.

18 Iancu TC, Neustein HB, Landing BH. The liver in thalassemia major: ultrastructural observations in iron metabolism. CIBA Foundation Symposium. 1977; 51: 293-307.

19 Cathew P, Edwards ER, Smith AG,Dorman B, Francis JE. Rapid induction of hepatic fibrosis in the gerbil after the parenteral administration of iron –dextran complex. Hepatology. 1991; 13: 534-539.



**Correspondence to:**

Dr. Meltem ÖZGÜNER
Kurtuluş mah. 137. cad.
Eralp apt. 7/9, Isparta
Turkey
e-mail: mozguner@hotmail.com

*Biomedical Research 2003; 14 (2): 185-188*

# Antisickling properties of *Parquetina nigrescens*

**I. J. Kade[1], O. O. Kotila[1], A. O. Ayeleso[1], A. A. Olaleye[2] and T. L. Olawoye[1]**

[1]Department of Biochemistry, Federal University of Technology, PMB 704 Akure, Nigeria
[2]Department of Pediatrics, Ondo State Specialist Hospital, Akure, Ondo State, Nigeria

**Key words:** *Parquetina nigrescens*, antisickling, sickle cells

*Accepted May 28 2003*

## Abstract

**Ethanolic extract of the roots of *Parquetina nigrescens* were prepared and used for *in vitro* studies on eight individual blood samples obtained from confirmed sickle cell patients in remission. The results obtained revealed that the aqueous partitions of ethanolic extracts of *Parquetina nigrescens* not only improved the morphology of already sickled cells, but it also inhibited and reversed the sickling process. The extracts of the root of the plant exhibited their inhibitory effect by delaying the time it takes for the cells to sickle in the presence of a powerful reducing agent, sodium metabisulphite. The phytochemical analyses showed that the plant contained alkaloids, tannins, saponins and cardiac glycosides.**

## Introduction

Management of sickle cell disease using local African herbs as medicinal plants has long been in practice. This is evident from the fact that local names had long been reported for this disease. Such names include *Chwechweechwe* by Ga tribe of Ghana, *Adep* by Banyangi tribe of Cameroun and *Arunmolegun* by the Yoruba tribe of Nigeria.

However, in recent times, researchers have directed efforts towards assessing medicinal plants for *in vitro* antisickling activities. These research efforts aimed at investigation of candidate plants for the management of sickle cell disease have been well described. Extract of the bark and root of Baobab have been reported to have beneficial effect in inhibiting and reversing the sickling process [1]. Also investigation of the antisickling potential of *Adansonia digitata* (Bombacaceae) showed that the plant significantly reverses already sickled cells but had little effect on the sickling process [2]. Elsewhere seeds of *Cajanus cajan* were reported to inhibit as well as, reverse the sickling of HbSS erythrocytes. Bioassay guided extraction and column fractionation of the seed extract yielded an active fraction, which delayed gelation of HbSS and increased its affinity for oxygen [3,4].

Earlier studies by Sofowora and others [5,6] had provided the pioneering impetus for laboratory study of these traditional medicaments.

There have been undocumented reports that *Parquetina nigrescens* (called *ewe ogbo* in Yoruba) is used in local treatment of sickle cell anaemia in Western part of Nigeria. We decided to investigate the efficacy and antisickling potentials of this plant to justify its unpublished use in the management of sickle cell disease.

## Materials and Methods

### *Plant Materials*

Roots of *P. nigrescens* were obtained from the herbal farm of Dr. Olaleye, Consultant Haematologist, State Specialist Hospital, Akure. The plants were later taken to the Crop Soil and Pest Management Department of the Federal University of Technology, Akure for botanical identification.

### *Extracts from plants*

Extraction of plant material was performed as described as elsewhere [3].

### *Blood collection*

Fresh venous blood (5-10ml) was obtained from eight confirmed volunteer sickle cell patients at the State Specialist Hospital, Akure. The patients were not in crises at the time of collection.

*Effect of Parquetina nigrescens on sickling*

The inhibition and reversion of sickling by *P. nigrescens* extract was investigated as described elsewhere [3].

*Phytochemical screeining*

The phytochemical screening tests were carried out as described by Sofowora [7].

## Results and Discussion

Figure 1 shows the mean inhibitory effect of extracts of *P. nigrescens* on sickling in the presence of a reducing agent (sodium metabisulphite). The data reveal that the number of cells sickled in the presence of *P. nigrescens* extract were significantly reduced when compared with control (cells treated with sodium metabisulphite only). The percentage inhibition (Figure 2) is the ratio (in percentage) of the positive difference between the number of cell sickled in the presence of sodium metabisulphite only and *P. nigrescens* extract to that of control.

There is apparently no documental evidence of the antisickling potential of *P. nigrescens*. This study is therefore the first to report on this subject. Unpublished information about *P. nigrescens* reveals that the aqueous extract of the leaves can be used locally to treat anaemic patients and was also found to be a potent blood builder.

Figure 2 shows the mean number of cells reverted in the presence of *P. nigrescens* extract. The baseline presickled cell is 100% and serves as the basis for calculation of percentage reversion which is the difference between the baseline and number of cell sickled in a given time (Figure 4).

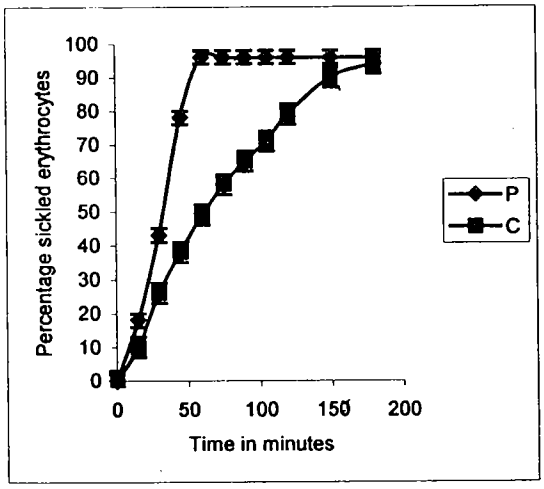


*Fig. 1: Inhibition of sickling by P. nigrescens*
*C- Sickling in sodium metabisulphite*
*P- Sickling in sodium metabisulphite and P. nigrescens*

Both the results obtained from the experiments for sickling reversion and inhibition indicate that in vitro action of the crude extracts of *P. nigrescens* are rapid. At least 50% of already sickled erythrocytes can be reversed within 10 minutes. The results show that *P. nigrescens* has great antisickling properties (Figures 1 and 3). The efficacy of the inhibitory effect of the extract was taken as the time ratio that the sodium metabisulphite was able to cause a 50% sickling of the HbSS erythrocyte in the presence and absence of extract. It takes about 60 minutes for almost 96% of the erythrocyte cells to sickle with sodium metabisulphite. On addition of *P. nigrescens* extract, the time interval was prolonged to about 180 minutes. In Figure 2, from the curve of percentage inhibition, it was observed that as the number of sickle cells reduce in the presence of *P. nigrescens*, the percentage inhibition increases due to inhibitory effect of the plant extract. With time the number of sickle cells increased and the percentage inhibition dropped. Peak activity was obtained at 45 minutes when there was maximum inhibition of sickling in the presence of *P. nigrescens* extract.

In the reversion of the already sickled erythrocytes (ISC's), *P. nigrescens* greatly reversed the already sickled erythrocytes to normal round shapes. The sickling reversal experiments were performed with erythrocytes with high percentage of already sickled cells (not less than 70%).

Figure 3 shows the curve for a typical set of result obtained using HbSS erythrocytes presickled in bulk as already described. The plant reverses almost 50% of the sickled cells to normal round shapes in about 10 minutes and microscopic observation revealed that there was a great improvement in the morphology of the sickled erythrocytes in contact with the plant extract.

The use of sodium metabisulphite in sickling induction is probably a more drastic approach than what actually happens in the vascular system. In that case, *P. nigrescens* extract may perform its antisickling action more efficiently under *in vivo* redox conditions than has hitherto been demonstrated.

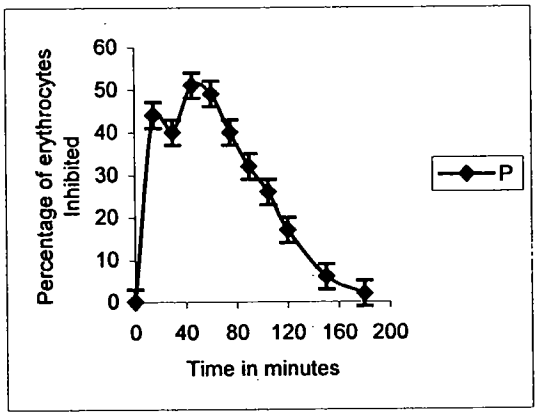


*Fig. 2: Percentage inhibition of sickling in the presence of P. nigerescens*

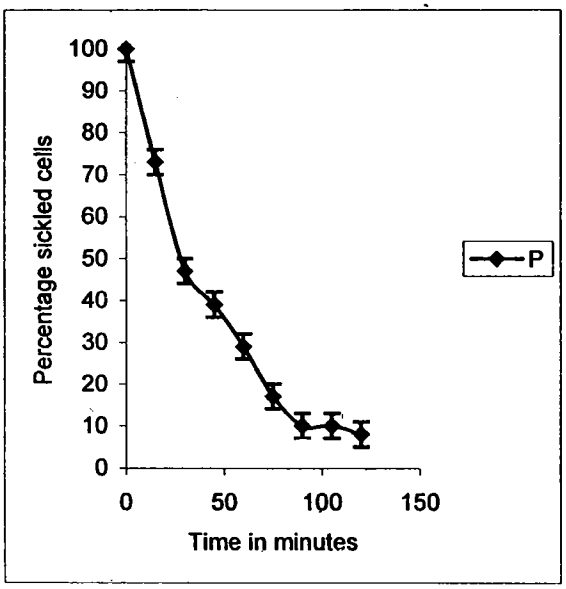


*Fig. 3: Reversion of sickling in the presence of P. nigerescens*

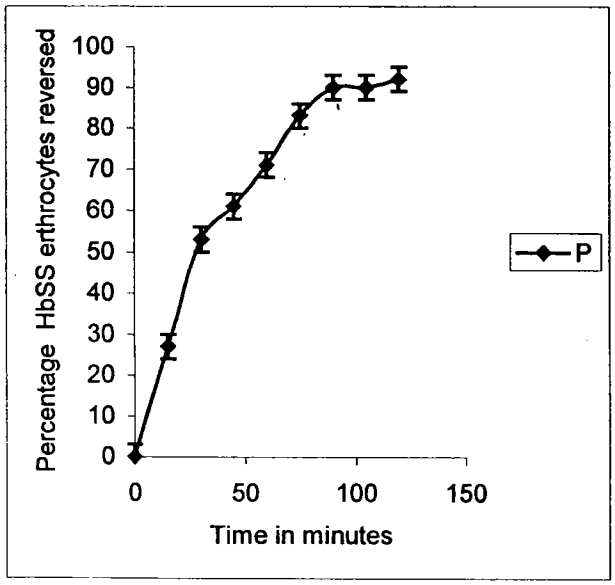


*Fig. 4: Percentage reversion of sickling by P. nigerescens*

In the phytochemical examination of the plants for secondary metabolites, *P. nigrescens* contained tannins, saponins and cardiac glycosides while phlobatannins and anthraquinones were absent. Some researchers in the past have isolated some plants and characterize them to contain secondary metabolites like amino acids aminoglycosides, which serve as the active principle in these plants, and the property enables them to be used in the treatment of sickle cell disease. An example of this is seen in *Fagara gilleti*, which have been found useful in inhibiting sickling and has been purified and found to give benzoic acid derivatives as the active principle [1]. It has also been reported that the aqueous extract of *Cajanus cajan* contains a high level of an essential amino acid, phenylalanine [8]. Other studies show that aromatic amino acids such as phenylalanine, tryptophan and tyrosine are potent inhibitors of HbSS gelation [9,10]. In a related study, it was found that the antisickling properties of thyroid hormone analogues like L-tyrosine were similar to those of the physiologically active thyroid hormones ($T_3$ and $T_4$), suggesting that the antisickling properties were not related to the hormonal function [11]. Further investigation of the secondary metabolites is essential in order to determine the active antisickling principle of this plant. The efficacy of an antisickling agent, whether *in vivo* or *in vitro*, must be associated by a set of reproductive criteria. It must act effectively and rapidly, especially in cases of severe crisis as well as possess minimal side effects. Since *P. nigrescens* is already being used as a local remedy in the management of sickle cell disease, it is hoped that pharmacological studies might prove that it possesses minimal toxic effects.

## References

1. Sofowora A. *The state of Medicinal plants research in Nigeria.* Eds. A. Sofowora. Faculty of Pharmacy Obafemi Awolowo University, Ile-Ife. 1983.

2. Adesanya SA, Idowa TB, Elujoba AA. Antisickling activity of *Adansonia digitata.* Planta Medica 1988; 54: 374.

3. Ekeke GI, Shode FO. The reversion of sickled cells by *Cajanus cajan.* Planta Medica 1985; 50: 505-506.

4. Iwu MM, Igboko OA, Onwubiko H, Ndu UE. Antisickling properties *of Cajanus cajan.* Effect on hemoglobin gelation and oxygen affinity. Planta Medica 1986; 53: 431-432.

5. Sofowora FA, Issacs WA. Reversal of sickling and crenation in erythrocytes by the roots of *Fagara xanthoxyloides.* Lloydia 1971; 34: 383-385.

6. Adesanya SA, Sofowora A. Biological standardization of *Zanthoxylum* roots for antisickling activity. Planta Medica 1983; 48: 27-33.

7. Sofowora A, *In: Medicinal plants and traditional medicine in Africa* 2nd Edition, Spectrum Books Limited Ibadan 1993; 150-152.

8. Ekeke GI, Shodo FO. Phenylalanine is the predominant antisickling agent in Cajanus seed extract. Planta Medica 1990; 56: 41-43.

9. Noguchi CT, Schechter . The inhibition of sickle hemoglobin gelation by amino acids and related compounds. Biochemistry 1978; 17: 54-55.

10 Schechter AR, Noguchi CT, Schwartz WA. Amino acids and peptides as inhibitors of sickle hemoglobulin gelation. Academic Press New York 1978; 129-142.

11. Olawoye TL, Dada OA. In vitro antisickling effects of thyroid hormones and some synthetic analogues. Nigerian Journal of Physiological Sciences 1989; 5: 133-136.

Correspondence:

Professor T.L. Olawoye
Department of Biochemistry
Federal University of Technology
PMB 704 Akure
Nigeria

*Biomedical Research 2003; 14 (2): 189-192*

# Effect of hemodialysis on ventricular repolarization in patients with end stage renal disease: A hospital based study

**A.S. Khan, S.F. Haque, Anshul Gupta, M. Singh**

Department of Medicine, Jawaharlal Nehru Medical College, Aligarh Muslim University, Aligarh, India

**Key words**: Hemodialysis, ventricular repolarization, renal disease, sudden cardiac death, arrhythmia,

*Accepted July 8, 2003*

## Abstract

**Sudden cardiac-death is a common consequence in the patients on hemodialysis and may also occur during immediate post dialysis period; higher incidence of ventricular arrhythmia has been described for such occurrence. QTc dispersion reflects the underlying regional heterogeneity of ventricular depolarization. The present pilot study had been conducted to evaluate the QTc dispersion before and after uncomplicated hemodialysis session.**

**50 patients of chronic renal failure, without CHF, diabetes mellitus (DM) and Ischemic heart disease (IHD) were selected. The QTc dispersion was determined by the difference between the largest and shortest QTc intervals measured on a 12 lead surface electrocardiogram. Following hemodialysis sessios in this pilot study, maximum QTc was increased from 500.16±52.81 to 539.16±62.18 ms ($p<0.05$) and QTc dispersion increased from 65.45±22.24ms to 99.56±25.23 ms ($p<0.001$).**

**In summary, hemodialysis perse does induce in increase of QTc dispersion, might be due to rapid changes in plasma electrolyte concentration which are all well known influencing factors to cause arrhythmogenic effects. Measurement of QTc dispersion therefore can provide a cheap and simple bedside method that could assess the increased myocardial inhomogeneity in the hemodialysis patients and to take necessary action accordingly.**

## Introduction

Evidence exists that patients of chronic renal failure on maintenance hemodialysis show high incidence of ventricular arrhythmias. Sudden cardiac death (SCD) is quite common in these patietns and may occur during and immediately after the dialysis session [1,2]. This arrhythmogenic effect of standard hemodialysis procedure is mainly attributed to the rapid change of intra-and extra cellular concentration of electrolytes [3,4]. It is well known that regional inhomogeneity of repolarisation time in adjusted areas of myocardium has been associated with higher risk of ventricular tachy-arrhythmias. Inter-lead variability of QT internal in surface electrocardiogram i.e. QTc dispersion reflects the regional differences in the ventricular recovery time [5,6] which inturn can elicit the re-entrant type of arrhythmias. The inter-lead QTc dispersion, therefore has been proposed as a simple and cheap indicator of arrhythmogenic risk and is able to predict more proneness to severe ventricular arrhythmia or sudden cardiac death in patients with hypertrophic obstructive cardiomyopathy myocardial infarction and congestive heart failure (CHF) [7].

The present pilot study had been conducted with the purpose of evaluating the effects of hemodialysis session on QT dispersion in patients with chromic renal failure (CRF) but without any clinical evedence of heart disease. The measurement of QT dispersion in chronic uremia patients on maintenance hemodialysis is an intriguing matter

of investigation and therefore recommended as a routine investigation before, during and after hemodialysis.

## Material and Methods

The present study included 50 patients of CRF (32 males, 18 females) with mean age of 51.46± 9.08 years on twice weekly maintenance hemodialysis. The patient had undergone hemodialysis 32±9.21 times.

The composition of dialysate used for hemodialysis was: Potassium 2mq/L, Calcium 3mq/L, Sodium 135 mq/L and Magnesium 0.75 mq/L, Chloride 106mq/L. The patients suffering from DM, CHF, IHD, AF or other conduction disturbances were excluded. No patient was under any pharmacological agent, which is known to affect the QT interval.

12 lead surface electrocardiogram were taken before and 15 minutes after the end of uncomplicated hemodialysis session.For each ECG recording, 3 consecutive QT intervals were measured from each lead and the arithmatic mean was calculated. QT values, these after were corrected for heart rate by using Bazett's formula to obtain corrected QT interval (QTc). The QTc dispersion dispersion was determined as the difference between the maximum and minimum value of QTc interval in different leads (at least 10 leads) of the same recording. The arithmetic mean of QTc from 12 leads was assumed to be QTc interval length.

Blood pressure and heart rate were noted during the same time of ECG recordings. Plasma level of electrolytes, blood urea, serum creatinine and hematocrit values were determined at the onset as well as at the end of hemodialysis session. Only the data of those sessions of hemodialysis were considered when no clinically significant hypotensive episode occurred.

All the results were expressed as mean ± SD. The statistical analysis was done by using studies 't' test for paired data and Pearson's correlation test. Differences were considered statistically significant when 'p' value was <0.05.

## Results

An increase in QTc dispersion was noted following hemodialysis session from pre-dialysis value of 65.45±22.24 ms to 99.56±25.23 ms which was found to be statistically significant (Table 1). Similarly, QTc interval also increased from 500.16±52.81 m sec to post dialysis value of 539.16±62.18 ms Following hemodialysis session, the plasma concentration of potassium was noted to be decreased (6.14±1.36 vs 3.95±0.52 meq/L), while calcium levels increased (9.25±0.65 Vs 10.42±0.82 mg/dl) (Table 2). However, no significant relations were observed between increase in QTc dispersion and blood pressure, hematocrit value at the onset of hemodialysis session as well as with age, sex or duration of hemodialysis.

*Table 1: Distribution of various particulars in the study subjects*

| S.No. | Particular | Males | Female | Total |
|---|---|---|---|---|
| 1. | Number | 32 | 18 | 50 |
| 2. | Age (Years) | 52.34±9.21 | 50.27±8.33 | 51.31±8.92 |
| 3. | Duration of CRF (Years) | 7.45±6.12 | 7.14±5.46 | 7.22±25.73 |
| 4. | TSP (gm/dl) | .82±10.83 | 7.42±0.87 | 7.61±0.83 |
| 5. | S. Albumin (gm/dl) | 4.18±0.65 | 3.92±0.75 | 408±0.71 |
| 6. | S. Globulin (gm/dl) | 3.71±1.18 | 3.54±1.12 | 3.62±1.14 |

*CRF: Chronic renal failur; $TSP^{+}$ : Total serum proteins*

*Table 2: Changes induced by hemodialysis (HD) on QTc dispersion, QTc length, heart rate and blood pressure in study group*

| S.No. | Variable | Before HD | After HD | P value |
|---|---|---|---|---|
| 1. | QTc Length (ms) | 65.45±22.24 | 99.56±25.23 | <0.001 |
| 2. | QTc Dispersion (ms) | 500.16±52.81 | 539.16±62.18 | <0.05 |
| 3. | Heart rate (bpm) | 74.34±18.17 | 80.17±20.16 | MS |
| 4. | Systolic B.P. (mmHg) | 160.18±28.46 | 146.74±20.18 | <0.001 |
| 5. | Diastolic B.P. (mmHg) | 92.48±12.68 | 85.56±10.26 | <0.001 |

## Discussion

Cardiac arrhythmias are very common in patients on maintenance hemodialysis and among them the ventricular arrhythmias are the most severe ones. They occur very frequently during and after the hemodialysis session [1,2,10]. They can be the cause of serious life threatening conditions although do not seem to predict the overall mortality in hemodialysis patients [8]

Rapid changes occur in both extra as well as intracellular fluid composition, which can account for the increased incidence of ventricular arrhythmias during and after the hemodialysis sessions. The rapid reduction of potassium and elevation of ionized calcium levels in plasma can cause cardiac arrhythmias [3]. Arrhythmogenic effects of hemodialysis also depends upon the plasma-dialysate potassium gradient. It has been demonstrated that the arrhythmogenic effect of hemodialysis was reduced when a constant plasma dialysate potassium gradient was used instead of the constant low potassium dialysate concentration [4].

It has been reported that regional inhomogeneity of duration of ventricular recovery and severe ventricular arrhythmias are linked to each other [5]. Since increased values of QTc dispersion reflect regional differences of myocardial repolarization, they are considered as a predictor of arrhythmigenic risk [5,9]

In the present investigation it has been noted that hemodialysis induces a significant increase of QTc dispersion. These findings aer closely similar to other studies [10-12].

Potassium is the most important factor along with Magnesium for maintaining the electrical stability of myocardium. They are also inv-olved in creating normal excitability, impulse propagation and regular ventricular recovery. Thus it is likely that the dialysis induced disequilibrium i.e. rapid reduction of extra-cellular potassium concentration might be an important reason for increased QTc dispersion.
The exact pathogenesis of increase in QTc dispersion following hemodialysis is not so clear because there are no well-defined study protocols in addition many dialytic composition and individual factors potentially affect this parameter. In present investigations, patients suffering from diabetes mellitus, congestive heart failure, ischemic heart disease, atrial fibrillation or other conduction disturbances were not included. Further studies are needed to be conducted in such patients of chromic renal failure to investigate if increased QTc dispersion is really associated with severe ventricular arrhythmias in them

## Conclusion

It can be concluded from this pilot study that the dispersion of QTc interval does increase after hemodialysis treatment indicating increased inhomogeneity of ventricular repolarization. Measurement of QTc and QTc dispersion is a cheap and simple bedside method to assess the increased myocardial inhomogeneity in dialysis patients. The role of dialysis induced increase in QTc dispersion as prediction of severe cardiac arrhythmias or sudden death remains to be assessed by further investigation involving more number of patients.

## References

1. Gruppo Emodialisi e patologie Cardiovascolari: Multicentre, cross-sectional study of ventricular arrhythmias in chronically hemodialysed patients. Lancet 1988; I: 305-309.

2. Morris ST, Galiatsou E, Stewart GA, Rodger RS, Jardine AG: QTdispersion before & after hemodialysis.J. Am Soc Nephrol 1999; 10: 160-163.

3. Nishimura M, Nakanishi T, Yasui A, Tsuji Y, Kunishige H, Hirabayashi M, Takahashi H, Yoshimura M: Serum calcium increases the incidence of arrhythmias during acetate hemodialysis. Am J Kidney Dis 1992; 19: 149-155.

4. Rombola G, Colussi G, De Ferrari MF, Frontini A, Minetti L: Cardiac arrhythmias and electrolyte changes during hemodialysis. Nephrol Dial Transplant 1992; 7: 318-322.

5. Higham PD, Hilton CJ, Aitchson DA, Furniss SS, Bourke JP, Campbell RWF: QT dispersion does reflect regional variation in ventricular recovery (abstract). Circulation 1992; 86: 392.

6. Lorincz I, Matyus J, Zilahi Z, Kun C, Karanyi Z, Kakuk G: QTdispersion in patients with end stage renal failure and during hemodialysis.J. Am Soc Nephrol 1999; 10: 1297-12302.

7. Tuncer C, Kulan K, Komsuoglu B, Ozdemir R, Guven A, Pekdemir H, Sezgin AT: Impact of hemodialysis on comprehensive ventricular repolarization. Acta Cardiol 1997; 52: 305-312.

8. Locati EH, Bagliani G, Saronio P, Stramba Badiale M, Timio M, Schwartz PJ: Increased QT interval dispersion following potassium hemodialysis; in Timio

M, Wizeman V, Venanzi S (eds): Cardionephrology.4. Consenza, Bios Ed, 1997, pp 173-177.

9. Erem C, Kulan K, Goldeli O, Tuncer C, Komsuoglu B, Mocan M: Impact of hemodialysis on QT interval. Acta Cardiol 1995; 50: 177-185.

10. Suzuki R, Tsumura K, Inoue T, Kishimoto H, Morii H: QT interval prolongation in patients receiving maintenance hemodialysis. Clin Nephrol 1998 Aprl; 49: 240-244.

11. Tun A, Khan IA, Wattanasauwan N, Win MT, Hussain A, Hla TA, Cherukuri VL, Vasavada BC, Sacchi TJ. Increased regional and transmyocardial dispersion of ventricular repolarization in end-stage renal disease. Can J Cardiol 1999; 15: 53-56.

12. Yetkin E, Ileri M, Tandogan I, Boran M, Yanik A, Hisar I, Kutlu M, Cehreli S, Korkmaz S, Goksel S. Increased QT interval dispersion after hemodialysis: role of peridialytic electrolyte gradients. Angiology 2000; 51: 499-504.

**Correpondence:**

Dr. Anshul Gupta
Department of Medicine
Jawaharlal Nehru Medical College
Aligarh Muslim University
Aligarh 202 002
India

Phone: 0091-571-2507040
Mobile: 9837077357
e-mail: dranshulgupta@yahoo.com

*Biomedical Research: 14 (2): 193-198*

# Referral pattern in primary care using the ICPC system and referrability rate

**Yousef I. Al-Jameel* and Khalid S. AL Gelban****

* Department of Family and Community Medicine, King Fahad National Guard, Hospital, Riyadh, Saudi Arabia.
** Department of Family and Community Medicine, Colloge of Medicine and Medical Sciences, King Khalid University, Abha, Saudi Arabia

**Key words**: Referral Patterns, primary care, referral rate, referrability rate

*Accepted August 31 2003*

## Abstract

**To describe the referral patterns in primary health care population using the International Classification of Primary Care Coding System (ICPC) and to compare with different estimator referrability rate Vs referral rate of the referral status.**

**A cross- sectional study in primary care setting was carried out. Modified encounter form was used for data collection from medical records using the ICPC coding system. The study was conducted on 2290 out of 200,000 encounters per year, which were randomly selected by utilizing a computerized random number generator. The concept of referrability rate as proposed by Smit et al (1997) to compare the pattern of referral was used.**

**At 2.53% of encounters (95% CI: 1.9% to 3.18%) at least one referral was recorded. The specialties mainly included were emergency room, obstetrician/gynecologist, surgery, dermatology and ophthalmology. The highest referral rates were observed for respiratory system (22%), skin (16.49%), reproductive system (13.55%) and eye (13.55%) giving referrability rates of 0.98%, 5.6%, 17.7% and 8.33%, respectively.**

**The referrability rate, when considered together with the referral rate, provided the general practitioners and specialists with a frame of reference for their own work which was also helpful for designing training and continuous medical education programs.**

## Introduction

Auditing the referral system from primary care to secondary care contributes to the improvement of the quality of care and lessening costs of medical services [1]. Wide variations in referral rates between doctors are observed and further investigation on this subject has been encouraged recently [2,3]. Many factors may contribute to this variation such as health care structure different nationalities of physicians and local morbidity patterns of general practice [3].

This international classification of health problems in primary care is based on problems as defined by the doctor [4], which allows collection of encountered data more reliably and constantly [5,6].

International referral studies using International Classification of Primary Care (ICPC) have found that 38.7% of referrals were described in symptomatic terms in Spain compared to 17.7% in Portugal while the rest of referrals were described in diagnostic terms. These two countries represent the extremes of the range of six European countries

[7,8]. In Australia, the percentage of new referrals to medical specialists is 6.5 per 100 encounters.

Since the implementation of referral system in Saudi Arabia in 1989, available studies have been examined for the effectiveness of the referral system, quality of referral letter and referral process indicating wide variation in referral rates from 2.6-6.6 per 100 encounters [9-12]. However, to the best of our knowledge no national study described referral pattern per encounter as an effective part of consultation process using the International Classificationof of Primary Care, 2nd edition ( ICPC2).

This study, aims to describe referral patterns of primary care setting at National Guard Housing (Iskan) over one year period, utilizing the ICPC2 in terms of referral rates and referrability rates for different diagnostic categories.

## Methods

This cross-sectional study was conducted at primary health care services at suburb of National Guard Housing (Iskan) Riyadh .All the ten-satellite clinics of Iskan, which were covered by non-board certified physicians supervised by a family medicine consultant for each clinic, were included in the study. These clinics serve as a catchment area of a total population of approximately 40,000 patients with estimated 200,000 encounters per year.

Data was collected from the data base of the Department of Family and community Medicine at King Fahad National Guard Hospital (KFNGH), was developed from January 1st to December 31st 1998 using the International Classification of Diseases, 10th edition (ICD-10).[13] These encounters were considered to be the sample frame of our study. The sample frame of the encounters was subjected to random selection process using computer-generated random numbers to select 2290 encounters and these represented the study sample size. The sample was determined based on an expected prevalence of approximately 50% with a 2% margin of error to provide 95% confidence limits for the estimates of population proportions ignoring finite population correction because of the large population size.

Collected data provided with a list of encounters including medical record numbers and date of encounters, which was drawn from the department's morbidity database, based on the previous randomization using modified encounter forms [8-14]. ICPC2 classification was used for diagnostic categorization and therapeutic procedures. Confidentiality was ensured by separating patient's identification and associated morbidity data. The modified structured encounter forms included sections for age and gender of patients; reasons for encounters (up to five); problems managed (up to four); status of the problem (old/new); treatments provided (up to five); tests and investigations (up to five); referrals and planned follow up (within 3 months). Researchers included only new referrals arising from recorded encounters. The new measure of referrability rates, introduced by Smit et al.[15] has been utilized to gain insight into the likelihood of a condition being referred. The referrability rate is defined as the frequency of referrals for particular problem per 100 encounters for that problem [8,15].

Data was collected, manually checked for completeness and verified for electronic coding by randomly selection of one to every ten encounter forms through an experienced ICPC2 coder who checked the coding against the forms. Statistical package (EPI info 6.04 version C) was used for data entry and analysis [16]. Analysis included descriptive statistics, proportions were presented as percentages. Chi square test was used to compare proportions among the groups. All morbidity data, both written and electronic, were maintained in a secure fashion in the department of Family Medicine, KFNGH, Riyadh.

## Results

This Survey included a total of 2290 encounters, 2592 problems and 3898 reasons for encounters. In this study, a total of 60 referrals resulted from the 58-referral encounters for a total of 59 problems. Two-thirds of referral encounters were of less than 12 years old and one third were of more than 12 years old. Males and females constituted 53% and 47% of the referral encounters, respectively. Seventy percent of all problems managed at all referral encounters were new while 30% of them were old. The highest rates of the referrals were recorded for 25-29 years old group (20%) whereas the lowest one was recorded for 0-3 years old (1.8%).

Table 1 displays that at 2.53% of encounters (95% CI: 1.9% to 2.18%) at least one referral was recorded whereas referral rate per 100 encounters was 2.62% (95% CI: 1.96 to 3.2%) .At 2.27% of total encounters at least one referral to a specialist was recorded.At least quarter of specialist referrals were to emergency room. Problems that were referred to emergency room included bronchiolitis (26.6%), pneumonia (13.3%) and laceration/cut (13.3%). Eighty percent of all problems referred and managed at emergency room were new whereas 20% of them were old.

Table 2 shows that acute bronchiolitis was the most frequently managed problem at referral encounters (8.62%). However, the referrability rate was low (7.35%). In contrast, strabismus was one of the least frequent problems managed at referral encounters (3.44%); however, its referrability rate was high (100%). A similar pattern was seen for refractive errors, pneumonia, alopecia and circumcision.

Table 3 shows that the most frequently managed problems at referral encounters were those of the respiratory tract (22%), skin (16.9%), reproductive (13.55%) and eye the

*Table 1. The distribution of the new referrals, National Guard Housing Primary Care Clinics, Riyadh*

| Diagnostic Categories | Number of Referrals (N=60) | Referrals per 100 Encounters (N=2290) | Percentage of Total Referrals (N=60) | Number of Referral Encounter (N=58) | Percentage Total of Encounters * (N=2290) |
|---|---|---|---|---|---|
| Emergency | (15) | 0.655 | 25.00 | (14) | 0.61% |
| OB/GYN | (10) | 0.437 | 16.67 | (10) | 0.43% |
| Surgery | (9) | 0.393 | 15.00 | (9) | 0.39% |
| Dermatology | (6) | 0.262 | 10.00 | (5) | 0.21% |
| Ophthalmology | (5) | 0.218 | 8.33 | (5) | 0.21% |
| Pediatrics | (5) | 0.218 | 8.33 | (5) | 0.21% |
| ENT | (3) | 0.131 | 5.00 | (3) | 0.131% |
| Family practice | (1) | 0.044 | 1.67 | (1) | 0.044% |
| **Total referrals to the specialists** | (54) | 2.358 | 90.00 | (52) | 2.27% |
| Optometrist | (4) | 0.175 | 6.67 | (4) | 0.175% |
| Dental | (2) | 0.087 | 3.33 | (2) | 0.087% |
| All referrals | (60) | 2.620 | 100.00 | (58) | 2.53 |

**Percentage of encounters at which at least one referral from the corresponding category was given.*

*Table 2:The most frequently managed problems according the ICPC coding system at referral encounters, National Guard Housing Primary care Clinics, Riyadh*

| ICPC Rubric (problems) | Number of Problems at Referral Encounters (N=59) | Rate per 100 Referral encounters (N=58 Encounters) | Number of Total for Each Problem at All Encounters | Rate per 100 Total Encounters (N=2290) | *Referrability rate |
|---|---|---|---|---|---|
| (1) (R78) Bronchiolitis | (5) | 8.62 | (68) | 2.9% | 7.35% |
| (2) (W78) Pregnancy | (4) | 6.89 | (26) | 1.13% | 15.38% |
| (3) (F95) Strabismus | (2) | 3.44 | (2) | 0.087% | 100% |
| (4) (F91) Refractive errors | (2) | 3.44 | (3) | 0.131% | 66.6% |
| (5) (R81) Pneumonia | (2) | 3.44 | (3) | 0.131% | 66.6% |
| (6) (R90) Hypertrophied/ chronic infection tonsilitis and adenoid | (2) | 3.44 | (3) | 0.131% | 66.6% |
| (7) (S11) Infected Post-traumatic wound | (2) | 3.44 | (7) | 0.3% | 28.57% |
| (8) (s18) Laceration/cut skin | (2) | 3.44 | (17) | 0.74% | 11.76% |
| (9) (S23) Alopecia | (2) | 3.44 | (2) | 0.087% | 100% |
| (10) (Y80) Circumcision | (2) | 3.44 | (2) | 0.087% | 100% |
| (11) Others | (34) | 58.6% | (445) | 19.4% | 7.6% |
| *Health professional | (6) | 0.262 | 10.00 | (6) | 0.262% |
| All referrals | (60) | 2.620 | 100.00 | (58) | 2.53 |

**Referrability rate is the frequency of referring a patient with this problem per 100 encounters of this condition encountered in General Practice*

*Table 3: The distribution of the problems managed according to the ICPC morbidity category at referral encounters, National Guard Housing Primary Care Clinics*

| ICPC Chapter | Number of Problems at Referral Encounters (N=59) | Percentage of Problems at Referral encounters (N=59) | Number of Problems at All Encounters | Percentage of Problems at all Encounters (N=2592) | *Referrabi-lity rate |
|---|---|---|---|---|---|
| (R) Respiratory | (13) | 22% | (1322) | 51% | 0.982% |
| (S)Skin | (10) | 16.94% | (178) | 6.88% | 5.61% |
| (W )Reproductive | (8) | 13.55% | (45) | 1.73% | 17.7% |
| (F) Eye | (8) | 13.55% | (96) | 3.7% | 8.33% |
| (D) Digestive | (6) | 10.16% | (257) | 9.91% | 2.18% |
| (A) General | (3) | 5.08% | (355) | 13.69% | 0.84% |
| (L)Musculoskeletal | (3) | 5.08% | (42) | 1.62% | 7.14% |
| (X) Female genital | (3) | 5.08% | (16) | 0.61% | 18.75% |
| (Y) Male genital | (2) | 3.38% | (6) | 0.23% | 33.3% |
| Others | (3) | 5.08% | (150) | 5.78% | 0.02% |

**Referrability rate is the frequency of referring a patient with this problem per 100 encounters of this condition encountered in general practice.*

*Table 4: The distribution of most important reasons for encounters by ICPC chapter at referral encounters, National Guard Housing, Riyadh*

| ICPC Chapter | Number of RFES (N=76) | Percentage of RFES at Referral Encounters (N=76) | Number of RFES at All Encounters | Percentage of RFES at All Encounters (N=3898) |
|---|---|---|---|---|
| (R). Respiratory | (20) | 26.3% | (1837) | 47.12% |
| (S) Skin | (11) | 14.47% | (190) | 4.8% |
| (A) General | (8) | 10.52% | (947) | 24.29% |
| (F) Eye | (7) | 9.2% | (120) | 3.07% |
| (W )Reproductive | (6) | 7.89% | (42) | 1% |
| (X) Female genital | (6) | 7.89% | (24) | 0.6% |
| (D) Digestive | (5) | 6.57% | (363) | 9.3% |
| (H) Ear | (3) | 3.94% | (84) | 2.15% |
| (L )Musculoskeletal | (3) | 3.94% | (49) | 1.25% |
| (Y )Male genital | (3) | 3.94% | (8) | 0.2% |
| (B) Blood | (2) | 2.63% | (77) | 1.97% |
| Others | (2) | 2.63% | (93) | 2.38% |

*REFS: Reasons for Encounters*

least frequent problems managed at referral encounters. (3.38%); however, it is referrability rate was high (33.3%).

Table 4 explores that the reasons related to respiratory tract system were the most frequent reasons for encounter (13.55%). Problems relating to male genitals were one of the least frequent problems managed at referral encounters. (3.38%); however, it is referrability rate was high (33.3%) Table 4 explores that the reasons related to respiratory tract system were the most frequent reasons for encounter (26.3%), which matches with the frequency of respiratory reasons for encounters in the total data (47.1%). In contrast , skin reasons for encounters were three times more frequent than over all data. A similar pattern was seen for eye, reproductive, female and male genitals and musculoskeletal systems. Furthermore, respiratory system reasons for encounters were most commonly expressed in term of symptoms such as "cough" (45%) and "Shortness of Breath" (15%). Skin complaints were also common particularly "laceration/cut (18%), hair loss (18%), and pruritus (18%). General symptoms were common, e.g. fever (62%) being the most frequent.

## Discussion

In the present study, a referral encounters rate of 2.53 per 100 encounters and referral rate of 2.62 per 100 encounters was observed. Referral rate was low when compared to other studies [8,14,17,18]. However, previous national studies showed comparable referral rate [9-12]. This low referral rate in the present study could be explained by the fact that majority of our study population at referral encounters belonged to pediatric age group (66.6%). Moreover, main problems managed at total encounters were related to respiratory tract (58%) while it was uncommon for a patient to be referred for respiratory tract conditions, and referral occurred when general practitioner had an important reason [15]. It was found in this study that referrals for specialist were mainly to emergency room and obstetrics/Gynecology Were higher in comparison with International studies which reported more referrals to general medicine and surgery [7,8].

On the other hand, the overall distribution of primary care referrals to various specialties observed in this study were in conformity with the findings of previous national studies[1,11,12]. However, there was no referral to general medicine and physiotherapists. This could be explained by the fact that our sample constituted young population. It was found that acute bronchiolitis was the most frequent problem managed at referral encounters as compared to other international studies, which had found that hypertension, was the most common problem managed at referral encounters [8]. Again this could be attributed to the study population which was belonged to pediatric group and cardiovascular problems in children were uncommon [15]. The high referrability rate for refractive errors and strabismus were consistent with studies conducted in Australia and Netherlands [8,15]. On the other hand, pneumonia and laceration/cut had high referrability rates of 66.6% and 11.7%, as compared to a study in Netherlands were it was reported as 6% and 4%, respectively [15]. Thus, the high referrability rates for problems such as: strabismus, alopecia, circumcision, refractive errors, chronic infection of tonsil and adenoid, pneumonia and laceration/cut might indicate that General practitioners lack training or equipment to deal with these conditions.

## Conclusion and Recommendations

This study explores that the referrability rate, especially when considered together with the referral rate, provides general practitioners and specialists with a frame of reference for their own workload. The knowledge of variation in the referability rates will enable the decision-makers to improve the training and CME programs. The participation of senior family physicians in clinical sessions in the satellite clinics of high referrability rate is recommended to improve the process and then the quality of care.

## Acknowledgement

I greatly appreciate the tremendous effort and help of Prof. Mohammad Yunus Khan of Family & Community Medicine, College of Medicine & Medical Sciences, King Khalid University, Abha in editing this manuscript.

## References

1. Badawi I, Khattab M, Champbell J. Referral rates and patterns in primary care department Khamis Mushayt, Saudi Arabia. Saudi Med J 1998; 19: 157-161.

2. Sara W, Margarat L. Prescribing and referral in general practice: A study of patient expectations and doctor's actions. Br J Gen Pract 1994; 44: 165-169.

3. Knottnerus J. A. Joosten J. Comparing the quality of referrals of general practitioners with high and average referral rates: an independent panel review. Br J Gen. Pract. 1990; 40: 178-181.

4. Driver B, Britt H, O'Toole B, Harris M, Bridges – Webb C and Neary S. How representative are patients in general practice morbidity surveys? Fam Pract 1991; 8: 261-268.

5. Mc Whiney I. R. A textbook of Family Medicine. 2nd edition. Oxford University Press; 1997.

6. WONCA Classification Committee. International Classification of Primary Care ($ICPC_2$). 2nd edition. Oxford Medical Publication; 1998.

7. Fleming DM. The use of ICPC in the European referral study. In: Lamberts H, Wood M, Hoffman I M.

The International Classification of Primary Care in European Community. Oxford, England; Oxford University, 1993.

8. Bridges-Webb C, Britt H, Miles D, Neary S, Charles J, Traynor V. Morbidity and treatment in general practice in Australia. 1990-1991. Med J Aust1992; 157 Suppl: S1-S56.

9. Al-Mazrou Y, Al-Shammari S, Siddique M, Jarallah J. A preliminary report on the effect of referral system in four areas of Saudi Arabia. Annals of Saudi Med 1991; 11: 663-668.

10. Khoja TA, Shehri AM, Abdul – Aziz AF, Khoja MS. Patterns of referral from health centers to hospitals in Riyadh region. East Medit Health J. 1997; 3: 236-243.

11. Jerallah J, the quality of referral letters in two health centers in Riyadh. Annals of Saudi Med 1991; 11: 658-662.

12. Khattab MS, Abolfotouh M, Al Khaldi Y, Khan MY. Studying the referral system family practice center in Saudi Arabia. Annals of Saudi Medicine 1999; 19: 167-170.

13. International Statistical Classification of Diseases and Related Health Problems. Tenth Revision. World Health organization, Geneva, 1992.

14. Britt H, Meza RA, Del Mar C. Methodology of morbidity and treatment data collection general practice in Australia: A comparison of two methods. J Fam Pract 1996; 13: 462-467.

15. Van Suijekom-Smit LWA, Bruijzeels MA, Van Der Woundern JC' Vanderveldan J, Visser HKA, Dokter HJ. Children referred for specialist care a nation wide study in Dutch general practice. Br J Gen Pract: 1997; 47: 19-23.

16. Dean AG, Dean JA, Coulombier D, Brendel KA, Smith DC, Burton AH et al. EPI info Version 6: a word processing data base and statistics program for public health on IBM-compatible microcomputers Centers for Disease Control and Presentation, Atlanta Georgia, USA. 1996.

17. Frrest CB, Reid RJ.Prevalence of health problems and primary care physicians'specialty referral decisions. J Fam Pract 2001; 50:427-32.

18. Forrest CB, Nutting PA, Strfield B, von Scrader S. family physicians, referral decisions: results from the ASPN referral study. J Fam Pract 2002; 51: 215-222.

**Correspondence to:**

Dr. Khalid S. Al Gelban
Department of Family and Community Medicine
College of Medicine and Medical Sciences
King Khalid University
P.O.Box 641,Abha
Saudi Arabia

Phone: ++96672247800 Ext. 2213
Fax. ++96672247570
e-mail: khalidgelban@hotmail.com

*Biomedical Research 2003; 14 (2): 199-202*

# The role of central noradrenergic system on FSH Secretion induced by excitatory amino acid

**S. Shahabi and A. A. Moghadamnia**

Department of Pharmacoloy and Physiology, Babol University of Medical Sciences, Babool, Iran

**Key words:** Central noradrenergic system, locus coeruleus nucleus, excitatory amino acid, follicle stimulating hormone (FSH)

*Accepted 11 August 2003*

## Abstract

**Excitatory amino acids (EAAs) and noradernaline are known as neurotransmiters which stimulate gonadotropin secretion in female and male animals. This study was designed to evaluate the involvement of central noradrenergic system on FSH secretion induced by EAA in adult male rats.**

**Rats were implanted with monolateral cannula through the locus coeruleus – sub coeruleus (LC-SC) by stereotaxy. Saline or glutamate was injected into the cannula. Blood samples were obtained just 10min later for radioimmunoassay. For investigating the involvement of LC-SC in noradrenergic system, DSP-4 was injected bilaterally one week before glutamate injection.**

**Microinjection of glutamate significantly increased the plasma levels of FSH in compared to that of the control group. Pretreatment with DSP-4 significantly decreased the plasma level of FSH in glutamate treated group.**

**The results indicate that the LC-SC in adult rats is one of the major sites affected by glutamate on FSH secretion by noradrenergic neurons.**

## Introduction

Excitatory amino acids (EAAs) neurotransmission is an essential component of the neuroendocrine transmission line that regulates gonadotropic hormone (FSH, LH) secretion [1,2]. The site of action of EAAs in the regulation of gonadotropin secretion pointed to the hypothalamus is based on the findings that:

A) Glutamate has no effect on gonadotropin release when injected in to the anterior pituitary [3].

B) Microinjection of glutamate in the third ventricle stimulates gonadotropin release [4].

C) EAAs such as glutamate and aspartate, are found in large concentrations in presynaptic buttons of a variety of important hypothalamic nuclei that regulates luteinizing hormone (LH) and follicle stimulating hormone (FSH) [5].

EAAs are able to excite virtually all neurons tested in the hypothalamus including the arcuate nucleus, the median eminance (two major sites of GnRH neurons) and other medial hypothalamic locations [6,7,8]. Administration of GnRH antagonist blocks EAA-induced gonadotropin release in a variety of species [5,9]. Therefore, EAAs possibly stimulate GnRH release through a direct effect.

But it is unclear whether EAAs stimulate GnRH release indirectly through regulation of other neunrotransmitter neurons means an extrahypothalamic site to influence by synaps on GnRH neurons. Catecholamins may mediate the effects of EAA on GnRH and gonadotropin release, but the exact neuronal pathway and the site of action are not yet clear [7,15].

In this present study, we evaluated the involvement of central noradrenergic on FSH secretion by EAA microinjection in locus coeruleus nucleus.

## Material and Methods

### *Animals*

Adult male Wistar rats, weighing 150-250 gm were used. Animals were kept in a controlled lighting schedule of 12h light and 12h darkness and at a constant temperature (20°-22°c). Rat feed and tap water were available ad libitum.

### *Drugs*

Nembutal, glutamate disodium, DSP-4 saline, were obtained from Sigma Chemical Co. Serum concentration of FSH was measured by FSH-IRMA I125 kit (0.1 Iu/L sensitivity).

### *Experimental protocol*

Monolateral cannula was implanted into Locus coeruleus (LC) 4 days prior to the experiments, as described (DV= 6ml , L=1.5ml and AP= -10.04ml) [10].

Microinjections of drugs were applied (2µl/sec) by hamilton syringe in to locus coeruleus nucleus via the cannula. Blood and serum samples were obtained 10 minutes after the drug microinjection into LC-SC nucleus, from orbital sinus of rat [11]. DSP-4 was utilized to induce a bilateraly lesion in locus coeruleus. Seven days before glutamate administration, DSP-4 was microinjected in stereotaxic surgury duration.

The appropriateness of the cannula sites was confirmed by 2µl of neutral red injection in to cannula and then the brain was removed and fixed by 10% formaldehyde. Sections were cut by vibrioslice. Animals containing injections restricted to the locus coeruleus were used in the analysis. FSH levels in plasma were measured using FSH- IRMA I125 kit with 0.1 Iu/l sensitivity.

### *Experimental groups*

Four groups of animals were recruited:

1. Un-manipulated group: Animals without surgery or drug treatment. Blood samples were collected and assayed by IRMA.
2. Control group: Cannulated animals were used after surgical recovery. 10µl of saline weremicroinjected into LC nucleus 10 minutes before blood sampling.
3. Glutamate group: Cannulated animals were used after recovery period. 20µg/ 10µl of glutamate (dilluted in-saline) were microinjected in to LC-SC nucleus 10 minutes before blood sampling.
4. Glutamat & DSP-4 group: Cannulated animals with chemical lesioning of LC-SC by DSP-4 (50µg/1µl, 7 days before glutamate injection) were used. Then 20µg/10µl of glutamate were microinjected into LC-SC nucleus 10 minutes before blood sampling.

Statistical analysis was performed utilising one- way ANOVA followed by Newman-Keuls post test. The difference between the data was considered statistical significant at $p<0.05$.

## Results

**Serum concentration of FSH (follicle-stimulating hormone) in adult male rat were 0.26-0.4 IU/l.**

Figure1. displays the effect of glutamate microinjection into LC on serum concentration of FSH in male rats in comparision with control and normal groups ($p<0.02$). As illustrated in Fig-2, chemical lesioning of LC-SC by DSP-4, 7 days before glutamate microjectionm, could completely reverse the glutamate effect on FSH release.

***Table 1: Effect of glutamate administration in LC-SC on serum concentration of FSH in rats***

| Groups | Number of rats | FSH concentration (IU/L) (mean±S.D) |
|---|---|---|
| Normal | 14 | 0.3279±0.011 |
| Control | 10 | 0.3380±0.016 |
| Glutamate | 11 | 0.8628±0.27 |
| Glutamate and DSP-4 | 9 | 0.3311±0.008 |

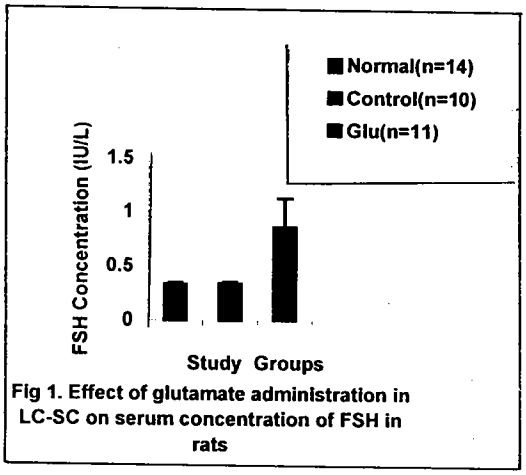


**Fig 1. Effect of glutamate administration in LC-SC on serum concentration of FSH in rats**

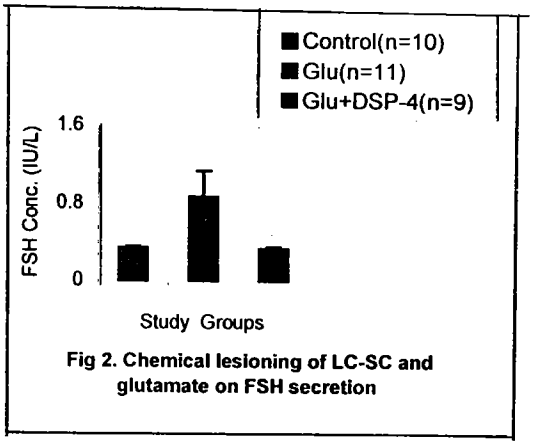


**Fig 2. Chemical lesioning of LC-SC and glutamate on FSH secretion**

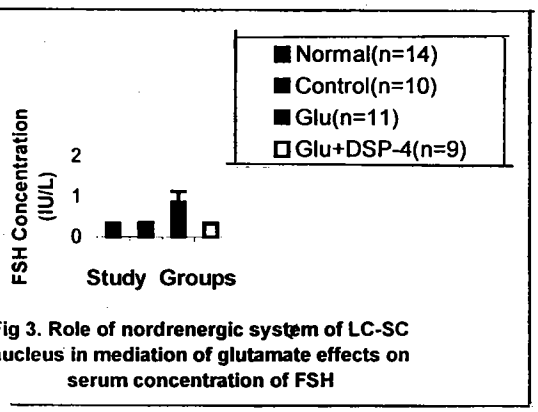


**Fig 3. Role of nordrenergic system of LC-SC nucleus in mediation of glutamate effects on serum concentration of FSH**

## Discussion

Several studies have reported that EAA can stimulate gonadotropin release [12] via inducing GnRH release in the medial hypothalamic region, preoptic area and arcuate nucleus. Other studies have reported that EAA can stimulate the nerve responsible for gonadotropin – releasing hormone (GnRH) [13,14].

The major site of NMDA (a kind of EAA) action apears to in preoptic area, where GnRH cell bodies reside. AMPA and kainate (another kinds of EAA) appear to act primarily at the arcuate nucleus/ median eminence, the site of GnRH nerve terminal. Hence the induction of the GnRH and gonadotropin release by involve enhanced EAA neurotransmission [15].

EAA stimulate GnRH release through a direct effect on GnRH neurons. Likewise EAAs could act at an extrahypothalamic site to influence GnRH release. For instance, NMDA has been shown to induced c- fos activation in noradrencergic cells in the LC , a major noradrencergic nucleus in the pons which sends projetions to the hypothalamus [15]. Since catecholamines are major regulators of GnRH and gonadotropin release. In addition, anatomical projections between locus coeruleus nucleus and median eminence and the other hypothalamic region was reported [1,15]. These evidences supporting the role of EAAs derived from CNS on gonadotropin and FSH (follicle stimulating hormone) release.

EAA also stimulate catecholamine release in the hypothalamus. Hence EAA effect on GnRH release could be mediated by activation of catecholamine neurons in LC nucleus.

In the present study we evaluated the involvement of central noradrenergic system on EAA stimulated FSH secretion by EAA microinjected in LC-SC nucleus in rats. Microinjection of glutamate significantly increased the serum level of FSH in comparsion to control and normal groups ($p<0.02$). Since glutamate is the most abundant amino acid in brain [16] and is major excitatory neurotransmitters in the neuroendocrin system (5), these results have demonstrated glutamate effect on FSH secretion via the activation in LC, a major noradrenergic system nucleus , in the pons which sends projections to the hypothalamus. Hence either hypothalmic regions or extrahypothalmic regions play a role in control of FSH release.

Therefore, glutamate could act to increase FSH via activation of LC neurons to colocalization secretion on GnRH neurons. Also, chemical lesioning of LC before glutamate microinjection by DSP-4 and decrease serum concentration of FSH clearly demonstrate that LC nucleus is an important component in the neurotransmission line responsible of regulating function in the hypothalamus. It is concluded that:

1. Locus coeruleus is an important extrahypothalamic regulatory center of GnRH and FSH secretion.

2. Excitatory amino acid affects the release of FSH by activation of central noradrenergic system in LC.

## Acknowledgement

This investigation was supported by a grant from Babol University of Medical Sciences, Iran. We would like to thank the members of the research department of the University for their supporting of this work.

## References

1 Saitoh Y, Silverman AJ, Gibson MJ. Norepinephrine neuronse in mouse locus coeruleus express c-fos protein after N-Methyl D,L- Aspartic Acid (NMDA) treatment. Brain Res 1991; 561: 11-19.

2 Honaramooz A, Cook SJ, Beard AP, Bartiewsk PM, Rawlling NC. Nitric oxide regulation of gonadtropin secretion in prepubertal heifersl. J Neuroendocrinol 1999; 11: 667-676.

3 Blandina P, Johnson D, Walcott J, Goldfrab J. Release of endogenous norepinephrine from rat hypothalamus by stimulation of N-Methyl D,L Aspartic Acid receptors. J Pharmacol Exp Ther 1992; 263: 61-68.

4 Lopez FJ, Donso AO, Negero– Villar A. Endogenous excitatory amino acid neurotransmission regulates the estradiol–induced LH surge in ovariectomized rats. Ecdocrinol 1990; 126: 1771-1773.

5 Lopez FJ, Donso AO, Negero– Villar A. Endogenous excitatory amino acids and glutamate receptor subtypes involved in the control of hypothalamic luteinizing hormone releasing hormone secretion. Endocrinol 1992; 130: 1986-1992.

6 Bettendorf M, De-Zegher F, Albers N, Hart CS, Kaplan SL, Grumbach MM. Acute N-Methyl D, L-Aspartate administration stimulates the luteinizing hormone pulse generator in the ovine fetus. Horm Res 1999; 51: 25-30.

7 Scacchi P, Carbone S, Szwarcfarb B, Wuttke W, Moguilevsky JA. Interaction between gabaergic and serotonergic systems with excitatory amino acid neurotransmission in the hypothalamic control of gonadotropin secretion in prepubertal female rats. Brain Res Dev Brain Res 1998; 105: 51-58.

8 Minegishist KH, Tano M, Kameda T, Hirakawa T, Miyamoto K. Control of FSH receptor mRNA expression in rat granulose cells by 3,5- cyclic adenosine monophosphate, activin, and follistain. Mol Cell Endocrinol 1999; 146: 71-77.

9 Brann DW, Mahesh VB. Endogenous excitatory amino acid involvement in the preovulatory and steroid induced surge of gonadotropins in the female rat. Endocrinol 1991; 128: 1541-1547.

10 Rodriguez MG. Blockade of the establishment of the sexual inhibition resulting from sexual exhaustion by the Coolidge effect. Behav Brain Res 1999; 100: 25-54.

11 Paxinose G. The rat nervous system. Vol 1 and 2, Academic Press, Australia 1985; 56.

12 Stone SH. Method for obtaining venius blood from the orbital sinus of the rat mouse. Science 1954; 100-119

13 Pinillal T, Sempere M, Aguilar E.Role of excitatory amino acid pathways in control of gonadotropin secretion in adult female rats sterillized by neonatal administration of estradiol or testosterone. J Reprod Fertill 1998; 113: 53-9.

14 Mahesh VB, Brann DW. Neuroendocrine mechanisms underlying the control of gonadotropin secretion by steroid. Steroids 1998; 63: 253-259.

15 Brann DW, Mahesh VB. Excitatory amino acids: function and significance in reproduction and neuroendocrine regulation. Front Neuroendocrinol 1994; 15:3-49.

16 Eonnum F. Glutamate: a neurotransmitter in mammalian brain. J Neurochem 1984; 42: 1-11.

**Correspondence to:**

Dr. A. A. Moghadamnia
Department of Pharmacoloy and Physiology
Babol University of Medical Sciences
Babool
Iran

e-mail: moghadamnia@yahoo.com

*Biomedical Research 2003; 14(2): 203-210*

# Vascular endothelial Growth Factor (VEGF) and Parathyroid Hormone (PTH)/PTH-Related Peptide (PTHrP) receptor in the femoral head of the growing rat

**M. Hyakutake, T. Saga, K. Yamaki and M. Yoshizuka**

Department of Anatomy, Kurume University School of Medicine, Kurume 830-0011, Japan

Key words: VEGF, PTH/PTHrP receptor, femoral head, developmental biology, vascularization, Rat

*Accepted August 22 2003*

## Abstract

**Recently, we clearly demonstrated that chondrocytes in the femur produce vascular endothelial growth factor (VEGF) before the beginning of ossification, and suggested that VEGF plays an important role in the penetration of blood vessels into the femoral head. In this study, we further examined the expression of parathyroid hormone (PTH)/PTH-related peptide (PTHrP) receptor in the growing femur using an immunocytochemical technique. In the fetus, VEGF immunoreactivity was demonstrated in the mesenchymal cells, periosteum, perichondrium and chondrocytes in the peripheral region of the femoral head. In the same stage, PTH/PTHrP receptors were distributed in almost the same regions as the VEGF-positive cells. For several postnatal days, VEGF immunoreactivity was observed in the osteoblasts, osteoclasts, periosteum, perichondrium and cartilage matrix of the femur. On the other hand, PTH/PTHrP receptors were not present in the cartilage matrix, but showed a similar distribution pattern to VEGF in the other regions. At a more advanced young stage, VEGF-immunoreactive chondrocytes appeared in the apex area of the femoral head and gradually increased in number. Thereafter, penetration of capillaries into the VEGF-immunopositive region was observed. In this stage, PTH/PTHrP receptors were distributed throughout the entire articular cartilage in the femoral head. In the adult, VEGF immunoreactivity disappeared in the articular cartilage, but immunoreactivity for PTH/PTHrP receptors was clearly observed. These results indicate that although the expression of VEGF and existence of PTH/PTHrP receptors were not equal, these factors have a close relationship for osteogenesis. VEGF plays an important role in the regulation of angiogenesis, and VEGF expression may be controlled by PTH/PTHrP via PTH/PTHrP receptors in the growing femur.**

## Introduction

VEGF is known to stimulate endothelial cell growth and angiogenesis [1,2,3], and to act as a vascular permeability factor (VPF) to induce microvascular hyperpermeability [4,5]. Furthermore, Horner et al [6] reported the immunolocalization of VEGF in human neonatal growth plate cartilage. They demonstrated that hypertrophic chondrocytes produced VEGF and suggested that VEGF may play a key role in the regulation of vascular invasion of the growth plate. Recently, Gerber et al [7] reported the role of VEGF in endochondral bone formation of the mouse. They indicated that VEGF is an essential coordinator of chondrocyte death, chondroclast function, extracellular matrix remodeling, angiogenesis and bone formation in the growth plate. Furthermore, chondrocytes originate from pluripotent mesenchymal progenitors which also give rise to osteoblasts, adipocytes and other cell types [8]. The expression of VEGF is upregulated with increasing differentiation of osteoblasts, adipocytes and myoblasts, suggesting that the production of VEGF is a common event linked to the differentiation of mesenchyme-derived cells [9,0]. It is also well known that VEGF is produced in various normal tissues [11], embryos and tumors [12]. However, little information is available about the occurrence of VEGF during bone formation in the femoral head of the growing rat. Therefore, we examined the appearance of VEGF in the rat femoral head during bone forma-

tion and discussed the relationship with vascularization [13]. The results indicated that some chondrocytes in the femoral head produced VEGF before the beginning of ossification, and that VEGF may play an important role in the penetration of blood vessels into the femoral head from the ligament of the femoral head.

Furthermore, in this study, the expression of PTH/PTHrP receptors was analyzed immunocytochemically as a factor concerned with osteogenesis. It is known that PTHrP and PTH/PTHrP receptors are expressed in many kinds of tissues [14] and act as modulators of cell differentiation and growth [15-23]. It has been reported that PTHrP appears in cartilage and bone in embryogenesis [24]. Moreover, Karaplis et al [25] reported that PTHrP gene knockout mice had osteochondrodysplasia that only existed for several postnatal hours. They suggested that PTHrP has a very important role in chondrogenesis. Recently, Amizuka et al [26] reviewed the biological action of PTHrP and PTH/PTHrP receptors in cartilage and bone.

However, the relationship between VEGF and PTH/PTHrP receptors in embryogenesis is not clear. In this study, we examined the appearance of VEGF and PTH/PTHrP receptors in the femoral head of the growing rat, and discuss the relationship between the expressions of VEGF and PTH/PTHrP receptors.

## Materials and Methods

This study was carried out after permission had been granted by the Committee for Animal Experimentation, Kurume University. Wistar rats (19-day fetuses and 1 - 60 day-old rats) were used in this study.

At least five animals at each stage were sacrificed by decapitation under deep anaesthesia at 10 a.m. and the femurs were extracted. The femurs were fixed in Bouin solution for 24 h - 2 weeks. The samples were then decalcified and dehydrated through a series of solutions containing increasing concentrations of ethanol. Samples were embedded in paraffin, and serial sagittal sections at 4 μm were mounted on glass slides. Sections were stained with Haematoxylin-Eosin and toluidine blue to permit observation of the general structure of the femur at each developmental stage.

## Immunocytochemistry

A primary antibody generated against human recombinant VEGF165 was used as an immunocytochemical probe (NeoMarkers, USA; diluted 1:500). This polyclonal antibody recognizes multiple isoforms of VEGF containing 206-, 188-, 165- and 121-amino acid residues in humans, mice and rats. The other primary antibody used was generated against PTH/PTHrP receptors (Santa Cruz Biotechnology Inc., USA; diluted 1:500).

Immunocytochemical staining was performed with a Histofine kit (Nichirei, Japan). Briefly, sections were deparaffinized in xylene, hydrated in a graded ethanol series, and washed in phosphate-buffered saline (10 mM sodium phosphate, 0.15 M sodium chloride, pH 7.5; PBS). All procedures were performed at room temperature, and incubations were performed in closed humid chambers. First, the tissue sections were incubated for 30 min in methanol containing 0.3% hydrogen peroxide to block endogenous peroxidase activity, and then washed in PBS. To reduce nonspecific staining of the biotinylated anti-rabbit IgG, sections were treated with normal goat serum for 30 min, and then washed in PBS. The primary antiserum was applied to the sections for 2 to 24 h, and then the biotinylated anti-rabbit IgG and peroxidase-conjugated streptavidin were applied for 1 h each. The final immunoreactive products were visualized with 3,3'-diaminobenzidine tetrahydrochloride in 50 mM Tris-HCl buffer (pH 7.6) containing 0.003% hydrogen peroxide. Sections were then counter-stained with haematoxylin, washed in running water, dehydrated through an increasing ethanol concentration series, and mounted in Diatex (Ab Wilh Becker, Sweden). To confirm the specificity of the immunocytochemical staining, the primary antiserum was replaced by PBS for the control sections.

## Results

In the 19-day-old fetus, almost all of the femoral head was composed of cartilage cells, and both VEGF and PTH/PTHrP receptor immunoreactivities were demonstrated. VEGF immunoreactivity was observed in the immature chondrocytes at the peripheral region of the femoral head. Moreover, mesenchymal cells around the femoral head were immunoreactive for the VEGF165 antibody (Fig. 1a). At the same stage, PTH/PTHrP receptor immunoreactivities were widely demonstrated on almost all of the immature chondrocytes in the femoral head and mesenchymal cells in the peripheral region (Fig. 1c). In the diaphysis, both VEGF and PTH/PTHrP receptor immunoreactivities were intensely demonstrated in the periosteum, perichondrium, osteoblasts and osteoclasts, and in the small number of chondrocytes in the distal end of the hypertrophic zone (Figs. 1b and d).

To confirm the specificity of these immunoreactivities, the primary antisera were replaced by PBS for the control sections, and no immunopositive reactions were found.

At one day after birth, immunoreactivities against VEGF and PTH/PTHrP receptor antibodies were demonstrated in the periosteum, perichondrium, osteoblasts and osteoclasts, and in chondrocytes in the distal end of the hypertrophic zone of the femur (Figs. 2a and b). In this stage, the femoral head consisted of mature chondrocytes that exhib ited no immunoreactivities with the VEGF and PTH/PTHrP receptor antibodies.

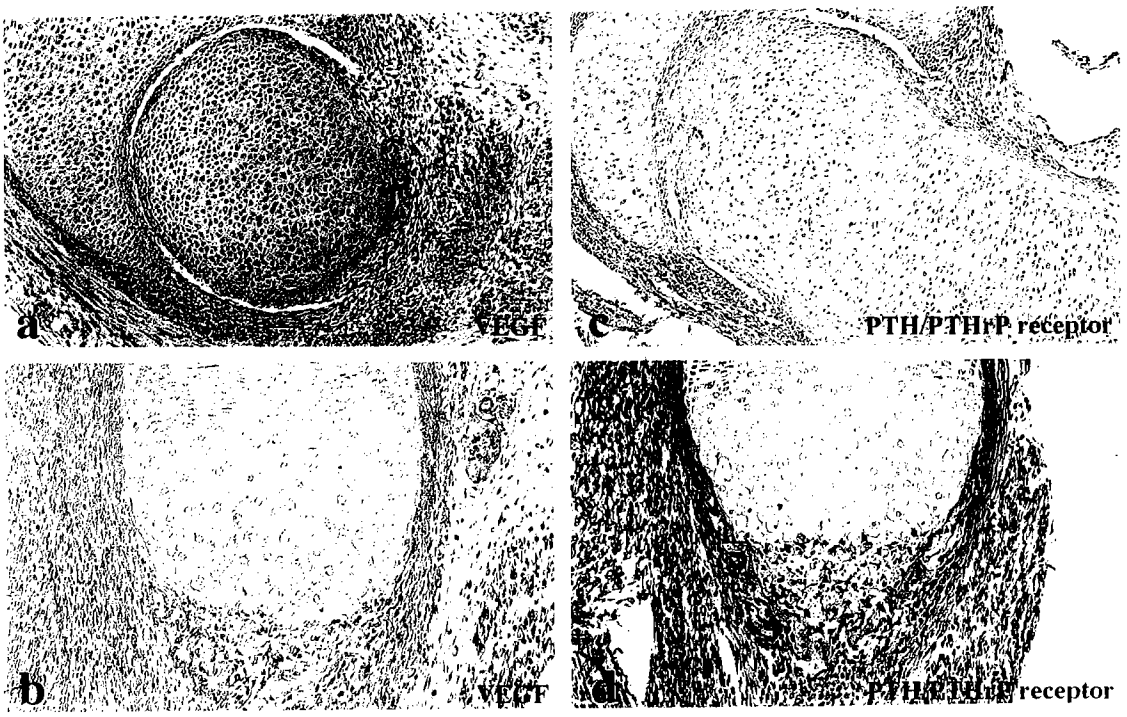


*Fig. 1: Femoral head of the 19-day-old fetus immunostained with VEGF antibody (a and c) and PTH/PTHrP receptor antibody (b and d). (a) VEGF immunopositive immature chondrocytes at the peripheral region of the femoral head and mesenchymal cells around the femoral head are shown. x75. (b) VEGF immunopositive periosteum, perichondrium, osteoblasts, osteoclasts and chondrocytes in the distal end of the hypertrophic zone. x90. (c) PTH/PTHrP receptors were widely demonstrated on almost all of the immature chondrocytes in the femoral head and mesenchymal cells. x75. (d) PTH/PTHrP receptors in the same region of (b). x90.*

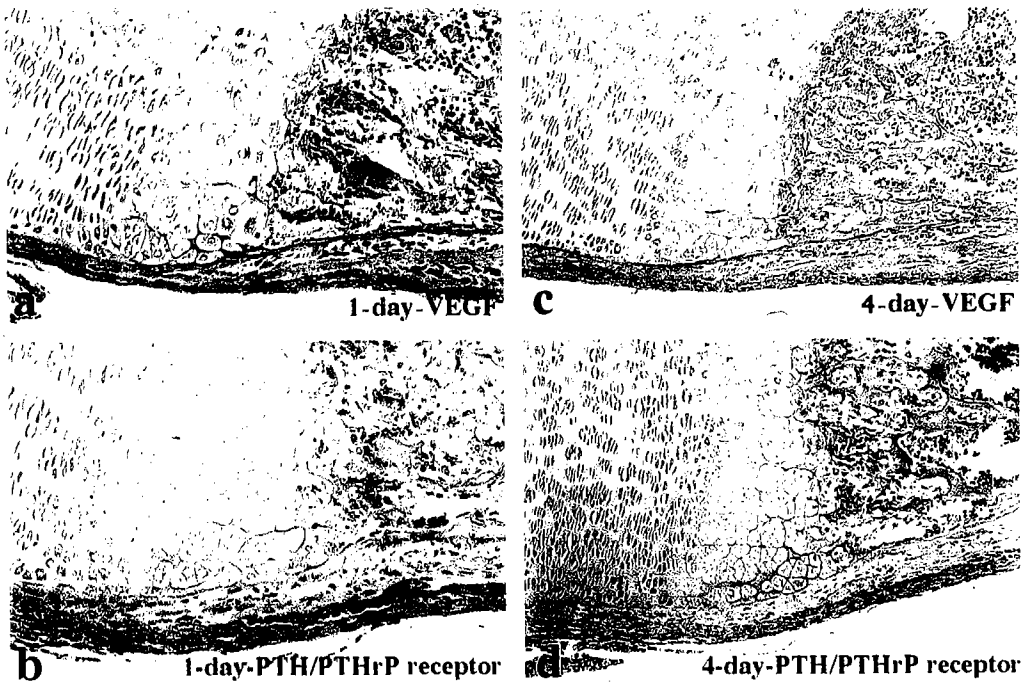


*Fig. 2: Boundary area of the femoral head and metaphysis. (a and b) One-day-old rat. Immunostained with VEGF antibody (a) and PTH/PTHrP receptor antibody (b). x70. (c and d) Four-day-old rat. Immunostained with VEGF antibody (c) and PTH/PTHrP receptor antibody (d). x60.*

At four days after birth, weak but apparent VEGF immunoreactivity appeared in the chondrocytes in the peripheral region of the proliferating zone and distal end of the hypertrophic zones (Fig. 2c). On the other hand, no PTH/PTHrP receptor immunoreactivity was observed in the chondrocytes in the peripheral region of the proliferating zone (Fig. 2d). Immunopositive periosteum, perichondrium, osteoblasts and osteoclasts were observed, similar to one day after birth (Figs 2c and d).

At seven days after birth, chondrocytes in the proliferating and hypertrophic zones, in particular, exhibited more intense immunoreactivity for the VEGF antibody. Moreover, the cartilage matrix around the chondrocytes demonstrated VEGF immunoreactivity, but no PTH/PTHrP receptor immunoreactivity (Fig 3a).

At 10 days after birth, more intense VEGF immunoreactivity was detected in the cartilage matrix at the peripheral region of the femoral head (Fig. 3c). Moreover, at the apex area of the femoral head, VEGF immunoreactivities appeared in the chondrocytes and cartilage matrix (Fig 3b). In this stage, PTH/PTHrP receptor immunoreactivity appeared in the chondrocytes at the peripheral region of the femoral head (Fig. 3d), whereas the cartilage matrix showed no immunoreactivity.

At 15 days after birth, apparent VEGF immunoreactivity was demonstrated in the chondrocytes at the apex area of the femoral head. Moreover, the perichondrial cells at the apex of the femoral head exhibited VEGF immunoreactivity (Fig. 4a).

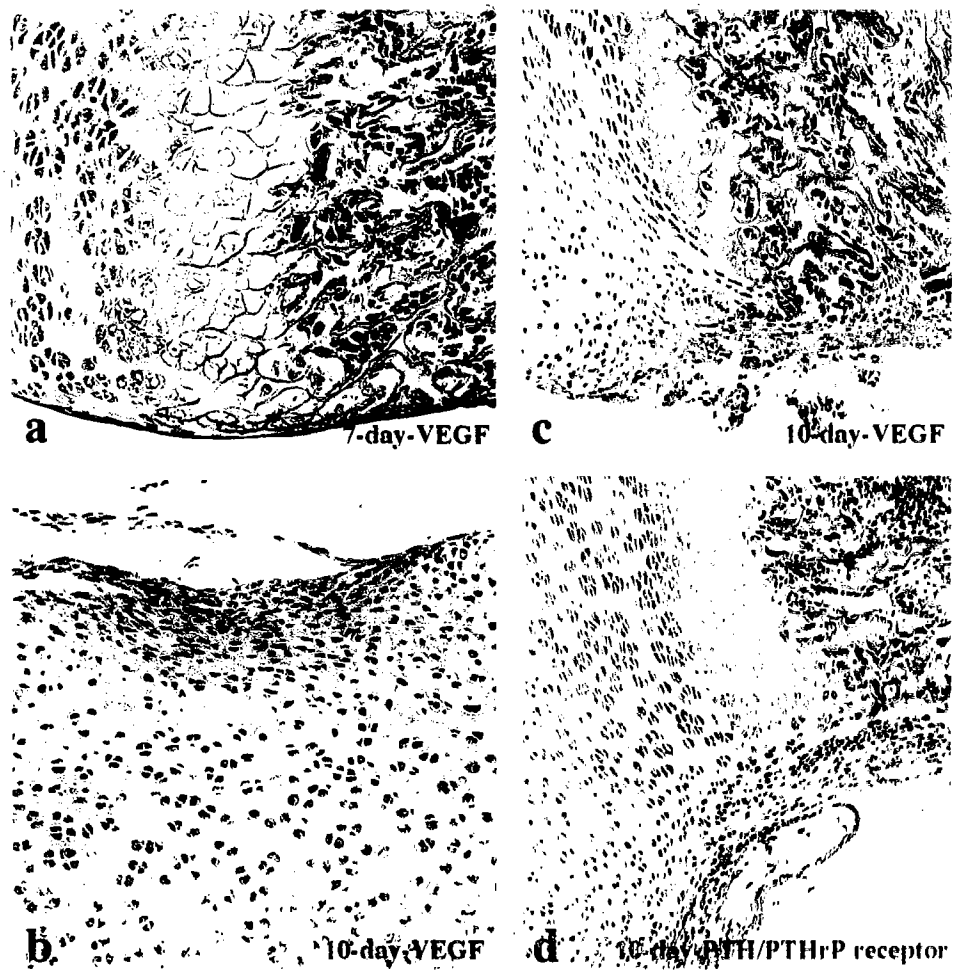


*Fig. 3: (a) Boundary area of the femoral head and metaphysis in the 7-day-old rat is shown. The cartilage matrix around the chondrocytes demonstrated VEGF immunoreactivity. x70. (b) The apex area of the femoral head immunostained with VEGF antibody in the 10-day-old rat. x100. Boundary area of the femoral head and metaphysis immunostained with VEGF antibody (c) and PTH/PTHrP receptor antibody (d) in the 10-day-old rat. x70.*

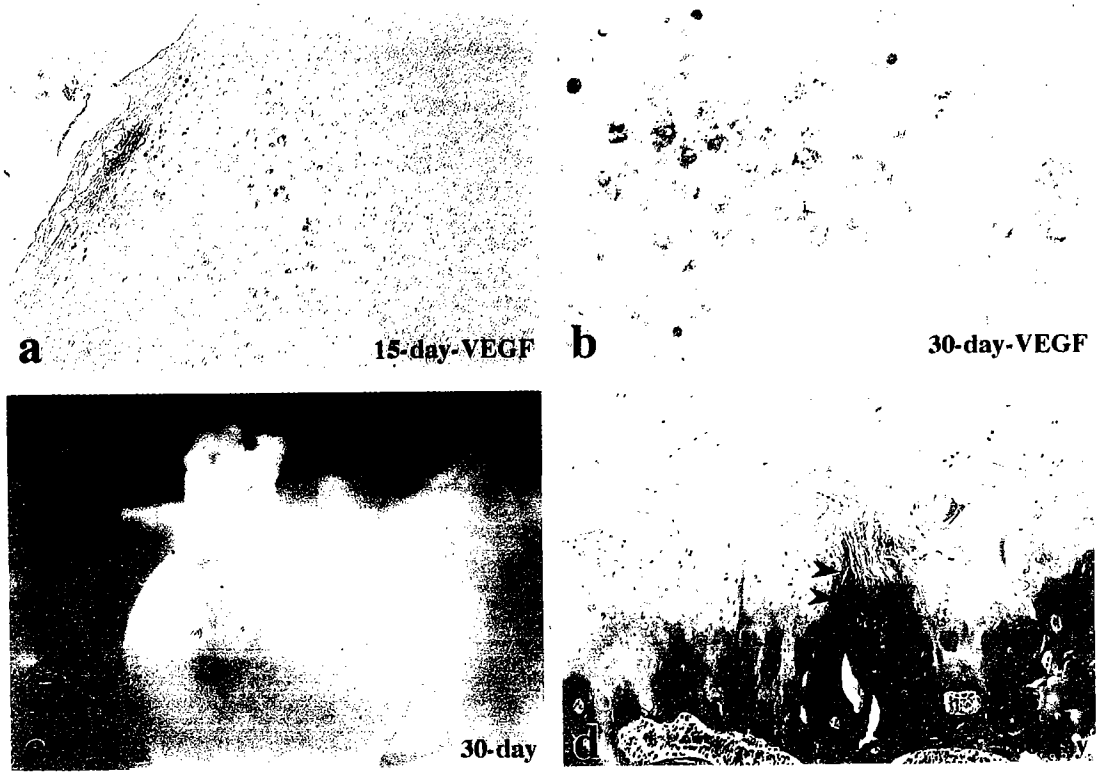


*Fig. 4: (a) Apex area of the femoral head immunostained with VEGF antibody in the 15-day-old rat. Immunopositive perichondrial cells and chondrocytes are shown. x45. (b) Apex area of the femoral head immunostained with VEGF antibody in the 30-day-old rat. Immunopositive chondrocytes developed and increased in number. x200. (c) In the 30-day-old rat, some capillaries were observed at the surface of the ligament of the femoral head. x17. (d) Apex area of the femoral head stained with H&E in the 60-day-old rat. A few capillaries (arrow heads) were observed in the ligament. x60*

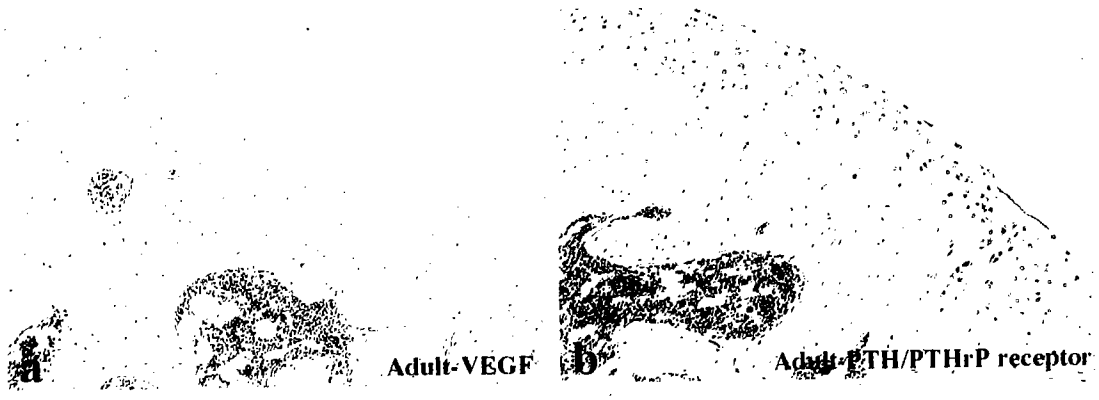


*Fig. 5: Femoral head of the adult rat immunostained with VEGF antibody (a) and PTH/PTHrP receptor antibody (b). x80.*

In this stage, the femoral head still consisted of chondrocytes, and no apparent vascular formation was observed in the femoral head.

At 20 days after birth, VEGF-immunoreactive chondrocytes in the apex area of the femoral head increased in number, and VEGF immunoreactivity was observed in the cartilage matrix around the VEGF-immunoreactive chondrocytes as mentioned above. Moreover, these immunopositive chondrocytes developed and further increased in number at 30 days after birth (Fig. 4b). At 15 to 30 days after birth, PTH/PTHrP receptor immunoreactivities were

demonstrated in all zones of the articular cartilage. In this stage, some capillaries were observed at the surface of the ligament of the femoral head (Fig 5a).

At 60 days after birth, a few capillaries were observed in the ligament of the femoral head. These capillaries penetrated into the apex area of the femoral head where VEGF-immunopositive chondrocytes and cartilage matrix had previously been identified (Fig. 5b).

In the adult rat, no apparent immunoreactivity against the VEGF antibody was demonstrated in the articular cartilage of the femoral head (Fig. 6a). On the other hand, PTH/PTHrP receptors were demonstrated in all zones of the articular cartilage of the femoral head (Fig. 6b).

## Discussion

This is the first report demonstrating the appearance of VEGF and PTH/PTHrP receptors in comparison with vascularization in the femoral head in the growing rat. In our previous report [13], the appearance of VEGF was clarified in the femoral head, and the results suggested that VEGF may have a very important role in the vascularization of the femoral head in the growing rat. In addition, we have now investigated the appearance of PTH/PTHrP receptors and discuss the relationship with VEGF.

It has been reported that VEGF stimulates the differentiation of mesenchyme-derived cells [9,10]. In this study, many VEGF- and PTH/PTHrP receptor-immunopositive mesenchymal cells were found around the femoral head in the 19-day-old fetus. These mesenchymal cells demonstrated no immunoreactivity with the PBS that was used as a negative control in place of the primary antisera. Therefore, we consider that these VEGF and PTH/PTHrP immunoreactivities are specific. Moreover, the results indicate that the VEGF produced by mesenchymal cells around the femoral head might induce angiogenesis toward the femur during early bone formation. PTH/PTHrP receptors were expressed by mesenchymal cells and more intensely produced by the perichondrial cells. Senior et al [24] reported that the cartilage cells and other cells expressed PTHrP mRNA at this stage. The PTHrP probably controls the differentiation of the PTH/PTHrP receptor-expressing cells. There was no PTH/PTHrP receptor immunopositivity in the chondrocytes of the femoral head in this stage, and this seems to be because the chondrocytes are actively proliferating and not differentiating into the prehypertrophic chondrocytes that are the target cells of PTHrP.

After birth, VEGF and PTH/PTHrP receptors were demonstrated in the osteoblasts, osteoclasts, periosteum and perichondrium around the femoral head. VEGF, an endothelial cell-specific mitogen, is an essential mediator of angiogenesis [12]. Angiogenesis is essential for bone growth and healing [27,28,29], and the recruitment of osteoblasts coincides with vascular invasion [30,31]. Therefore, the VEGF produced in osteoblasts and osteoclasts might play a key role in the formation of microvessels at the metaphysis of the newborn rat. Moreover, the existence of VEGF in the periosteum and perichondrium suggests that VEGF has an intimate relationship with the angiogenesis in the periosteum and perichondrium. Karaplis et al [25] suggested the importance of PTHrP during chondrogenesis using PTHrP gene knockout mice. Therefore, the fact that VEGF and PTH/PTHrP receptors are expressed in the same cells suggests the possibility that PTHrP has an effect on the cells expressing VEGF.

At a more advanced stage, VEGF appeared in the chondrocytes at the proliferative and hypertrophic zones and in the cartilage matrix at the peripheral region of the femoral head. On the other hand, PTH/PTHrP receptors were not expressed in the chondrocytes and cartilage matrix in the same region where VEGF was expressed. It seems that the VEGF demonstrated in the proliferative and hypertrophic zones may play a role in the regulation of vascular formation in the elongation of the femur. Since there were no PTH/PTHrP receptors in the chondrocytes of the epiphysis, it is considered that PTHrP does not affect the chondrocytes in this area and the chondrocytes actively proliferate. The VEGF demonstrated in the cartilage matrix may be considered to be secreted by chondrocytes, whereas PTH/PTHrP is not secreted by the chondrocytes since the PTH/PTHrP receptor is the membrane receptor for PTHrP.

In the young rat, VEGF was demonstrated in the chondrocytes at the apex area of the femoral head. The apex area of the femoral head is the presumptive secondary ossification area. On the surface of this region, a few capillaries penetrated within the ligament of the femoral head at 60 days after birth. Recently, Morini et al [32] reported that capillary invasion into the femoral head first occurred in 9-week-old rats. These results indicate that the VEGF appearing in the chondrocytes at the apex area of the femoral head may play an important role in the microvascular invasion of the ligament of the femoral head. In fact, since the blood vessels from the ligament of the femoral head are not abundant, the femoral head is mainly supported by blood vessels originating from the metaphysis. We consider that the vessels coming from the metaphysis are induced by the VEGF secreted from the chondrocytes in the proliferative and hypertrophic zones. PTH/PTHrP receptors were expressed in the articular cartilage from the young to the adult rat, and this fact suggests that PTHrP suppresses the differentiation of articular cartilage to hypertrophic chondrocytes and osteogenesis. Naturally, VEGF was not expressed in the articular cartilage, since blood vessels are not formed there.

In conclusion, the early expression of VEGF and PTH/PTHrP receptors have a close relationship for osteogenesis. VEGF, in particular, plays an important role in regulating the angiogenesis at each site of endochondral bone

formation. PTH/PTHrP may control the expression of VEGF by regulating the differentiation of the osteoblasts, osteoclasts and chondrocytes in early developmental stages.

## Reference


1. Ferrara N, Henzel WJ. Pituitary follicular cells secrete a novel heparin-binding growth factor specific for vascular endothelial cells. Biochem Biophys Res Commun 1989; 161: 851-858.

2. Gospodarowicz D, Abraham JA, Schilling J. Isolation and characterization of a vascular endothelial cell mitogen produced by pituitary-derived folliculo stellate cells. Proc Natl Acad Sci USA 1989; 86: 7311-7315.

3. Leung DW, Cachianes G, Kuang EJ, Goeddel DV, Ferrara N. Vascular endothelial growth factor is a secreted angiogenic mitogen. Science 1989; 246: 1306-1309.

4. Senger DR, Galli SJ, Dvorak AM, Perruzzi CA, Harvey VS, Dvorak HF. Tumor cells secrete a vascular permeability factor that promotes accumulation of ascites fluid. Science 1983; 219: 983-985.

5. Connolly DT, Heuvelman DM, Nelson R, Olander JV, Eppley BL, Delfino JJ, Diegel NR, Leimgruber RM, Feder J. Tumor vascular permeability factor stimulates endothelial cell growth and angiogenesis. J Clin Invest 1989; 84: 1470-1478.

6. Horner A, Bishop NJ, Bord S, Beeton C, Kelsall AW, Coleman N, Compston JE. Immunolocalization of vascular endothelial growth factor (VEGF) in human neonatal growth plate cartilage. J Anat 1999; 194: 519-524.

7. Gerber HP, Vu TH, Ryan AM, Kowalski J, Werb Z. Ferrara N. VEGF couples hypertrophic cartilage remodeling, ossification and angiogeneis durin endochondral bone formation. Nature Med 1999; 5: 623-628.

8. Rodan GA, Noda M. Gene expression in osteoblastic cells. Crit Rev Eukaryotic Gene Expression 1991; 1: 85-98.

9. Claffey KP, Vilkison WO, Spiegelman BM. Vascular endothelial growth factor; regulation by cell differentiation and activated second messenger pathways. J Biol Chem 1992; 23: 16317-16322.

10. Harada S, Nagy JA, Sullivan KA, Thomas KA, Endo N, Rodan GA, Rodan SB. Induction of vascular endothelial growth factor expression by prostaglandin E2 and E1 in osteoblasts. J Clin Invest 1994; 93: 2490-2496.

11. Fan L, Iseki S. Immunohistochemical localization of vascular endothelial growth factor in the endocrine glands of the rat. Acta Histol Cytol 1998; 61: 17-28.

12. Ferrara N, Davis-Smyth T. The biology of vascular endothelial growth factor. Endocr Rev 1997; 18: 4-25.

13. Ichigatani M, Saga T, Yamaki K, Yoshizuka M. Appearance of vascular endothelial growth factor (VEGF) in femoral head in the growing rat. Histol Histopathol 2001;16: 463-468.

14. Ureña P, Kong XF, Abou-Samra AB, Jüppner H, Kronenberg HM, Potts Jr JT, Segre GV. Parathyroid hormone (PTH)/PTH-related peptide receptor messenger ribonucleic acids are widely distributed in rat tissues. Endocrinology 1993; 133: 617-623.

15. Merendino Jr JJ, Insogna KL, Milstone LM, Broadus AE, Stewart AF. A parathyroid hormone-like protein from cultured human keratinocytes. Science 1986; 231: 388-390.

16. Ikeda K, Weir EC, Mangin M, Dannies PS, Kinder B, Deftos LJ, Brown EM, Broadus AE. Expression of messenger ribonucleic acids encoding a parathyroid hormone-like peptide in normal human and animal tissues with abnormal expression in human parathyroid adenomas. Mol Endocrinol 1988; 2: 1230-1236.

17. Thiede MA, Rodan GA. Expression of a calcium-mobilizing parathyroid hormone-like peptide in lactating mammary tissue. Science 1988; 242: 278-280.

18. Drucker DJ, Asa SL, Henderson J, Goltman D. The parathyroid hormone-like peptide gene is expressed in the normal and neoplastic human endocrine pancreas. Mol Endocrinol 1989; 3: 1589-1595.

19. Thiede MA, Daifotis AG, Weir EC, Brines ML, Burtis WJ, Ikeda K, Dreyer BE, Garfield RE, Broadus AE. Intrauterine occupancy controls expression of the parathyroid hormone-related peptide gene in preterm rat myometrium. Proc Natl Acad Sci USA 1990; 87: 6969-6973.

20. Moseley JM, Hayman JA, Danks JA, Alcorn D, Grill V, Southby J, Horton MA. Immunohistochemical detection of parathyroid hormone-related protein in human fetal epithelia. J Clin Endocrinol Metab 1991; 73: 487-484.

21. Kaiser SM, Laneuville P, Bernier SM, Rhim JS, Kremer R, Goltzman D. Enhanced growth of a hu-

man keratinocyte cell line induced by antisense RNA for parathyroid hormone-related peptide. J Biol Chem 1992; 267: 13623-13628.

22. Kaiser SM, Sebag M, Rhim JS, Kremer R, Goltman D. Antisense-mediated inhibition of parathyoid hormone-related peptide production in a keratinocyte cell line impedes differentiation. Mol Endocrinol 1994; 8: 139-147.

23. Deftos LJ, Burton DW, Brandt SW. Parathyroid hormone-like protein is a secretory product of atrial myocytes. J Clin Invest 1993; 92: 727-735.

24. Senior PV, Heath DA, Beck F. Expression of parathyroid hormone-related protein mRNA in the rat before birth: demonstration by hybridization histochemistry. J Mol Endocrinol 1991; 6: 281-290.

25. Karaplis AC, Luz A, Glowacki J, Bronson RT, Tybulewicz VLJ, Kronenberg HM, Mulligan RC. Lethal skeltal dysplasia from targeted disruption of the parathyroid hormone-related peptide (PTHrP) gene. Genes Dev 1994; 8: 277-289.

26. Amizuka N, Henderson JE, White JH, Karaplis AC, Goltzman D, Sasaki T, Ozawa H. Recent studies on the biological action os parathyroid hormone (PTH)-related peptide (PTHrP) and PTH/PTHrP receptor in cartilage and bone. Histol Histopathol 2000; 15: 957-970.

27. Streeten EA, Brandi ML. Biology of bone endothelial cells. Bone Mine 1990; 10: 85-94.

28. Mori S, Yoshikawa H, Hashimoto J, Ueda T, Funai H, Kato M, Takaoka K. Antiangiogenic agent (TNP-470) inhibition of ectopic bone formation induced by bone morphogenetic protein-2. Bone 1998; 22: 99-105.

29. Ryan AM, Eppler DB, Hagler KE, Bruner RH, Thomford PJ, Hall RL, Shopp GM, O'Neill CA. Preclinical safety evaluation of rhuMabVEGF, an antiangiogenic humanized monoclonal antibody. Toxicol Pathol 1999; 27: 78-86.

30. Holder N. The onset of osteogenesis in the developing chick limb. J Embryol Exp Morphol 1978; 44: 15-29.

31. Carrington JL, Reddi AH. Parallels between development of embryonic and matrix-induced endochondral bone. Bioessays 1991; 13: 403-408.

32. Morini S, Pannarale L, Franchitto A, Donati S, Gaudio E. Microvascular features and ossification process in the femoral head of growing rats. J Anat 1999; 195: 225-233.

**Correspondence:**

Dr. Tsuyoshi Saga
Department of Anatomy
Kurume University
School of Medicine
Asahi-machi, Kurume 830-0011
Japan

Phone: ++81-942-31-7540
Fax. ++81-942-33-3233
e-mail. saga@med.kurume-u.ac.jp

Biomedical Research

Volume 11 Number 2 Special issue on Smooth Muscle* May-August 2000

CONTENT



*Guest Editor: ***Professor C.Y. Kwan, Ph.D.*** Price: US$ 50.00

**Order could be placed directly to: Biomedical Research, 6-B Manzar, Sir Syed Nagar, Aligarh 202 002, India**

CONTENT

# Biomedical Research

**Volume 14 Number 1** **April 2003**

# INSTRUCTIONS TO AUTHORS

*Biomedical Research* is an interdisciplinary Research Journal for publication of original research work in all major disciplines of Basic and Applied Medical Sciences. Invited and submitted review articles on current topics will also be included.

Manuscripts are received with the understanding that they have not been published or are not under consideration for publication elsewhere. Manuscripts are accepted after the recommendations of the referees. Published papers become the sole property of *Biomedical Research* and will be copyrighted by the Scientific Publishers of India.

The journal considers for publication manuscripts prepared in accordance with the guidelines laid down by the International Committee of Medical Journal Editors (Br Med J 1988; 296: 48-50).

***Preparation of Manuscripts***

Manuscript should consist of the following subdivisions: Title page, Key words, Abstract, Introduction, Material and Methods, Results/ Observations, Discussion, Acknowedgments, References, Tables, Figures and Legends. All manuscripts should be written in English and typed double-spaced throughout on one side of A4 (206x294 mm) with a wide margin. Number all the pages consecutively beginning with the title page.

The original and one copy of the manuscript along with two sets of figures should be sent to Receiving Editors or directly to the Chief Editor:

**Professor M.A. Qayyum**
**Editor in chief: Biomedical Research**
**6 B- Manzar, Sir Syed Nagar**
**Aligarh-202 002**
**India**

**e-mail:** biomedical@sancharnet.in qayyum@del3.vsnl.net.in **Fax: +91571-400678** **Tel: +91571-502043**

***Title page***

The title page should include the complete title of the manuscript, the author(s) name, address of the institute where the work was conducted, running title and the name and address of the author to whom the whom correspondence could be sent. A running title should also be given on the title page.

*Key words: 3-8 key words is essential.*

***Abstract***

The abstract should not exceed 250 words. It should be written in complete sentences and should give factual information.

***Abbreviations***

*Abbreviations of unitis should conform with those shown below:*

| | | | |
|---|---|---|---|
| Decilite | dl | micrometer | µm |
| gram(s | g | minute(s | m |
| kilogram | Kg | molar | mol/l |
| milligram | mg | milliliter(s) | ml |
| hour(s) | h | percent | % |

Other abbreviations and symbols should follow the recommendations on units, symbols and abbreviations: a guide for Biological and Medical Editors and Authors (The Royal Society of Medicine London 1977).

***References***

A list of all the references cited in the text should be given at the end of the manuscript. The references should be cited according to the Vancouver agreement. They should be typed with double spacing, and numbered consecutively in the order in which they are first mentioned in the text. Identify references in the text by Arabic numerals [in square brackets]. Authors must check and ensure the accuracy of all references cited. All authors should be cited. Abbreviations of titles of medical periodicals should conform to those used in the latest edition of Index Medicus. The volume of the periodical should be followed by the page number of each reference cited. Some examples are given below:

*Journal article*

Griffin JH, Evatt B, Zimmermann TS, Kleiss AJ. Deficiency of protein C in congenital thrombotic disease. J Clin Invest 1981; 311: 1373-1378.

*Personal authors' book*

Carr KE, Toner PG. Cell structure: An introduction to Biomedical Electron Microscopy. 3rd ed Edinburgh Churchill Livingstone 1982.

*Edited book*

Dausset J, Columbani J eds. Histocompatibility 1972. Copenhagen Muksgaard 1973.

*Chapter in a book*

Fenichel GM. Hemiplegia. In: Clinical Neurology. 2nd ed. W.B. Saunders Co., Philadelphia 1993: pp 246-260.

*Tables:* The tables should be typed on separate sheets. Place explanatory matter as footnote.

*Figures*

All figures (photographs, photomicrographs, electron micrographs, drawings, graphics and illustrations) should be listed together. Figures should not exceed 6x8.2 inches and should be numbered. Each figure should have on its back the author's name, figure number and an arrow indicating the top side of the figure.

*Page charge*

No page charges for the first 3 pages. Each additional printed page is charged to the author/s at US$ 100.00. For short papers of 1-4 pages US$50.00 per page will be charged.

*Reprints*

15 reprints will be supplied free. Additional reprints may be ordered on the approved forms. Reprint order forms and price list are sent with the galley proofs.

## Annual Subscription: US $ 150.00

**Manuscripts should be sent to one of the following Editors or Chief Editor directly:**



*Floppy diskette*

***Authors may submit manuscripts on floppy diskette using Microsoft Word Programme. It will speed up the publication of your manuscript and will cut the cost.***


Edited, Printed and Published by M.A. Qayyum for Scientific Publishers of India, 87-Greater Azad Enclave, Aligarh 202 002, Indiia

**Printed at : Taj Mahal Printing Press, Delhi-6**